SYNTHESIS AND FUNCTIONALITY OF POLYMERIC DIAZENIUMDIOLATES IN THE USE AND CONTROL OF NITRIC OXIDE RELEASE FOR SEVERE MEDICINAL ATHEROSCLEROTIC PLAQUE APPLICATIONS AND HUMAN PAPILLOMAVIRUS TREATMENT

A Dissertation

Presented To

The Graduate Faculty of The University of Akron

In Partial Fulfillment

of the Requirements for the Degree

Doctor of Philosophy

Chanda L. Elam

August, 2008

SYNTHESIS AND FUNCTIONALITY OF POLYMERIC DIAZENIUMDIOLATES IN THE USE AND CONTROL OF NITRIC OXIDE RELEASE FOR SEVERE MEDICINAL ATHEROSCLEROTIC PLAQUE APPLICATIONS AND HUMAN PAPILLOMAVIRUS TREATMENT

Chanda L. Elam

Dissertation

Approved:

_____
Advisor
Dr. Daniel J. Smith

_____
Committee Member
Dr. Stephanie Lopina

_____
Committee Member
Dr. Michael Taschner

_____
Committee Member
Dr. Chris Wesdemiotis

_____
Committee Member
Dr. Weiping Zheng

Accepted:

_____
Department Chair
Dr. Kim C. Calvo

_____
Dean of the College
Dr. Ronald Levant

_____
Dean of the Graduate School
Dr. George R. Newkome

_____
Date

ABSTRACT

Current research utilizing nitric oxide for its wound healing properties has propelled researchers to expand current applications. One application is the use of polymeric diazeniumdiolates to increase nitric oxide's vasodilation properties, namely in the area of atherosclerotic plaque[1]. Earlier commercial use of coated stents in the pharmaceutical arena for arterial blockage showed great promise with the exception of remission of plaque buildup within the stent [2]. The same procedure has been applied to relieve thrombogenic plaque, which has lead to restenosis (re-narrowing) of the coronary artery due to trauma at the site of the stent or coiling[3]. The body's natural instinct is to cause clotting (thrombosis), thus restenosis, at that site. Instead of using polymeric diazeniumdiolates for stent coating and long-term usage, the polymeric diazeniumdiolate could be used to alleviate the body's response to restenosis as well as increase the release time of nitric oxide from several days to weeks or longer[4.] The body will naturally process the diamine to its biodegradable by-products and thereby remove them as waste from the body.

Studies have shown that nitric oxide-producing PEG derivatives in conjunction with hydrogels have been able to release nitric oxide over a period of a couple of days with a short release time [5]. However, flexibility in the release profile will prove useful in the treatment of atherosclerotic thrombosis and restenosis. At the same time these diazeniumdiolates were tested for applicable use for the treatment of the high-risk human papillomavirus (HPV) types 16 and types 18.

Previous research shows that nitric oxide has been effective in the treatment of low-risk HPV, namely plantar warts and the like. It is hypothesized that if the virus is responsive to nitric oxide

in its cutaneous, benign growth stage then it is possible that the mucosal, malignant growth is susceptible to nitric oxide treatment.

A study using HeLa (wild type, HPV type 18), C33A (mutant, HPV negative) and CaSki (wild type, HPV type 16) cervical cancer cells has been used to determine the effectiveness of nitric oxide on high-risk HPV and determine the genetic process effected in the treatment[6]. Bioavailability testing was performed to determine future drug therapy for nitric oxide producing compounds in the treatment of HPV–induced cervical cancer.

ACKNOWLEGEMENTS

First and foremost, I would like to thank my advisor Professor Daniel J. Smith for his patience and guidance throughout my graduate experience. Secondly, I would like to thank the other members of Dr. Smith's group for providing me with insightful discussions and a wonderful graduate experience: Nathaniel Beres, Wilmarie Flores-Santana, Piyaporn Kampeerapappun (Oh), Melinda Carnahan, Jurapun Parapoon (Tung), and Marcos Lopez for his contribution of characterization of the synthesized materials. I would also like to express gratitude to Dr. Stephanie Lopina of the Unversity of Akron and Dr. Angelo DeLucia of NEOUCOM who have allowed me to think critically and more in-depth of my research aspiration. Lastly, I would like to thank an undergraduate student Jeremy Setser, who assisted with the nitric oxide analysis.

I am grateful for the financial support from the Department of Chemistry and the Graduate School of the University of Akron, as well as the Millipore Company.

Finally, I would like to dedicate this dissertation to my family especially my parents, the late Mrs. Lillian C. Elam, Robert and Doris Ivey Elam and my sisters Sabrina Walker and Dedrey Elam, who never doubted my abilities and who encouraged, sacrificed and cheered for me throughout this process.

I would like to give a special acknowledgement to some very close friends that have been with me throughout this process and more than likely deserve a doctorate in patience: Mrs. Joy Mason, Mrs. Mathilda Reeves-Jones, Dr. Trocia Clasp, Mrs. Mariam Kea, Ms. Vanessa Browne, Dr. Dorothy Jones, Ms. Leticia S. Williams, the late Mr. A. Glenn Nevels and Ms. Katrice Sterling.

TABLE OF CONTENTS

Page

LIST OF TABLES

LIST OF FIGURES

Figure Page

BACKGROUND

Although, the NO Analyzer has been utilized to determine the nitric oxide profile of many diazeniumdiolates, it does have some limitations. The diazeniumdiolates made by Michael's addition reaction used either 1,4-diaminobutane (putrescine) or ethylenediamine with the desired acrylate. After a multi-step synthesis, the resulting diazeniumdiolate were analyzed. The problem encountered with these types of nitric oxide donors is their solubility in the phosphate, buffered aqueous media. Analysis using one chemiluminiscent method (Nitric Oxide Analyzer) does not give an accurate detection of the total amount of NO in these compounds; additionally a more quantitative analytical method is required for analyzing these lipophilic, materials.

For spectrophotometric determination, a Griess reagent is a cost efficient opportunity to determine total nitric oxide release. In the case of this study, the reagent is a potassium phosphate buffered, neutral, sulfanilic acid and N-(1-naphthyl)ethylenediamine dihydrochloride chemiluminescence reagent. The Griess reagent methodology will be compared to the current NO Analyzer technique in order to fully understand its benefits and its practicality in nitric oxide release profile development. Furthermore, a diazeniumdiolate pro-drug will be prepared and examined to determine its bioavailability in the treatment of the human papillomavirus (HPV).

The human papillomavirus has been linked to low-risk warts such as plantar and butchers warts and high-risk cervical cancer, depending on the virus gene-type. In some cases, there has been research to support treatment of these warts utilizing nitric oxide products. However, there has not been any research of nitric oxide in the treatment of high-risk, HPV-induced cervical cancer cells. Utilizing several cell lines, a study was performed to determine the effect of nitric

oxide on HPV-induced, cervical cancer cells. The intriguing element of the study was the response of differing HPV cell lines to the pro-drug. The data would have indicated that diazeniumdiolates have the potential to treat the virus. The implications of such a treatment with minimal side effects, based on knowledge of nitric oxide's physiological need, development and usage, would have significant impact over current therapies.

CHAPTER I

INTRODUCTION

1.1 The Fundamentals of Nitric Oxide and its Therapeutic Nature

Nitric oxide has been utilized over the years for many medical applications associated with its most common property: vasodilation. Nitric oxide has been determined to regulate vasorelaxation of smooth muscle cells, regulate blood pressure and expedite the healing process, and control the inhibition of platelet aggregation. The history of nitric oxide, as such, has been studied extensively. Accordingly, the metabolic synthesis of NO has been identified and defined by multiple researchers. All studies support that nitric oxide is the by-product of the conversion of L-arginine to L-citrulline by nitric oxide synthase. It works as a "…biological messenger molecule"[13] and its effectiveness is determined by its concentration.

The synthesis of nitric oxide involves two pathways working in conjunction to process L-arginine into L-citrulline[14]. The first pathway is the conversion of L-arginine to citrulline via the intermediate N^G-Hydroxy-L-arginine. The second pathway follows the course of electrons transferring with the utilization of nicotinamide adenine dinucleotide phosphate hydride (NADPH), 6R-tetrahydrobiopterin (BH_4), flavin ademine dinucleotide (FAD), flavin mononucleotide (FMN), ferrous ions (Fe^{+2}), ferric ion (Fe^{+3}), calcium/calmodulin (Ca/CaM), oxygen (O_2) and water (H_2O)[15]. This process takes place at the heme and requires BH_4 in conjunction with nitric oxide synthase (NOS), to synthesize nitric oxide. NOS isoforms are derived by location, functionality and regulation of the body[16]. The endothelial, inducible and

neuronal NOS are used to synthesize NO in muscle tissue, the liver and the central and peripheral neurons, respectively. As seen in Table 1.1, the characteristicsand locations of the enzymes are directly proportional to nitric oxide synthesis and functionality.

Table 1.1: Nitric Oxide Synthases Isoforms Functionality and Locale[23, 51]

Type (gene bp)	Common Name	Tissue/Cell Locale	Functionality and Activation
NOS-1 (155kD)	Neuronal NOS or Type I-NOS	• Central and peripheral neurons • Endometrium • Skeletal muscles • Brain	• Constitutive • Calcium/Calmodulin dependent to neurons
NOS-2 (125 kD)	Inducible NOS or Type II-NOS	• Macrophages • Liver • Smooth muscles • Endothelium • Heart	• Inducible by endotoxins (lipopolysaccharides) • Cytokines and glucocorticoids • Calcium/Calmodulin independent to macrophages
NOS-3 (133 kD)	Endothelial NOS or Type III-NOS	• Endothelium • Brain • Heart	• Constitutive • Calcium/Calmodulin dependent to endothelium • Modified by acylation and phosphorylation

NOS-1 and NOS-III are constitutive enzymes, but the enzyme expression is dependent upon the tissue locale; while NOS-II is induced by endotoxins, interleukins and pro-inflammatory cytokines. The calcium dependent isoforms exist as homodimers and work with BH_4 and the heme to form dimers.

In this process, as L-arginine is converted to the intermediate two electrons are transferred from NADPH to FAD fueled by the consumption of one mole of oxygen. The transfer of the electrons to FMN from FAD is perpetuated by the calcium/calmodulin complex, whereas the calmodulin acts as a carrier of electrons to the heme, thus reducing the ferric ion. As seen in figure 1.1, the conversion from the N^G-Hydroxy-L-arginine to L-citrulline takes place via the reductase domain, whereby only one electron is transferred. BH_4 is present in both phases of the

electron transfer, due to the fact that without pterin, NADPH would continue to oxidize oxygen. The reduced and unbound oxygen will lead to the superoxide (O_2^-) species.

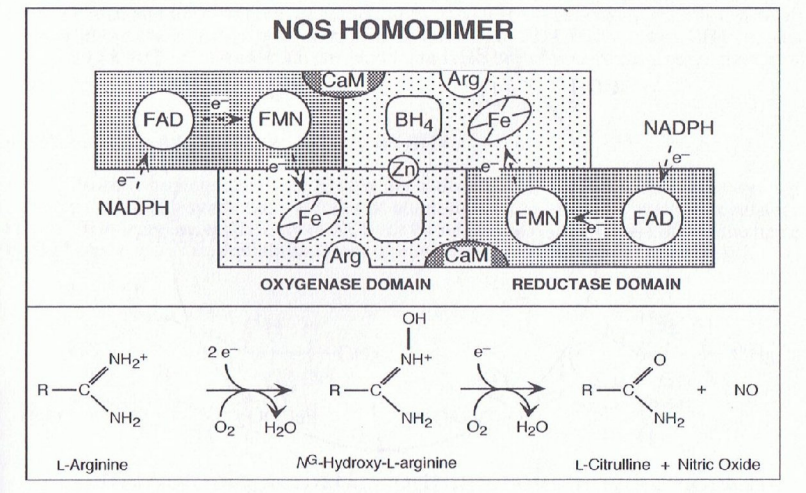

Figure1.1: The conversion of L-arginine to L-citrulline and nitric oxide: the combination of two cycles working in conjunction with each other aids in the generation of nitric oxide. Copyright permission has been granted by the publisher.

Accordingly figure 1.2 provides the mechanism by which NOS (noted as the enzyme) must bind to heme in order for L-arginine to bind and convert to citrulline. By binding NOS to the sulfur, the L-arginine is conformationally aligned with iron (III) to reduce the amine and yield the intermediate and lead to the release of nitric oxide. According to Beckman[18], there are multiple formulas and oxidative states of nitrogen oxides. Nitrogen functions differently when bound to oxygen, due to varied oxidative states of nitrogen. As seen in Table 1.2, the oxidative states range from +1 to +6. However, nitrogen has more commonly known oxidative states such as 0, -1, -2 and -3 (N_2, NH_2OH, $R{=}NH_2$, N_2H_2 and NH_3, $R\text{-}NH_2$, respectively).

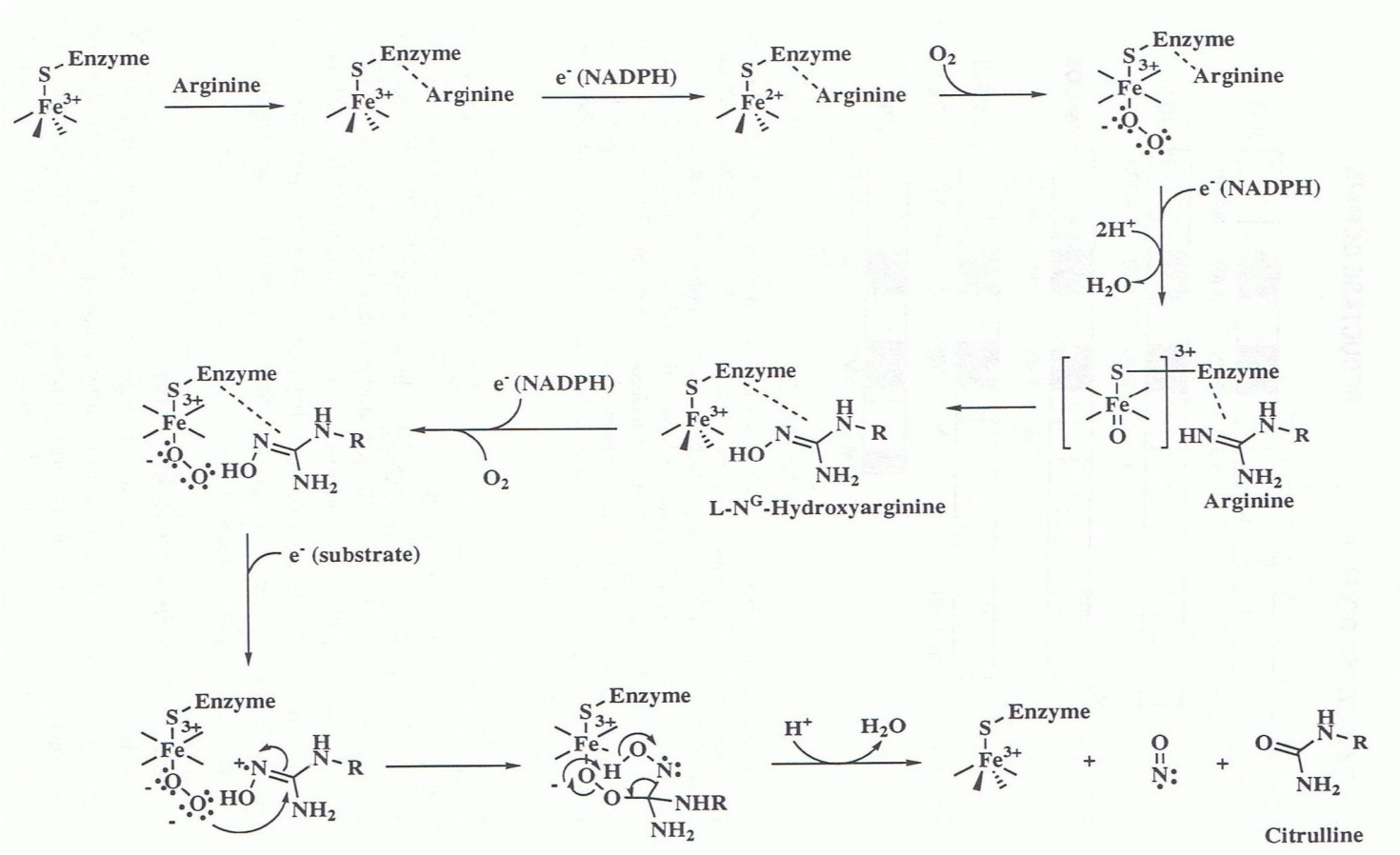

Figure 1.2: The mechanism of L-arginine conversion to L-citrulline and NO. The mechanism takes into account the enzyme NOS, the ferric ion, oxygen and the heme. Copyright permission has been granted by the publisher.

Table 1.2. Common Oxidative States of Nitrogen Oxide

Oxidative State	Molecular Formulas	Common Names
+1	N_2O	Nitrous Oxide
+2	NO	Nitric Oxide
+3	NO_2^-	Nitrite
+4	NO_2	Nitrogen Dioxide
+5	$ONOO^-$, NO_3^-	Peroxynitrite; Nitrate
+6	$ONOO^{\cdot}$, $NO_3^{\cdot}$	Nitrosyldioxyl radical; Nitrate radical

Due to the particular interest in nitric oxide, the oxidizing elements of this molecule must be significant to understand the physiological changes that occur during the metabolism of the molecule[19].

$$N^+\equiv O \longrightarrow {}^{\cdot-}N=O \longrightarrow N=O^- \qquad [1]$$

The nitric oxide ($^{\cdot}NO$) free-radical exists as the intermediate between the conversions of the nitrosonium ion (NO^+) to the nitroxyl anion (NO^-) per equation 1. Nitric oxide is a one electron oxidizing agent which forms the nitroxyl compound (NO^-) for biological interactions. Nitric oxide is mediated in this process by the reaction of a transition metal, which is seen by the reduction of the ferric ion to the ferrous ion. This is due to the fact that nitric oxide can not "…directly nitrosate organic molecules" without a proper electron acceptor[20, 21]. Also, nitric oxide does not form the dimer intermediate of dinitrogen dioxide, N_2O_2 from its one-electron state, but instead disproportionally forms NO_2 and N_2O as seen in equation 2:

$$3NO \rightarrow NO_2 + N_2O \qquad [2]$$

A more in-depth review of nitric oxide shows that this is the result of an unpaired electron in the highest occupied molecular orbital (HOMO). In this molecule, nitrogen maintains five valence

electrons while oxygen holds six valence electrons leaving one an unpaired electron. The nitric oxide molecule is weakened by the lone electron, thus the conversion to nitrosonium ion by removing one electron. Dimerization of the nitric oxide to N_2O_2 is not thermodynamically stable: 1) N-N bonds can be broken at room temperature due to the zero electronegative charge, 2) Gibb's free energy of the dimer is equal to the free energy of two nitric oxide molecules[22]. However, the more common reaction is nitric oxide reacting with air to form a brown gas, nitrogen dioxide as seen in equation 3.

$$2NO + O_2 \rightarrow 2NO_2 \quad [3]$$

This occurs when nitric oxide is in a lower concentration than the oxygen. The reaction is slow and has a third order rate constant, which leads to the possibility of dimerization to dinitrogen tetraoxide. However, under physiological conditions this is impossible due to the slow rate of nitrogen dioxide formation.

Also, due to nitric oxide's slight solubility in water, it can react with oxygen in the water to form nitrite products per equation 4. This is helpful in the use of biomaterials which are activated by water.

$$4NO + O_2 + 2H_2O \rightarrow 4H^+ + 4NO_2^- \quad [4]$$

Analysis of this phenomenon has been enhanced to detect nitrate levels as the nitrite reacts with ozone (O_3) in nitric oxide analyzer instrumentation to reveal nitric oxide profiles of biomaterials.

1.2 Nitric Oxide Communication with Tissue

Nitric oxide is a small messenger molecule. As documented in previous research, the nitric oxide synthase (NOS) isoforms communicate with the cell tissue. The three isoforms (i.e. e-nos, c-nos and i-nos) which are expressed in cells, of which e-nos and i-nos are involved in the synthesis of L-arginine to citrulline[43, 44, 45]. Figure 1.3 shows the effect of nitric oxide in the system of a healthy endothelium cell and the permeability of nitric oxide to the vascular smooth

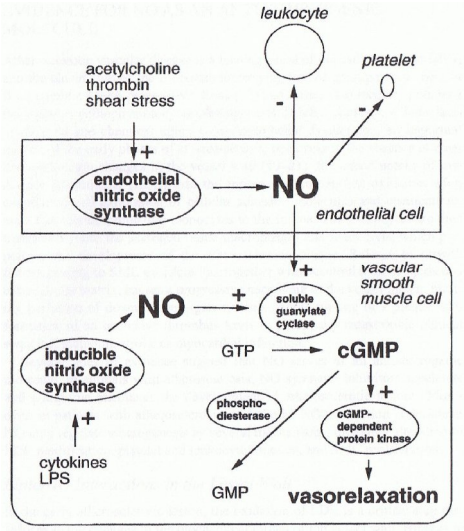

Figure 1.3: Nitric oxide production in a healthy endothelium cell. Nitric oxide complexes with NOS in both the endothelium and vascular smooth muscle cells to retard platelet activation and platelet adhesion as well as control vascular homeostasis via a conversion of GTP to cGMP. Copyright permission has been granted by the publisher.

muscle cell. Within the endothelium cell, e-NOS complexes with nitric oxide to inhibit the leukocytes and platelet adhesion, while i–NOS complexes with nitric oxide to control the vaso-relaxation, thus relieving smooth muscle cell proliferation. Also, nitric oxide is known to: 1) act as a barrier between the bloodstream and vessel walls, 2) regulate arterial vasomotor tone (vascular reactivity) and blood flow, 3) produce a range of proteins involved in the control of coagulation, 4) maintain the anti-adhesive properties of the endothelial surface, 5) play a critical role in the control of the circulatory system and maintenance of normal cardiovascular system function, 6) have a primary role in controlling vasomotor tone and thus regulating blood flow and pressure (acts as a vaso-relaxant), and 7) have an important anti-atherogenic effect (inhibition of platelet aggregation and anti-inflammatory properties).

Figure 1.4 demonstrates the role of nitric oxide in an unhealthy endothelium cell, which leads to complications of the vascular smooth muscle cells via abnormal vaso-regulation. Chapter two will discuss the complications from unhealthy nitric oxide production and causality

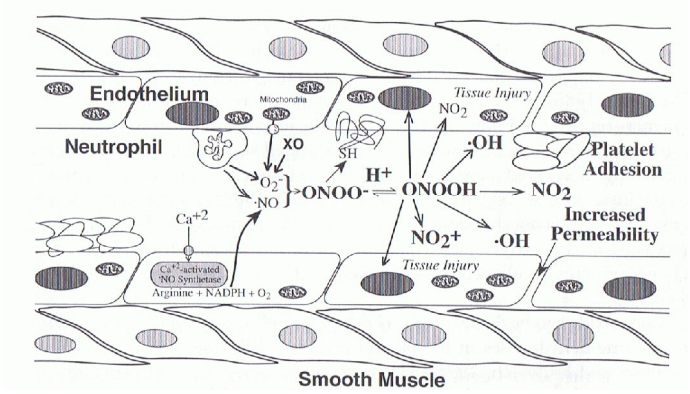

Figure 1.4: Role of nitric oxide in an unhealthy endothelium cell. The production of peroxynitrite leads to compromises in the vascular smooth muscle cells. The lack of nitric oxide will lead to the activation of platelet and platelet adhesion. The increase in the peroxynitrite increases the permeability of nitric oxide and superoxide which leads to abnormal vaso-regulation. Copyright permission has been granted by the publisher.

of atherosclerotic vascular disease due to a process of plaque adhesion along the cell wall. Additionally, chapter two will discuss both low-risk and high-risk human papillomavirus (HPV), which has been attributed to the initiator of cervical cancer and its current medicinal therapies.

CHAPTER II

DISEASES AFFECTED BY NITRIC OXIDE COMPLICATIONS AND THEIR THERAPIES

2.1 Motivation for Studying Atherosclerotic Plaque and HPV Therapy

In every aspect of daily life, chemistry and its benefits can be seen, particularly in regards to the medical benefits of biotechnological and biomaterial applications[7, 8]. The application with respect to our discussion is the medicinal applications of nitric oxide biomaterials and their derivatives[9, 10].

Two existing physical conditions have employed the vasodilating, nitric oxide (NO) releasing compounds in their therapies[11]. The first condition is atherosclerotic plaque and the second is low-risk human papillomavirus (HPV)-induced warts. These conditions are created by pathological processes that arise from either insufficient production of NO or physiological barriers that lead to reduced production of NO, such as diabetes and hypertension.

In this dissertation, the usefulness of polymeric diazeniumdiolate derivatives will be tested and their effectiveness evaluated. It will be shown that the traditional methods for the analysis of these nitric oxide compounds is inefficient and time-consuming, while new approaches to determine the release profile are more effective and straightforward. The discussion will lead to analysis of lipophilic, insoluble diazeniumdiolates and their attractiveness in the future of polymeric diazeniumdiolates applications. The theoretical approach to creating nitric oxide (NO) donating compounds has been to utilize a secondary amine and react with monomers, such as alkylated acrylates, polyurethanes and polyethylene glycol derivatives[12]. In

chapter one, the discussion centered on the origin of nitric oxide, while chapter two will focus on the two medical conditions, their origins and current therapies.

This background is the source to understanding the practical use of nitric oxide to effectively treat these conditions.

2.2 Models of Atherosclerotic Plaque

One aspect of endothelial dysfunction, namely the lack of nitric oxide production, occurred when the body is not readily able to control inflammation or endothelial trauma. The lack of metabolic nitric oxide was caused by numerous metabolic causes such as diabetes, dyslipidaemia, hypertension, and obesity to name a few. With the lack of nitric oxide there are increased interactions of reactive oxygen species (peroxides, etc) with low-density lipoproteins (LDL) to create oxidized LDL. As seen in figure 2.1[73, 74], the reaction of oxidized LDL and macrophages lead to the creation of foam cells which build up to a thrombus, the major cause of atherosclerotic plaque. Also, inflammation is noted by monocytes which induced C-reative

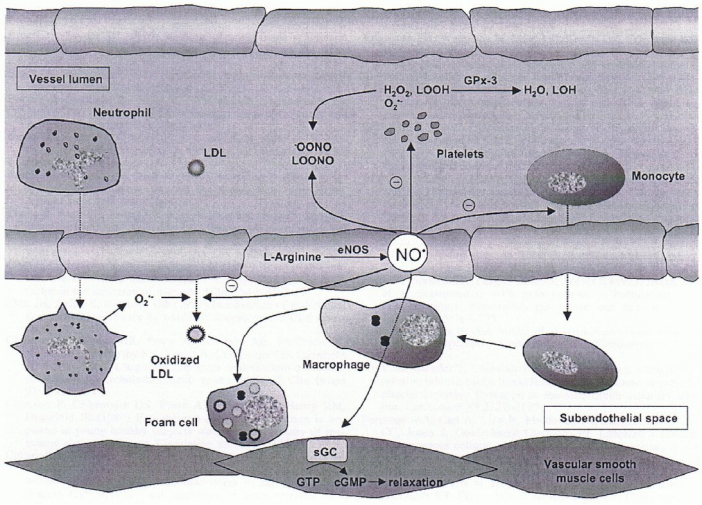

Figure 2.1 Schematic of the initial formation of a foam cells. With increase inflammation, a chain effect of the interaction of macrophages with oxidized LDL occurs, thereby leading to atherosclerotic plaque. Copyright permission has been granted by the publisher.

proteins (CRP) response. The response of CRP led to the activation of the interleukin via the macrophages. A recent study has shown that with the increase in inflammation and CRP, it was noted that the nitric oxide levels decreased. The instances of the body correcting the inflammation decreases as well. . The figure shows an in-depth view of nitric oxide forming nitrates by interacting with reactive oxygen species (ROS). However, interations of ROS and oxidized low-density lipoproteins (LDL) will lead to the formation of foam cells, a precursor for plaque[85, 86]. The build-up of plaque in the arterial walls can lead to: 1) coronary arterial dysfunction, 2) brain spasm, 3) aneurysm and, 4) thromboembolic incidents. As the foam cells continue their generation, plaque aggregation and adhesion (atherosclerotic plaque) will eventually create a thrombus, or clot. The formation of the thrombosis will eventually lead to restenosis (narrowing) of the endothelial smooth muscle[75]. Atherosclerosis (formation of arterial plaque) is a slow forming disease and has been defined as types I-V lesions. Type I and II are defined as early lesion with "…small lipid deposit" on the intima of the blood vessel. Type III lipid formation has been described as extracellular. Type IV is the buildup of the lipid core below the smooth muscle surface. Type V has been described as the fibrous thrombus material which can be seen in figure 2.2[5, 76, 77].

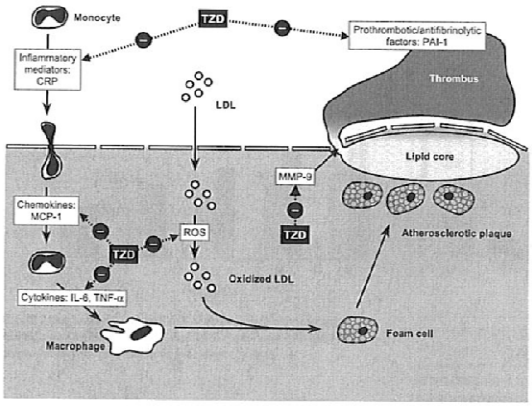

Figure 2.2 Schematic of the formation of a thrombus. With increased inflammation, a chain effect of CRP, interleukin and macrophage activation occurs. Due to hindered nitric oxide production, the macrophages react with oxidized LDL, thereby leading to atherosclerotic plaque accumulation. Copyright permission has been granted by the publisher.

2.2.1 Current Therapeutic Practices

There are numerous avenues to overcome atherosclerosis plaque. Namely, nitric oxide donating drug therapies, heparin-coated and uncoated stents, probucol in conjunction with balloon angioplasty, polyethylene oxide biomaterials, aspirin therapy, and tissue repair[5, 78, 79, 80, 81]. The nitric oxide drug therapy involved replacing endothelial nitric oxide synthesis. Nitrovasodilator such as nitroglycerin, amyl nitrite and isosorbide dinitrate have been known treatments of cardiovascular disease, traditionally. Other therapies such as L-arginine, tetrahydrobiopterin, hydralazine can be used to induce nitric oxide release without invasive, corrective surgery[82]. There are enzymatically-activated drugs such as nitro-aspirins that release nitic oxide, as welll as sinitrodil that target specifically large arteries[83]. When there is extensive artherosclerotic plaque build-up, the uses of stents, whether heparin-coated or uncoated, are used to expand narrowed arterial passageway. While uncoated stents in conjuction with angioplasty traditionally have been used, significant complications from thrombosis have been reported either from a lack of or no anticoagulation post-operative therapies, as well as the re-accumulation of platelets along the stent[75]. However, heparin-coated stents (utilized for heparins have well-documented anticoagulating properties) has shown to reduce coagulation, but can lead to one of the most significant complications, namely restenosis.

2.2.2 Hazards of Current Therapies

The chance of restenosis (re-narrowing) of the coronary artery due to trauma or injury at the site of the angioplasty or stent implantation is highly likely. The injury, an effect of the overstretching of the arterial intima, can reduce the healing process initially intended by the angioplasty, since the body's natural instinct is to cause clotting (thrombosis) when an injury occurs. Therefore, the use of post-operative, anticoagulating drug therapies to retard the clotting process have been found a necessary precaution.

Restenosis starts with initial trauma to the endothelial smooth muscle cells. As the trauma progress, the smooth muscle cells migrate and form a hyperplasia of extracellular material in the intima. The hyperplasias lead to hypertrophy which can depress the blood flow and results in a vascular lesion. Therefore stenting in conjunction with the angioplasty resolve the issue to restenosis after angioplasty[3]. According to Figure 2.3, angioplasty alone would leave the artery exposed to continual plaque buildup versus stenting with the angioplasty would stretch the artery and hindered build-up. Current therapies have shown that the use of nitric oxide donating drugs have been effective in the treatment of atherosclerosis, thombosis, restenosis, cerebral vasospasm and hypertension. These nitric oxide therapies, which have a known indication as a vasodilator and vasorelaxant, help maintain a barrier between the bloodstream and vessel wall, produce a range of proteins involved in the control of coagulation and maintain the anti-adhesive properties of the endothelial surface[87].

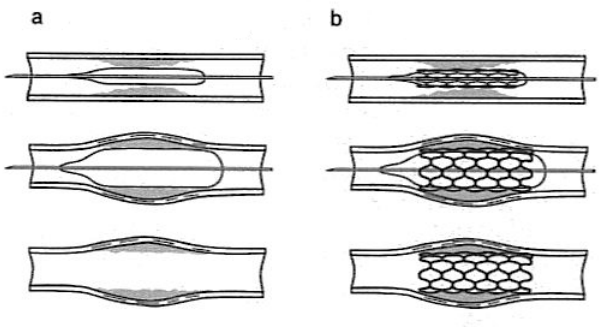

Figure 2.3: Arteial repair from atherosclerotic plaque. A. The arterial repair was completed via balloon angioplasty. Without preventive, post-operative coagulation therapy, the artery would be impacted by more plaque. B. Arterial repair utilizing balloon angioplasty and stenting to prevent arterial closing after treatment. Copyright permission has been granted by the publisher.

However, the greatest hazard associated with the use of these drugs is excess drug remediation. The body naturally produces 1uM of NO; any amount above that level is detrimental to the

patient's health as it reduces blood pressure and can lead to metabolic diseases (such as diabetes, hypertension, etc).

2.2.3 Outcomes of Current Therapies

According to research by Miketic, et al. there was no significant difference between the uncoated, untreated stent and the coated stent implantation.[89] Furthermore, work by Lea, Bohl, et al and McGrowder, et al suggest that the use of nitric oxide prodrug therapies and polyethylene glycol in conjunction with nitric oxide drug remediation have proven most effected in the treatment of impairments (restenosis, thrombosis, hypertension, etc) occurring from cardiovascular disease.[1, 36, 78] Recently, Gombotz, et al, determined that polyethylene oxide surfaces, which has been documented to decreased protein absorption when used as a coating of biomaterials, may not adhere to the surfaces "…in a solution containing proteins".[90] However, by covalently bonding the ethylene oxide with other polymers such as polyether polyurethanes, the elution of polyethylene oxide from the surface is negated.

2.3 Human Papillomavirus Background

Historically, the human papillomavirus (HPV) has been linked with other sexually transmitted diseases (STDs) as a side effect. Later, it was determined that these venereal diseases (gonorrhea and syphillis) provided HPV with its mode of transmission via mucosal exposure.[95]

2.3.1. Human Papillomavirus Background

The human papillomavirus is approximately 8000 base pair (bp), circular, double-stranded DNA, non-enveloped virus. There are approximately 200 types of the papillomavirus. Of these differing types, the virus has been divided into two disease types: non-genital cutaneous and anogenital (or mucosal) in type. In both disease types there is a designation of high risk or

low risk. The low-risk designation referred to a localized, benign growths or warts in which the host cell displayed non-integrated extrachromosomal HPV DNA.[91] However, the high-risk designation displayed malignant cells or lesions with integration of the HPV genes with the host chromosome. Table 2.1 displayed the HPV disease types and lesion type. Based on the table, the non-genital cutaneous HPV types have the propensity to exist as warts, while the anogenital type yields the high-risk, malignant cancerous lesions.

Table 2.1 HPV disease types and lesion type

Lesion	Disease Type	HPV Type
Common Warts	Non-genital Cutaneous	1-4
Plantar Warts		1,4
Flat Warts		3, 10
Butcher's Wart		3,7
Epidermodysplasia verruciformus		3,5, 8-10, 12, 14, 15, 17, 19-25, 28, 29
Respiratory	Non-genital Mucosal	6, 11, 30, others
Genital	Anogenital	6, 11, 16, 18, 30, 31, 33-35, 39, 40, 42-45, 51-59, 66, 68, 70

According to Anderson, the HPV gene has been divided eight gene sequences, E1 through E8.[91, 92] However, the E3 and E8 gene functionalities have not been determined. The eight genes are divided into two categories: the early and late gene. As presented in Table 2.2, the early gene has been segmented into five genes: E1-E7. The late gene consisted of two genes: L1 and L2. The early (E) region encodes nonstructural proteins while the late (L) region encodes the two capsid proteins. For the discussion of the human papillomavirus and its connection to cervical cancer, the genes E6 and E7 were particularly necessary to understand viral transcription and cell proliferation due their involvement in the mutagenesis and spread of the disease.

Table 2.2 HPV Gene Functionality

Gene Category	Gene	Functions
Early Gene	E1	Viral Replication
	E2	Modulation of Transcription and Replication
	E4	Productive Viral Infections
	E5	Transforming Properties
	E6	Oncoproteins, interaction with p53 (functions to restrain the uninhibited cell proliferation that is characteristic of cancer)
	E7	Oncoproteins, interaction with Rb (DNA binding proteins that interact with E2F)
Late Gene	L1	Major Capsid Protein
	L2	Minor Capsid Protein

The process of a healthy cell and cell proliferation initially occurred as levels of p53, the tumor suppression protein, are at low levels during normal cellular functions. DNA damage, infection and cellular stressors activate p53 to higher levels resulting in apoptosis (cell death) or cessation of cell cycle at G1 with the support of p21, the cyclin dependent kinase inhibitor.[93] Trans-infection of a healthy cell with the human papillomavirus cause the activation of the E6 and E7 genes, as seen in figure 2.4.

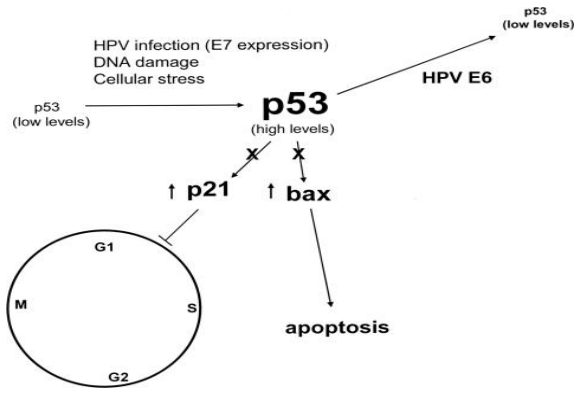

Figure 2.4: Function of p53 in a healthy cell. The levels of p53 are low during normal functions. However, the activaton of p53 transpires as a function of possible DNA damage, cellular stress and infection. By activating p53to a higher level, the impaired cell begins the process of apoptosis or cessation of cellular transcription. Copyright permission has been granted by the publisher.

According to Howley, and Munger, et al, the infection by both E6 and E7 lead to the degradation of the p53 and the deregulation of pRB, respectively. [93, 94] It has been noted that the papillomavirus initially interferes with cellular regulations by compromising pRB, a known transcription activator. In the G0/G1 stage, pRB form a complex with E2F, a transcription repressor. As seen in figure 2.5, the E7 gene will complex with the pRB protein in its hypophosphorylated form. The binding of the E7 gene will cause the release of E2F from pRB, thereby activating continual DNA transcription into the S phase of the cell cycle. E7 can not completely immortalize cellular functions. The E6 gene is necessary and must work in conjunction with the E7 gene to deregulate normal cell death cause by the protein p53.

The E6 gene has been shown to interrupt p53 activity. Upon further inspection it was noted that the E6 gene can not bind directly with p53 in its normal state and requires the assistance of E6-associated protein (E6AP), an E3 ubiquitin protein ligase.

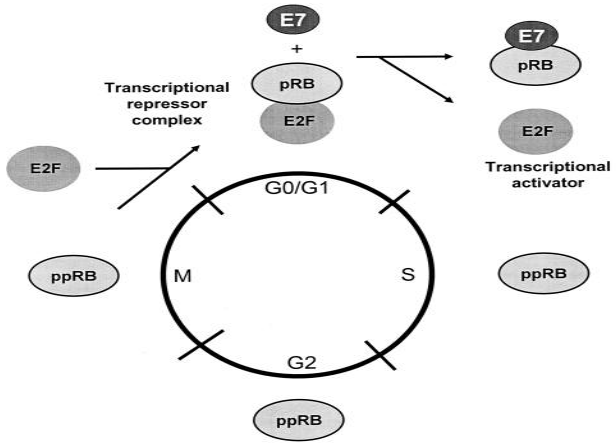

Figure 2.5: Function of the E7 gene in the deregulation of pRB. pRB is initially bound to E2F, to regulate cellular transcription. In the deactivated state, the hypophosphorylated state, pRB hinders DNA transcription. E7 ruptures the complex, promoting DNA transcription. Copyright permission has been granted by the publisher .

The complex of E6 and E6AP, having bonded to p53, promoted the ubiquitylation and proteolysis of p53 as seen in figure 2.6. The ubiquitylation of p53 extended cellular proliferation and instead leads to continuous cell mutation.

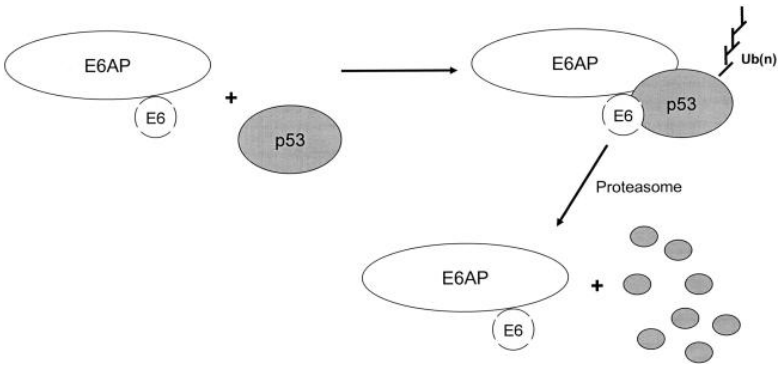

Figure 2.6: Function of the E6 gene in the deactivation of p53. With p53 levels low, during normal functions, the activation of p53 transpires as a function of possible DNA damage, cellular stress and infection. At that time, the activation of p53 leads to apoptosis or cessation of cellular transcription. Copyright permission has been granted by the publisher.

According to Lowry, Crum and Phelps, et al, viral infection of the papillomavirus occurred within a microtrauma or cut in the skin or upper epidermis.[96, 97, 92] Viral transcription of the non-capsid HPV began once the virion migration to the basal keratinocytes had occurred. Figure 2.7 illustrated the process by which the basal layer provided the virus with continual cell growth due to the longevity and rapid turnover of keratinocytes at the basal level. As the virus was reproduced in the process, the skin cells continue their migration to the surface of the epidermis. The process can range from months to years without symptoms of the virus.

The severity of the HPV infection has been graded by the progression of the cellular mutation from normal cellular growth to highly invasive carcinoma.[99, 100, 101] The initial infection classified the cell as mild dysplasia, or as cervical intraepithelial neoplasia (abnormal tissue)

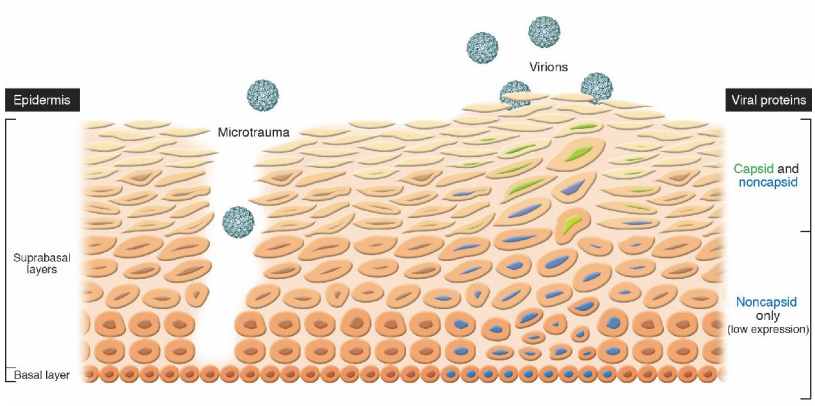

Figure 2.7: Pathway of HPV infection. With the trans-infection of the basal layer, the papillomavirus begins the process of viral DNA replication. As the skin cells migrate to the surface of the epidermis, a viral assembly occurs with the encapsulation of the virus and it release in the dead skin cells. Copyright permission has been granted by the publisher.

(CIN) or low-grade squamous intraepithelial lesion (abnormal cell growth) (LSIL). Figure 2.8 showed the active progression of the virus from mild dysplasia to the on-set of cancer occurring via viral transcription.

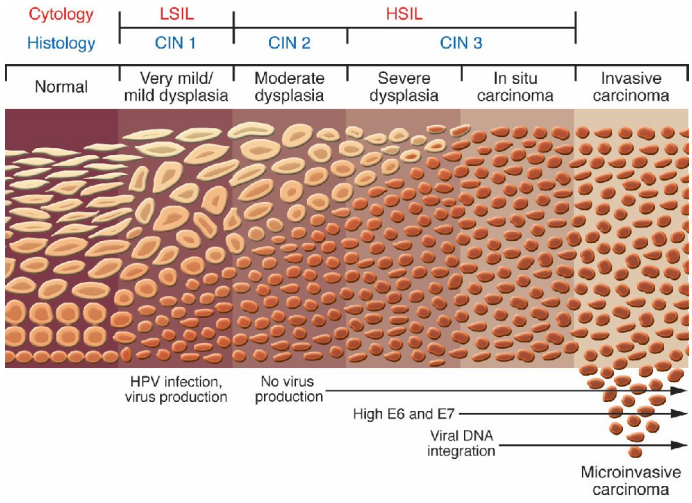

Figure 2.8: Cellular and Tissue Classification of the HPV infection. With the trans-infection of the basal layer, the virus begins to affect the cellular structure. The abnormal growth of the cells and tissue determine the severity of the infection. The most severe of the infection is the on-set of invasive carcinoma. Copyright permission has been granted by the publisher.

2.3.2 Current Treatments of HPV

Due to the nature of the papillomavirus, there are several forms of treatment for the disease based on the severity and progression of the disease. The treatments range from immediate, chemical treatment over the span of several months to radical surgeries to prevent cancerous cell growth in patients that have displayed severe dysplasia to carcinoma in situ. Most recently, a vaccine for young women that have not been exposed to the virus has been developed and marketed as a preventative measure.

2.3.2.1. Chemical Therapies

According to the Center for Disease Control and Prevention (CDC) published report, there are several chemical treatments used for less invasive HPV infection.[102] These treatments are listed as: Immune response modifiers, cytotoxins, and keratolytic agents. Immune response modifiers such as imiquimod, interferon Alfa and 5-fluorouracil are topical treatments which act to destroy the underlying tissue of warts or abnormal growths.[103] Imiquimod caused tumor necrosis factors and the secretion of interluken-1, -6 and -8 to activate an immune response. Interferon alfa suppress external anogenital warts by stimulating the immune system, impedding viral division and by fortifying the surrounding normal cells from infection. Most treatments by interferon alfa and imiquimod require several treatments until the abnormality is no longer detectable. 5-Fluorouracil acts as part of the chemotherapy protocol following vulvar and ovarian cancer. As seen in figure 2.9, 5-fluorouracil (5.136) undergoes a convertion to 5-fluoro-2-dexoyuridylate (5.137) leading to the inactivation of thymidylate synthase. 5-Flourouracil diminished the biosynthesis of pyrimidine by inhibiting thymidylate synthase, thereby inhibiting DNA synthesis for mutagenic cells.

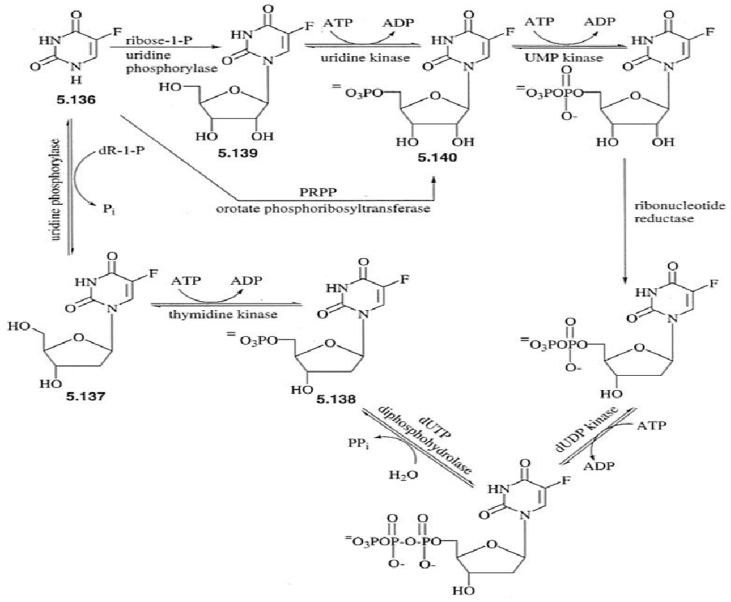

Figure 2.9: 5-Fluorouracil Mechanism to5-fluoro-2-deoxyruidylate. The mechanism displays the conversion of 5-fluorouracil to the intermediate 5-fluoro-2-deoxyuridylate. 5-Fluoro-2-deoxyuridylate is responsible for the inactivation of thymidylate synthase. Copyright permission has been granted by the publisher.

The cytotoxins are a class of drugs which act to eradicate abnormal cells. Two drugs within this category are podofilox and podophyllin. Podofilox antimitotic properties are known to stimulate necrosis of infected tissue; while podophyllin externally eliminated genital warts via arrest of cellular mitosis. Keratolytic or chemodestructive agents are used to externally eradicate genital warts via tissue necrosis.[104] The keratolytic chemcials associated with the curative procedure are salicylic acid, trichloroacetic acid (TCA) and bichloracetic acid (BCA). In all instances, the agents are topically applied and allowed to sloth away the surface layer of the treated area (cervix). Several rounds of treatment are necessary until the virus is undetectable. In the case where the infection has progressed to cervical intraepithelial neoplasia -3 (CIN-3) or severe dysplasia, chemical therapies may not completely eradicate the virus. Modern surgical treatments have become the method of recovery from the more significant forms of HPV transinfection.

2.3.2.2 Surgical Remedies

Surgical treatments of severe dysplasia to invasive carcinoma range from conization and electrosurgery to more radical extractions of the vulva and/or the reproductive organs (hysterectomy) to prevent further cellular destruction.[104] Electrosurgery consist of a loop electrosurgical excision procedure (LEEP) to cauterize and remove an abnormal area of the cervix. This technique has assisted in the removal of large external warts as well. Based on research, it has been documented that traces of HPV DNA exist in the smoke plumes released during these surgeries. Therefore, smoke inhalation must be prevented at all cost. For more progressive forms of HPV infection other procedures have been utilized.

One particular treatment occurred due to the cervical tissue becoming extremely abnormal and more invasive surgical methods must be employed. Conization, which involved the excision of the endocervical canal, offered the possibility to treat deep-rooted infection of the cervix.[105] Figure 2.10, demonstrated the conization technique employed to treat a HPV infection.

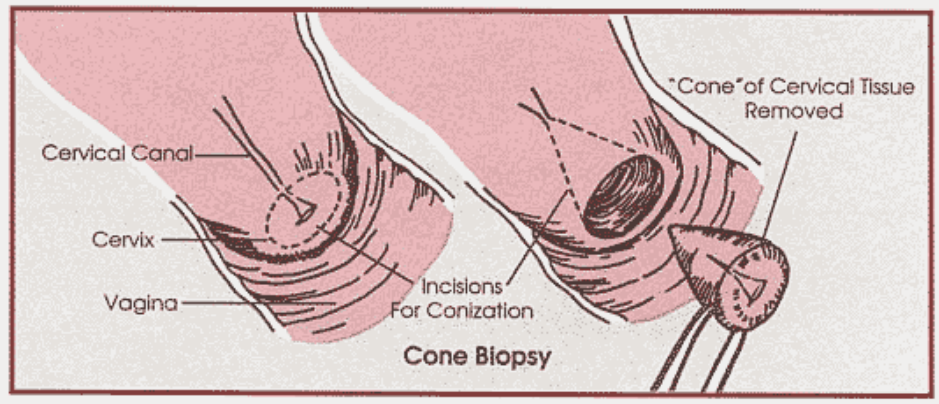

Figure 2.10: Conization procedure. The procedure removed subcutaneous, trans-infected tissue from the cervix. The tissue removed during the procedure undergoes a biopsy to determine the extent of the carcinoma. Copyright permission has been granted by the publisher.

In the case of advanced carcinoma, the only option was the removal of the tumorogenetic tissue. The suggestion of a radical vulvectomy and/or hysterectomy by physicians in the most severe

cases has been accomplished as the greatest opportunity for patient survival. These treatments, while effective, are highly disfiguring, remove chances for reproductive possibilities and reduce ones chances at normal sexual contact.

2.3.3 Outcome of Current Therapies

The current therapies for resolving infections of anogenital warts to cervical carcinoma have been very effective. However, these treatments have required numerous medical vistis and treatments over a significant period of time. In some cases, the treatment has been extremely painful, disfiguring and have reduced the quality of life for some.

2.4 Current Treatments of Atherosclerotic Plaque and HPV using Nitric Oxide

Treatments for atherosclerotic plaque have evolved over time to address not only the therapies associated with the disease, but the complications that arise from trauma associated with those corrective procedures.

2.4.1 Nitric Oxide Treatment of Atherosclerotic Plaque

Balloon angioplasty had been the corrective action for atherosclerotic plaque. However, the modification did not last long, due to re-narrowing and reoccurring blockage of the artery. As an improvement to the side effect of the balloon angioplasty, the stent was incorporated in the surgery to prevent re-narrowing of the artery. The improvement of the stent was immediately observed, but improvements to the stent were needed once more to retard a side effect of the angioplasty: restenosis. There have been several improvements to the stent: 1. coating the stent with heparin to retard coagulation, 2. use of a complex of heparin and nitric oxide to more effectively prevent coagulation as well as heal initima trauma associated with the insertion of the stent and 3.

2.4.2. Nitric Oxide Treatment of low-risk HPV Plantar Warts

The most common treatment for plantar warts has been the topical therapy employing imiquimod 5% and salicylic acid.[107] However, the solitarytreatment for low-risk plantar warts utilizing nitric oxide has been the electrospun nano-fibers of linear poly(ethylenimine) diazeniumdiolates. The electrospun fibers form a patch, which when activate releases a controlled quantity of nitric oxide.[106] The use of the patch over several weeks has proven highly effective in completely healing the plantar wart.

2.5 Organization of this Dissertation

The remainder of this dissertation is organized as follows: Chapter III describes the use and some limitations of the nitric oxide analyzer in the analysis of lipophilic diazeniumdiolates. In Chapter III, there is the discussion of an alternative process for the analysis of insoluble and polymeric, lipophilic diazeniumdiolates. Also, there is a discussion of polymeric diazeniumdiolates in the treatment of atherosclerotic plaque. The application of these diazeniumdiolates on high-risk, cervical cancer cells is evaluated in Chapter VI. Chapter V is a summary of the results of this dissertation.

CHAPTER III

COMPARISON AND QUANTITATIVE USES OF REAGENT IN NITRIC OXIDE RELEASE PROFILE GENERATION FOR INSOLUBLE DIAZENIUMDIOLATES

Experimental nitric oxide release profiles of diazeniumdiolates are essential in designing biomaterials with long, constant releasing capabilities. These profiles reveal the importance of the diazeniumdiolate's inherit molecular structure and opportunities to either enhance or retard nitric oxide release by the scaffolding of these materials[24]. Accordingly these biomaterials must reflect the natural synthesis of NO compounds and their biodegradation. Diazeniumdiolates biomaterials must have the fundamental backbone structure, secondary amine, to fully show evidence of its wound healing potential[25]. In the process of synthesizing these materials, it was determined that both soluble and insoluble materials were created. These compounds possess a property that is exhibited with most organic compounds, as the molecular weight of the material grows, the physical property changes[26], namely dispersion forces and dipole-dipole interactions. This occurs in three ways: 1. change in physical state from a liquid to solid materials, 2. change in the solubility of these bio-materials in the digesting media, which should reflect an in-vitro or in-vivo environment and 3. the increase and/or decrease in the amount of nitric oxide generated in the release profile[27]. The investigation of a more efficient and practical application of the reagent to analyze all diazeniumdiolates is beneficial to analyze insoluble, lipophilic diazeniumdiolates and reduces the need for continuous hands-on data generation in order to determine the nitric oxide profile using the current instrumentation. The nitric oxide analyzer has proven to yield inaccurate data when compared to other quantitative techniques for the analysis of soluble, lipophilic diazeniumdiolates. The reagent creates a chemical azo compound which, when

scanned at a certain wavelength over a period of time and using a first order analysis of the data, generates experimental values to comparable the nitric oxide analyzer, but with less manipulation of the instrumentation. In this chapter, a brief introduction of the experimental synthesis as well as observations (clear to orange color vs plateau of analysis) used to detail the analysis of both polymeric and insoluble, lipophilic diazeniumdiolates will be discussed by comparison of differing analytical techniques. The third section discusses the analysis of polymeric diazeniumdiolates via multiple analytical techniques in order to best describe possible cross-linking patterns and its utility and differing applications for its use (spun fiber vs hydrogels vs direct in-vitro application). Finally, a discussion of the results obtained from both the Reagent analysis and the nitric oxide analyzer and the impact both techniques offers are documented in section 2.4 as well as derivatives of the polymeric diazeniumdiolates.

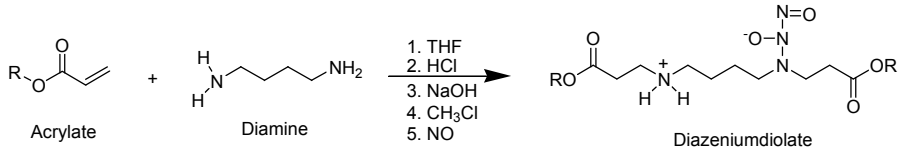

[14]

Equation 14 represents the reaction of a secondary amine with an acrylate to yield the diazeniumdiolate compound via multiple in-situ reactionary sets. The intermediate of this reaction is a sodium salt that can be isolated upon addition of concentrated hydrochloric acid. The free-base material is liberated by the addition of the base, sodium hydroxide (1M), to remove the chloride ion. This step allows for the intermediate to undergo modification by nitric oxide gas at 75psi in a high-pressure glass reaction charger.

3.1 Experimental Observations

The experimental observations between the Nitric Oxide Analyzer and the Reagent are discussed in the following sections.

3.1.1 An Experimental Observation of the Nitric Oxide Analyzer in Determining a Nitric Oxide Profile

Zweier and Samouilov[26] used the Nitric Oxide Analyzer (NOA) to analyze nitrosothiols (thionitrites) as found in biological samples. According to Ewing and Janero[27], these thionitrites represent "…naturally occurring nitric oxide surrogates" acting as intermediates in their transformation to nitric oxide during biological metabolism. Analysis of these compounds using the nitric oxide analyzer acid reflux chamber to digest the material and release nitric oxide is a method available to quantitatively analyze nitric oxide at a level of 16.3-3500 pmol. In other cases, the sample is placed in a chamber with potassium phosphate buffered saline and allowed to react. The release profile is generated over a period of time as the buffered solution begins to interact with the diazeniumdiolate. In either case, the nitric oxide sample is collected for a period of time. The vessel is then evacuated with a non-reactive gas, such as helium, which carries the sample through the NOA. At the same time that the sample is being carried to the reaction cell of the NOA, oxygen is purged into the system where is converted to ozone via an ozone generator. Once this conversion occurs, the ozone is carried to the reaction cell where it reacts with the nitric oxide as seen below in equations 15.

$$\cdot NO + O_3 \longrightarrow \cdot NO_2^* + O_2 \qquad [15]$$

$$\cdot NO_2^* \longrightarrow h\nu + \cdot NO_2 \qquad [16]$$

From the reaction in equation 16, the excited nitrite intermediate is generated. The excited nitrite is analyzed via the photomultiplier tube (PMT) and detected via the amplifier to yield quantitative data of nitric oxide production via soluble, lipophilic diazeniumdiolates as seen in Fig 3.1.[52] As the samples increased in molecular weight and exhibited greater insolubility to the phosphate buffered saline (PBS) solution, it became increasingly difficult to utilize the nitric oxide analyzer.

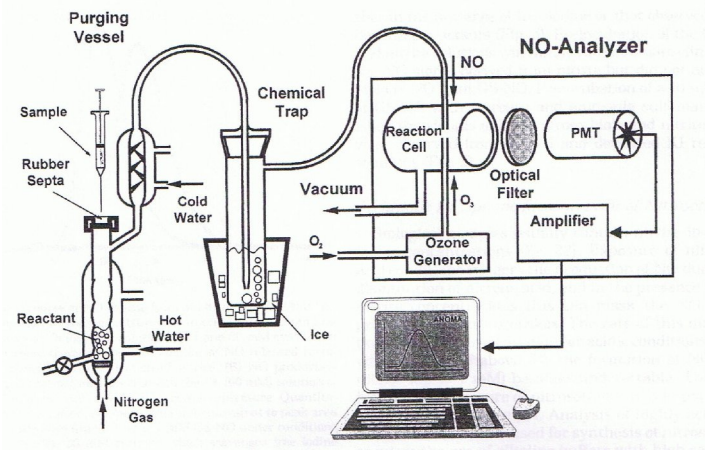

Figure 3.1 Schematic of Nitric Oxide Analyzer: Nitric Oxide analyzer setup for the analysis of diazeniumdiolate includes the reaction cell, photomultiplier tube, ozone generator, glass purging vessel and chemical trap. Copyright permission has been granted by the publisher.

In Fig. 3.2 and 3.3, multiple lipophilic diazeniumdiolates of lower molecular weight have been analyzed by the nitric oxide analyzer to generate a nitric oxide profile.

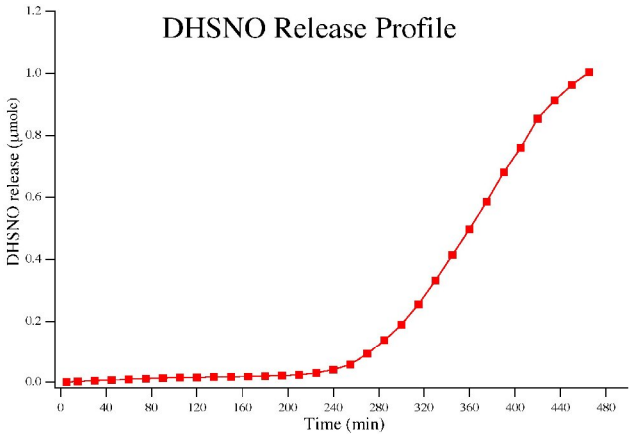

Figure 3.2: NO profile of Dihexyl Spermeate Diazeniumdiolate yielded by NO Analyzer. Sample shows a delay of four hours prior to initial release of NO. The sample yielded a total release of 8nmole of nitric oxide.

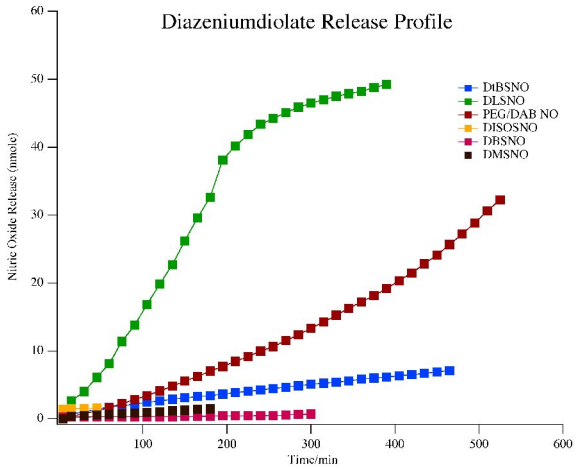

Figure 3.3 NO Profile of insoluble, lipophilic diazeniumdiolates by nitric oxide analyzer. The samples yielded values of 1-50 nmole. Samples were integrated using the NO_2 signal of the NOA.

Figure 3.4 exhibited the portion of figure 3.3 that yielded values below 1 nmole. Due to these lower values, it was determined that the materials did not successfully yield adequate levels of nitric oxide levels.

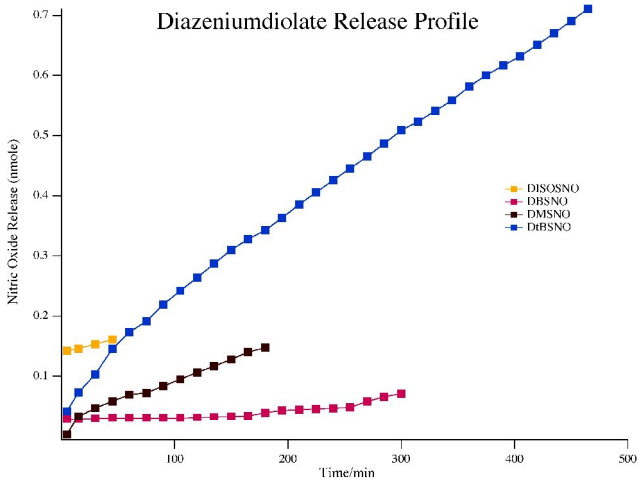

Figure 3.4 In-depth view of insoluble, lipophilic diazeniumdiolates with low release profiles via NO Analyzer. The samples yielded values less than 1nmole. Samples data were integrations of NO_2 signal of over time.

The raw data of these diazeniumdiolate compounds, located in Appendix K, showed that the total release profile was less than 1 nmole as seen in Table 3.1.

Table 3.1. Total NO Release Analysis for Nitric Oxide Analyzer

Diazeniumdiolate	**Total Nitric Oxide Release (nmol)**
DHSNO	8.01
DtBSNO	13.0
DLSNO	83.9
PEG/DAB NO	45.8
DISOSNO	0.60
DBSNO	0.80
DMSNO	1.10

3.1.1.1 Manipulation of Reagents

The preparation of the diazeniumdiolates, as stated previously, requires the synthesis of the intermediate, followed by the conversion of the intermediate to the free-base molecule, which is then converted to the modified, nitric oxide producing compound. The synthesis of the intermediate is a 1 to 2 ratio utilizing one mole equivalent of the diamine monomer to two mole equivalents of the diacrylate monomer. During this preparation, the solvent is determined by the low molecular weight diacrylate. Hence, methanol was used as the solvent for methyl diacrylate and ethanol for ethyl diacrylate. However, for monomeric diacrylates with higher molecular weights, distilled tetrahydrofuran (THF) was used as the solvent.

3.1.1.2 Experimental Procedure

Discussion of the preparation, processing and characterization of the synthesized compounds have been included for structural determination.

3.1.1.2.1 Michael's Addition of 1,4-diaminobutane and methyl acrylate

The initial reaction was carried out in a flamed-dried, nitrogen flushed 1000-mL round-bottom flask containing 17.0 g (0.200 mol) of 1,4-diaminobutane with 150-mL of methanol. The methyl acrylate monomer, 34.7 g (36.3 mL, 0.40 mol) was added to a pressure-equalizing addition funnel containing 250-ml of methanol. The methyl acrylate monomer was then added drop-wise to the round-bottom. The reaction was left to stir for 24 hours. Afterwards, the reaction flask was removed from the stir plate and submerged in ice. Next, an equimolar volume of concentrated hydrochloric acid (50-mL) was added to the reaction flask and left in refrigerated conditions for a minimum of 24 hours. The intermediate, 1, 4-diaminobutane-N, N'-bis-3-propanoate dimethyl ester dihydrochloride, is neutralized with equimolar volume of 1M NaOH. The solution was next heated to completely dissolve the hydrochloride salt. The solution was allowed to cool before extracting the dimethylspermeate, with diethyl ether (3-25ml) in a 250-ml separatory funnel. The pH was confirmed at pH=9 or greater. The dimethylspermeate was dried over sodium sulfate. Once the dimethylspermeate was liberated, the material was dissolved in acetonitrile (100ml) and loaded with nitric oxide at 75 psi in the nitric oxide reactor. The solvent was roto-evaporated to recover the dimethylspermeate diazeniumdiolate. The final product was confirmed by NMR, FT-IR and ESI-MS. ^{1}H DMS $CDCl_3$ (δ): -NH-CH_2-CH_2-CH_2-CH_2-NH- 1.10 (t), -NH-CH_2-CH_2-CH_2-CH_2-NH- 1.41 (s), -CH_2-C(O)-O- 2.33 (t), C(O)O-CH_3 2.56 (s), -O(O)C-CH_2-CH_2-NH- 2.72 (t), and –NH-CH_2-CH_2-CH_2-CH_2-NH- 3.96 (dd). ^{13}C DMS $CDCl_3$ (δ): 172, 60, 48, 44, 34 and 14 ppm. FT-IR (cm^{-1}) 1180 C-O (s), 1730 C=O (s), 2790-3706 CH_2 (s) and 3340 H-N (w). ESI-MS (m/z) $[M+H]^+$ 261.1.

3.1.1.2.2 Michael's Addition of Ethylenediamine and Methyl Acrylate

The synthesis was carried out as described in section 2.1.1.2.1 utilizing ethylenediamine (11.1 mL, 0.17 mol) in methanol (100 mL) and methyl acrylate (29.7 mL, 0.33 mol) in methanol (150 mL) to produce the intermediate ethyldiamine-N, N'-bis-3-propanoate dimethyl ester dihydrochloride with the addition of equimolar quantities concentration hydrochloric acid. The liberation of dimethyl ethylenediamine was attempted with the addition of equimolar volumes of 1M NaOH as described in section 2.1.1.1., but was unstable and unable to isolate from the aqueous phase.

3.1.1.2.3 Michael's Addition of 1, 4-Diaminobutane and Ethyl Acrylate

The synthesis was carried out as described in section 2.1.1.2.1 utilizing 1, 4-diaminobutane (15.3 mL, 0.15 mol) in ethanol (100 mL) and ethyl acrylate (30.0 g, 0.30 mol) in ethanol (150 mL) to produce the intermediate 1, 4-diaminobutane-N, N'-bis-3-propanoate diethyl ester dihydrochloride with the addition of equimolar quantity (50-mL) of concentrated hydrochloric acid. Diethyl spermeate was liberated from the hydrochloride salt with the addition of equimolar volumes of 1M NaOH as described in section 2.1.1.2.1. Diethyl spermeate was dissolved in 100 mL of acetonitrile and modified with nitric oxide gas by the same procedure as described in section 2.1.1.2.1 to yield diethyl spermeate diazeniumdiolate. The final product was confirmed by NMR, FT-IR and ESI-MS. ^{1}H DES $CDCl_3$ (δ): -C(O)O-CH_2-CH_3 0.80 (t), -NH-CH_2-CH_2-CH_2-CH_2-NH- 1.05 (t, b), -NH-CH_2-CH_2-CH_2-CH_2-NH- 1.35 (b), -CH_2-C(O)-O- 2.04 (t), -NH-CH_2-CH_2-CH_2-CH_2-NH- 2.16 (t, b), -O(O)C-CH_2-CH_2-NH- 2.41 (t), and –C(O)O-CH_2-CH_3- 3.68 (q). ^{13}C DES $CDCl_3$ (δ): 171, 59, 48, 44, 34, 27 and 13 ppm. FT-IR (cm^{-1}) 1180 C-O (s), 1730 C=O (s), 2790-3710 CH_2 (s) and 3340 H-N (w). ESI-MS (m/z) $[M+H]^+$ 289.0.

3.1.1.2.4 Michael's Addition of Ethylenediamine and Ethyl Acrylate

The synthesis was carried out as described in section 2.1.1.2.1 utilizing ethylenediamine (9g, 1 mol) in ethanol (150 mL) and ethyl acrylate (30g, 2 moles) in ethanol (300 mL) to produce ethylenediamine-N, N'-bis-3-propanoate diethyl ester dihydroxychloride with the addition of equimolar volumes (50mL) of concentrated hydrochloric acid. Diethyl ethylenediamine was liberated from the hydrochloride salt with the addition of equimolar volumes of 1M NaOH as described in section 2.1.1.2.1. Diethyl ethylenediamine was dissolved in 100 mL of acetonitrile and modified with nitric oxide gas by the same procedure as described in section 2.1.1.2.1 to yield diethyl ethylenediamine diazeniumdiolate. The final product was confirmed by NMR, FT-IR and ESI-MS. ^{1}H DEEDA $CDCl_3$ (δ): CH_3-CH_2-O(O)C- 0.93 (t), -NH-CH_2.CH_2-NH- 1.67 (s), -O-(O)C-CH_2-CH_2-NH- 2.22 (t), --NH-CH_2-CH_2-NH- 2.44 (s), -O(O)C-CH_2-CH_2-NH- 2.60 (t), and CH_3-CH_2-O(O)C- 3.87 (q). ^{13}C DEEDA $CDCl_3$ (δ): 172, 59, 48, 44, 34 and 13 ppm. FT-IR (cm^{-1}) 1261 C-O (s), 1733 C=O (s), 2451-2948 CH_2 (s). ESI-MS (m/z) $[M+H]^+$ 261.2.

3.1.1.2.5 Michael's Addition of 1, 4-Diaminobutane and Butyl Acrylate

The synthesis was carried out as described in section 2.1.1.2.1 utilizing 1, 4-diaminobutane (15.1 mL, 0.15 mol) in butanol (100 mL) and butyl acrylate (43.0 mL, 0.30 mol) in butanol (150 mL) to produce the intermediate 1, 4-diaminobutane-N, N'-bis-3-propanoate dibutyl ester dihydrochloride with the addition of equimolar quantity (50-mL) of concentrated hydrochloric acid. Dibutyl spermeate was liberated from the hydrochloride salt with the addition of equimolar volumes of 1M NaOH as described in section 2.1.1.2.1. Dibutyl spermeate was dissolved in 100 mL of acetonitrile and modified with nitric oxide gas by the same procedure as described in section 2.1.1.2.1 to yield dibutyl spermeate diazeniumdiolate. The final product was confirmed by NMR, FT-IR and ESI-MS. ^{1}H DBS $CDCl_3$ (δ): C(O)O-CH_2-CH_2-CH_2-CH_3 0.79(t), C(O)O-CH_2-CH_2-CH_2-CH_3 1.23 (m),-NH-CH_2.CH_2-CH_2-CH_2-NH- 1.38 (t, b), C(O)O-CH_2-CH_2-CH_2-

CH_3 1.45 (m), -CH2-C(O)-O- 2.35 (t), -NH-CH_2-CH_2-CH_2-CH_2-NH- 2.47 (t, b), O(O)C-CH_2-CH_2-NH 2.72 (t), and -O(O)C-CH_2-CH_2- 3.93 (t). ^{13}C DBS $CDCl_3$ (δ): 171, 64, 49, 45, 34, 30, 27, 19 and 13 ppm. FT-IR (cm^{-1}) 1180 C-O (s), 1730 C=O (s), 2790-2990 CH_2 (s) and 3340 H-N (w). ESI-MS (m/z) $[M+H]^+$ 345.0.

3.1.1.2.6 Michael's Addition of Ethylenediamine and Butyl Acrylate

The synthesis was carried out as described in section 2.1.1.2.1 utilizing ethylenediamine (8.9 mL, 0.17 mol) in n-butanol (100 mL) and butyl acrylate (42.6 mL, 0.33 mol) in n-butanol (150 mL) to produce ethylenediamine-N, N'-bis-3-propanoate di-butyl ester dihydroxychloride with the addition of equimolar volumes (50mL) of concentrated hydrochloric acid. Di-butyl ethylenediamine was liberated from the hydrochloride salt with the addition of equimolar volumes of 1M NaOH as described in section 2.1.1.2.1. Di-butyl ethylenediamine was dissolved in 100 mL of acetonitrile and modified with nitric oxide gas by the same procedure as described in section 2.1.1.2.1 to yield di-butyl ethylenediamine diazeniumdiolate. The final product was confirmed by NMR, FT-IR and ESI-MS. ^{1}H DBEDA $CDCl_3$ (δ): CH_3-CH_2-CH_2-CH_2-O(O)C- 0.75 (t), CH_3-CH_2-CH_2-CH_2-O(O)C- 1.21 (m), CH_3-CH_2-CH_2-CH_2-O(O)C- 1.42 (m), -O-(O)C-CH_2-CH_2-NH- 2.31 (t), --NH-CH_2-CH_2-NH- 2.53 (s), -O(O)C-CH_2-CH_2-NH- 2.70 (t), and -CH_2-O(O)C- 3.90 (t). ^{13}C DBEDA $CDCl_3$ (δ): 172, 64, 48, 44, 34, 30, 18 and 13 ppm. FT-IR (cm^{-1}) 1195 C-O (s), 1735 C=O (s), 2448-2957 CH_2 (b) and 3340 H-N (w). ESI-MS (m/z) $[M+H]^+$ 317.0.

3.1.1.2.7 Michael's Addition of 1, 4-Diaminobutane and Hexyl Acrylate

The synthesis was carried out as described in section 2.1.1.2.1 utilizing 1, 4-diaminobutane (15.1 mL g, 0.15 mol) in tetrahydrofuran (100 mL) and hexyl acrylate (52.8 mL, 0.30 mol) in tetrahydrofuran (150 mL) to produce the intermediate 1, 4-diaminobutane-N, N'-bis-3-propanoate dihexyl ester dihydrochloride with the addition of equimolar quantity (50-mL) of concentrated

hydrochloric acid. Dihexyl spermeate was liberated from the hydrochloride salt with the addition of equimolar volumes of 1M NaOH as described in section 2.1.1.2.1. Dihexyl spermeate was dissolved in 100 mL of acetonitrile and modified with nitric oxide gas by the same procedure as described in section 2.1.1.2.1 to yield dihexyl spermeate diazeniumdiolate. The final product was confirmed by NMR, FT-IR and ESI-MS. ^{1}H DHS $CDCl_3$ (δ): -CH3 0.77 (t), -CH_2-CH_2-CH_2-CH_3 1.19 (m), -CO(O)-CH_2-CH_2- 1.41 (t), -NH-CH_2-CH_2-CH_2-CH_2-NH- 1.48 (t), -CH_2-C(O)-O- 2.40 (t), -NH-CH_2-CH_2-CH_2-CH_2-NH- 2.48 (t, b), -O(O)C-CH_2-CH-$_2$-NH- 2.75 (t), and C(O)O-CH_2-CH_2 3.95 (t). ^{13}C DHS $CDCl_3$ (δ): 172, 64, 49, 44, 34, 31, 28, 27, 25, 22 and 13 ppm. FT-IR (cm^{-1}) 1180 C-O (s), 1730 C=O (s) and 2800-2990 CH_2 (s). ESI-MS (m/z) $[M+H]^+$ 401.2.

3.1.1.2.8 Michael's Addition of Ethylenediamine and Hexyl Acrylate

The synthesis was carried out as described in section 2.1.1.2.1 utilizing ethylenediamine (8.9 mL, 0.15 mol) in tetrahydrofuran (100 mL) and hexyl acrylate (52.8 mL, 0.30 mol) in tetrahydrofuran (150 mL) to produce ethylenediamine-N, N'-bis-3-propanoate dihexyl ester dihydroxychloride with the addition of equimolar volumes (50mL) of concentrated hydrochloric acid. Dihexyl ethylenediamine was liberated from the hydrochloride salt with the addition of equimolar volumes of 1M NaOH as described in section 2.1.1.2.1. Dihexyl ethylenediamine was dissolved in 100 mL of acetonitrile and modified with nitric oxide gas by the same procedure as described in section 2.1.1.2.1 to yield dihexyl ethylenediamine diazeniumdiolate. The final product was confirmed by NMR, FT-IR and ESI-MS. ^{1}H DHEDA $CDCl_3$ (δ): CH_3-CH_2-CH_2-CH_2-CH_2-CH_2-O(O)C- 0.80 (t), CH_3-CH_2-CH_2-CH_2-CH_2-CH_2-O(O)C- 1.21 (m), -CH_2-CH_2-O(O)C- 1.44 (m), -(O)C-CH_2-CH_2-NH- 3.48 (m), --NH-CH_2-CH_2-NH- 3.67 (s) and -CH_2-O(O)C- 3.98 (t). ^{13}C DHEDA $CDCl_3$ (δ): 173, 62, 44, 43, 32, 31, 30, 25, 22 and 14 ppm. FT-IR (cm^{-1}) 1060 C-O (s), 1736 C=O (s), 2451-2948 CH_2 (s) and 3345 H-N (w). ESI-MS (m/z) $[M+H]^+$ 373.1.

3.1.1.2.9 Michael's Addition of 1, 4-Diaminobutane and Lauryl Acrylate

The synthesis was carried out as described in section 2.1.1.2.1 utilizing 1, 4-diaminobutane (15.1 mLg, 0.15 mol) in tetrahdyrofuran (100 mL) and lauryl acrylate (81.6 mL, 0.30 mol) in tetrahydrofuran (150 mL) to produce the intermediate 1, 4-diaminobutane-N, N'-bis-3-propanoate dilauryl ester dihydrochloride with the addition of equimolar quantity (50-mL) of concentrated hydrochloric acid. Dilauryl spermeate was liberated from the hydrochloride salt with the addition of equimolar volumes of 1M NaOH as described in section 2.1.1.2.1. Dilauryl spermeate was dissolved in 100 mL of chloroform and modified with nitric oxide gas by the same procedure as described in section 2.1.1.2.1 to yield dilauryl spermeate diazeniumdiolate. The final product was confirmed by NMR, FT-IR and ESI-MS. ^{1}H DLS D_2O (δ): -CH_3 0.847 (t), -$(CH_2)_9$-CH_3 1.26 (m), -NH-CH_2-CH_2-CH_2-CH_2-NH- 1.65 (b), -NH-CH_2-CH_2-CH_2-CH_2-NH- 1.41 (s), C(O)O-CH_2-CH_2 1.74 (b), -CH_2-C(O)O- 2.82 (t), and –NH-CH_2-CH_2-CH_2-CH_2-NH- 3.02 (b), -O(O)C-CH_2-CH_2-NH- 3.35 (b), and C(O)O-CH_2-CH_2 4.15 (t). FT-IR (cm^{-1}) 1203 C-O (s), 1731 C=O (s), 2454-2951 CH_2 (s) and 3396 H-N (w). ESI-MS (m/z) $[M+H]^+$ 569.6.

3.1.1.2.10 Michael's Addition of Ethylenediamine and Lauryl Acrylate

The synthesis was carried out as described in section 2.1.1.2.1 utilizing ethylenediamine (8.9 mL, 0.15 mol) in tetrahydrofuran (100 mL) and lauryl acrylate (81.6 mL, 0.30 mol) in tetrahydrofuran (150 mL) to produce ethylenediamine-N, N'-bis-3-propanoate dilauryl ester dihydroxychloride with the addition of equimolar volumes (50mL) of concentrated hydrochloric acid. Dilauryl ethylenediamine was liberated from the hydrochloride salt with the addition of equimolar volumes of 1M NaOH as described in section 2.1.1.2.1. Dilauryl ethylenediamine was dissolved in 100 mL of acetonitrile and modified with nitric oxide gas by the same procedure as described in section 2.1.1.2.1 to yield dilauryl ethylenediamine diazeniumdiolate. The final product was confirmed by NMR, FT-IR and ESI-MS. ^{1}H DLEDA D_2O (δ): CH_3-$(CH_2)_{11}$-O(O)C- 0.83 (t), CH_3-$(CH_2)_9$-CH_2-CH_2-O(O)C- 1.21 (m), -CH_2-CH_2-O(O)C- 1.50 (m, w), -O-(O)C-CH_2-CH_2-NH-

2.45 (t), --NH-CH_2-CH_2-NH- 2.68 (s), -O(O)C-CH_2-CH_{-2}-NH- 2.78 (t), and -CH_2-O(O)C- 3.53 (t). ^{13}C DLEDA D_2O (δ): 173, 64, 48, 45, 34, 32, 29, 25, 22 and 14 ppm. FT-IR (cm^{-1}) 1190 C-O (s), 1740 C=O (s), 2860-2930 CH_2 (s) and 3380 H-N (w). ESI-MS (m/z) $[M+H]^+$ 541.5.

3.1.1.2.11 Michael's Addition of 1, 4-Diaminobutane and Isobornyl Acrylate

The synthesis was carried out as described in section 2.1.1.2.1 utilizing 1, 4-diaminobutane (15.1 mL, 0.15 mol) in tetrahydrofuran (100 mL) and isobornyl acrylate (63.4 g, 0.30 mol) in tetrahydrofuran (150 mL) to produce the intermediate 1, 4-diaminobutane-N, N'-bis-3-propanoate diisobornyl ester dihydrochloride with the addition of equimolar quantity (50-mL) of concentrated hydrochloric acid. Diisbornyl spermeate was liberated from the hydrochloride salt with the addition of equimolar volumes of 1M NaOH as described in section 2.1.1.2.1. Diisobornyl spermeate was dissolved in 100 mL of chloroform and modified with nitric oxide gas by the same procedure as described in section 2.1.1.2.1 to yield diisbornyl spermeate diazeniumdiolate. The final product was confirmed by NMR and ESI-MS. ^{1}H DIBORNS $CDCl_3$ (δ): -$(CH_3)_2$ (bicyclo) 0.74 (s), -CH_3 (bicyclo) 0.87 (s), -CH/CH_2 (bicyclo) 1.62 (m), -CH-C(O)O- 4.58 (m), -O(O)C-CH_2-CH_{-2}-NH- 2.75 (t), and –NH-CH_2-CH_2-CH_2-CH_2-NH- 2.49 (b). ^{13}C DIBORNS $CDCl_3$ (δ): 171, 80, 49, 48, 46, 44, 38, 34, 33. 26, 19 and 11 ppm. ESI-MS (m/z) $[M+H]^+$ 505.5.

3.1.1.2.12 Michael's Addition of Ethylenendiamine and Isobornyl Acrylate

The synthesis was carried out as described in section 2.1.1.2.1 utilizing ethylenediamine (8.9 mL, 0.175 mol) in tetrahydrofuran (100 mL) and isobornyl acrylate (63.4 mL, 0.30 mol) in tetrahydrofuran (150 mL) to produce ethylenediamine-N, N'-bis-3-propanoate diisobornyl ester dihydroxychloride with the addition of equimolar volumes (50mL) of concentrated hydrochloric acid. Diisobornyl ethylenediamine was liberated from the hydrochloride salt with the addition of equimolar volumes of 1M NaOH as described in section 2.1.1.2.1. Diisobornyl ethylenediamine

was dissolved in 100 mL of acetonitrile and modified with nitric oxide gas by the same procedure as described in section 2.1.1.2.1 to yield diisobornyl ethylenediamine diazeniumdiolate. The final product was confirmed by NMR, FT-IR and ESI-MS. ^{1}H DIBORNEDA $CDCl_3$ (δ): CH_3-(bicyclo) 0.80, 0.90 (s), CH/CH2 (bicyclo) 1.68 (m), -NH-CH_2-CH_2-NH- 2.65 (s), -O(O)C-CH_2-CH_2-NH- 2.43 (t) and –NH-CH_2-CH_2-O(O)C- 2.80 (t). ^{13}C DIBORNEDA $CDCl_3$ (δ): 172, 80, 48, 46, 44, 38, 35, 33, 26, 19 and 11 ppm. FT-IR (cm^{-1}) 1180 C-O (s), 1730 C=O (s), 2840-3010 CH_2 (s) and 3360 H-N (w). ESI-MS (m/z) $[M+H]^+$ 261.2.

3.1.1.2.13 Michael's Addition of 1, 4-Diaminobutane and Isobutyl Acrylate

The synthesis was carried out as described in section 2.1.1.2.1 utilizing 1, 4-diaminobutane (15.1 mL, 0.15 mol) in tetrahydrofuran (100 mL) and isobutyl acrylate (43.3 mL, 0.30 mol) in tetrahydrofuran (150 mL) to produce the intermediate 1, 4-diaminobutane-N, N'-bis-3-propanoate diisobutyl ester dihydrochloride with the addition of equimolar quantity (50-mL) of concentrated hydrochloric acid. Diisobutyl spermeate was liberated from the hydrochloride salt with the addition of equimolar volumes of 1M NaOH as described in section 2.1.1.2.1. Diisobutyl spermeate was dissolved in 100 mL of acetonitrile and modified with nitric oxide gas by the same procedure as described in section 2.1.1.2.1 to yield diisobutyl spermeate diazeniumdiolate. The final product was confirmed by NMR, FT-IR and ESI-MS. ^{1}H DISOS $CDCl_3$ (δ): $(CH_3)_2$-HC-CH_2-O(O)C- 0.70 (d), -NH-CH_2-CH_2-CH_2-CH_2-NH- 1.32 (b), -NH-CH_2-CH_2-CH_2-CH_2-NH- 1.27 (m), $(CH_3)_2$-CH-CH_2-O(O)C- 1.68 (m), -O(O)C-CH_2-CH-$_2$-NH- 2.27 (t), and –NH-CH_2-CH_2-CH_2-CH_2-NH- 2.38 (b). ^{13}C DISOS $CDCl_3$ (δ): 172, 70, 49, 44, 34, 27 and 18 ppm. FT-IR (cm^{-1}) 1187 C-O (s), 1735 C=O (s), 2440-2959 CH_2 (s) and 3456 H-N (w). ESI-MS (m/z) $[M+H]^+$ 345.2.

3.1.1.2.14 Michael's Addition of Ethylenediamine and Isobutyl Acrylate

The synthesis was carried out as described in section 2.1.1.2.1 utilizing ethylenediamine (8.9 mL, 0.15 mol) in tetrahydrofuran (100 mL) and isobutyl acrylate (43.3 mL, 0.30 mol) in tetrahydrofuran (150 mL) to produce ethylenediamine-N, N'-bis-3-propanoate diisobutyl ester dihydroxychloride with the addition of equimolar volumes (50mL) of concentrated hydrochloric acid. Diisobutyl ethylenediamine was liberated from the hydrochloride salt with the addition of equimolar volumes of 1M NaOH as described in section 2.1.1.2.1. Diisobutyl ethylenediamine was dissolved in 100 mL of acetonitrile and modified with nitric oxide gas by the same procedure as described in section 2.1.1.2.1 to yield diisobutyl ethylenediamine diazeniumdiolate. The final product was confirmed by NMR, FT-IR and ESI-MS. ^{1}H DISOEDA $CDCl_3$ (δ): $(CH_3)_2$-CH-CH_2-O(O)C- 0.94 (d), -NH-CH_2-CH_2-NH- 3.42 (s), -CO(O)-CH_2-CH-$(CH_3)_2$- 1.90 (m), -NH-CH_2-CH_2-CO(O)- 2.47 (t), -O(O)C-CH_2-CH_2-NH- 2.76 (t), and -CH_2-O(O)C- 3.85 (d). ^{13}C DISOEDA $CDCl_3$ (δ): 174, 70, 49, 45, 32, 27 and 19 ppm. FT-IR (cm^{-1}) 1180 C-O (s), 1730 C=O (s) and 2830-3010 CH_2 (s). ESI-MS (m/z) $[M+H]^+$ 317.2.

3.1.1.2.15 Michael's Addition of 1, 4-Diaminobutane and t-butyl Acrylate

The synthesis was carried out as described in section 2.1.1.2.1 utilizing 1, 4-diaminobutane (15.1 mL, 0.15 mol) in t-butanol (100 mL) and t-butyl acrylate (43.5 mL, 0.30 mol) in t-butanol (150 mL) to produce the intermediate 1, 4-diaminobutane-N, N'-bis-3-propanoate di-t-butyl ester dihydrochloride with the addition of equimolar quantity (50-mL) of concentrated hydrochloric acid. Di-t-butyl spermeate was liberated from the hydrochloride salt with the addition of equimolar volumes of 1M NaOH as described in section 2.1.1.2.1. Di-t-butyl spermeate was dissolved in 100 mL of acetonitrile and modified with nitric oxide gas by the same procedure as described in section 2.1.1.2.1 to yield di-t-butyl spermeate diazeniumdiolate. The final product was confirmed by NMR, FT-IR and ESI-MS. ^{1}H DTBUS $CDCl_3$ (δ): -NH-CH_2-CH_2-CH_2-CH_2-NH- 1.21 (b),(CH3)3-C-O(O)C 1.13(s), -O(O)C-CH2-CH2-NH- 2.51 (t), -O(O)C-CH_2-CH_2-

NH- 2.08 (t), and –NH-CH_2-CH_2-CH_2-CH_2-NH- 2.32 (b). ^{13}C DTBUS $CDCl_3$ (δ): 173, 79, 49, 44, 35 and 27 ppm. FT-IR (cm^{-1}) 1160 C-O (s), 1730 C=O (s), 2792-2975 CH_2 (s) and 3330 H-N (w). ESI-MS (m/z) $[M+H]^+$ 345.3.

3.1.1.2.16 Michael's Addition of Ethylenediamine and t-butyl Acrylate

The synthesis was carried out as described in section 2.1.1.2.1 utilizing ethylenediamine (8.9 mL, 0.15 mol) in t-butanol (100 mL) and butyl acrylate (43.5 mL, 0.30 mol) in t-butanol (150 mL) to produce ethylenediamine-N, N'-bis-3-propanoate di-t-butyl ester dihydroxychloride with the addition of equimolar volumes (50mL) of concentrated hydrochloric acid. Di-t-butyl ethylenediamine was liberated from the hydrochloride salt with the addition of equimolar volumes of 1M NaOH as described in section 2.1.1.2.1. Di-t-butyl ethylenediamine was dissolved in 100 mL of acetonitrile and modified with nitric oxide gas by the same procedure as described in section 2.1.1.2.1 to yield di-t-butyl ethylenediamine diazeniumdiolate. The final product was confirmed by NMR, FT-IR and ESI-MS. ^1H DTBUEDA $CDCl_3$ (δ): $(CH_3)_3$-C-O(O)C- 1.45 (s), -O(O)C-CH_2-CH_2-NH- 2.83 (t), --NH-CH_2-CH_2-NH- 3.53 (s) and -O(O)C-CH_2-CH_2-NH- 3.38 (t). ^{13}C DTBUEDA $CDCl_3$ (δ): 172.8, 80.2, 48.7, 44.8, 35.5 and 27.7 ppm. FT-IR (cm^{-1}) 1151 C-O (s), 1727 C=O (s) and 2676-2980 CH_2 (b). ESI-MS (m/z) $[M+H]^+$ 317.0.

3.1.1.2.17 Michael's Addition of 1, 4-Diaminobutane and 2-Hydroxyethyl Acrylate

The synthesis was carried out as described in section 2.1.1.2.1 utilizing 1, 4-diaminobutane (15.1 mL, 0.15 mol) in tetrahydrofuran (100 mL) and 2-hydroxyethyl acrylate (35.9 g, 0.30 mol) in tetrahydrofuran (150 mL) to produce the free base dihydroxyethyl spermeate without the addition of equimolar quantity (50-mL) of concentrated hydrochloric acid. Diethyl spermeate was dissolved in 100 mL of acetonitrile and modified with nitric oxide gas by the same procedure as described in section 2.1.1.2.1 to yield diethyl spermeate diazeniumdiolate. The final product was confirmed by NMR, FT-IR and ESI-MS. ^1H DHES D_2O (δ): -NH-CH_2-CH_2-CH_2-CH_2-NH- 1.52

(b), -NH-CH_2-CH_2-CH_2-CH_2-NH- 2.62 (b), -O(O)C-CH2-CH2-NH- 2.96 (t), HO(CH2)2-C-O(O)C- 3.47 (s), HO-CH2-CH2-CO(O)C- 3.66 (b) and HO-CH2-CH2-C-O(O)C- 4.08 (b). ^{13}C DHES D_2O (δ): 173, 66, 62, 46, 44, 33 and 23 ppm. FT-IR (cm^{-1}) 1186 C-O (s), 1725 C=O (s), 2859-2929 CH_2 (b) and 3259 H-N (w). ESI-MS (m/z) $[M+H]^+$ 321.1.

3.1.1.2.18 Michael's Addition of Ethylenediamine and 2-Hydroxyethyl Acrylate

The synthesis was carried out as described in section 2.1.1.2.1 utilizing ethylenediamine (33.4 mL, 0.17 mol) in n-butanol (100 mL) and 2-hydroxyethyl acrylate (34.5 mL, 0.33 mol) in tetrahydrofuran (150 mL) to produce ethylenediamine-N, N'-bis-3-propanoate di-butyl ester dihydroxychloride with the addition of equimolar volumes (50mL) of concentrated hydrochloric acid. Di-butyl ethylenediamine was liberated from the hydrochloride salt with the addition of equimolar volumes of 1M NaOH as described in section 2.1.1.2.1. Di-butyl ethylenediamine was dissolved in 100 mL of acetonitrile and modified with nitric oxide gas by the same procedure as described in section 2.1.1.2.1 to yield di-butyl ethylenediamine diazeniumdiolate. The final product was confirmed by NMR, FT-IR and ESI-MS. ^1H DHEDA $CDCl_3$ (δ): CH_3-$(CH_2)_5$-O(O)C- 0.80 (t), CH3- CH2-CH2-CH2-(CH2)2-O(O)C- 1.21 (m), -CH_2-CH_2-O(O)C- 1.44 (m), -NH-CH_2-CH_2-NH- 3.67 (s), and -CH_2-O(O)C- 3.98 (t). ^{13}C DHEDA $CDCl_3$ (δ): 173, 62, 44, 43, 32, 31, 30, 25, 22 and 14 ppm. FT-IR (cm^{-1}) 1060 C-O (s), 1733 C=O (s), 2860-2970 CH_2 (s) and 3345 H-N (w). ESI-MS (m/z) $[M+H]^+$ 373.1.

3.1.1.2.19 Michael's Addition of Diaminobutane and Polyethylene (700) Glycol Diacrylate

The synthesis was carried out as described in section 2.1.1.2.1 utilizing 1, 4-diaminobutane (3.8 mL, 0.038 mol) in tetrahydrofuran (100 mL) and polyethylene glycol (700) diacrylate (23.4 g, 0.038 mol) in tetrahydrofuran (150 mL) to produce the intermediate 1, 4-diaminobutane-N, N'-bis-3-propanoate di-polyethylene oxide ester dihydrochloride with the addition of equimolar quantity (50-mL) of concentrated hydrochloric acid. The material did not immediately create the

hydrochloride salt. The viscous material was roto-evaporated to remove any excess solvent. Then, placed in the freezer for several months at which time, the excess solvent was removed as it was observed. As this process continued, the material began to solidify and form a gel. Without using any solvent, di-polyethylene glycol spermeate was modified with nitric oxide gas by the same procedure as described in section 2.1.1.2.1 to yield di-polyethylene glycol spermeate diazeniumdiolate. The final product was confirmed by NMR, FT-IR and ESI-MS

3.1.1.2.20 Michael's Addition of Ethylenediamine and Polyethylene (700) Glycol Diacrylate The synthesis was carried out as described in section 2.1.1.2.1 utilizing ethylenediamine (2.23 mL, 0.038 mol) in tetrahydrofuran (100 mL) and polyethylene glycol (700) diacrylate (23.4mL, 0.038 mol) in tetrahydrofuran (150 mL) to produce ethylenediamine-N, N'-bis-3-propanoate di-polyethylene glycol ester dihydroxychloride with the addition of equimolar volumes (50mL) of concentrated hydrochloric acid. Di-polyethylene glycol ethylenediamine was not converted to the free base by the addition of equimolar volumes of 1M NaOH as described in section 2.1.1.2.1., but instead was dissolved in 100 mL of chloroform and modified with nitric oxide gas by the same procedure as described in section 2.1.1.2.1 to yield di-polyethylene glycol ethylenediamine diazeniumdiolate. The final product was confirmed by NMR, FT-IR and ESI-MS.

3.1.2 Materials

All materials have been purchased via University of Akron funding. Instrumental analysis was completed at the University of Akron.

3.1.2.1 Solvents

Anhydrous Ethyl Ether, Fisher Scientific
Tetrahydrofuran, Fisher Scientific
Chloroform, Fisher Scientific
Acetonitrile, Fisher Scientific
Methanol, Fisher Scientific
n-Butanol, Fisher Scientific
t-Butanol, Fisher Scientific
Sodium Sulfate, Aldrich Chemical Company
Sodium Hydroxide, Fisher Scientific
Hydrochloric Acid, Fisher Scientific

3.1.2.2 Gases

Prepurified Nitrogen, National Welders Supply Company
Prepurified Nitric Oxide, National Welders Supply Company
Prepurified Oxygen, National Welders Supply Company
Prepurified Helium, National Welders Supply Company

3.1.2.3 Reagent

Ethylenediamine, Aldrich Chemical Company
Methyl Acrylate, Alrdrich Chemical Company
Ethyl Acrylate, Aldrich Chemical Company
Butyl Acrylate, Aldrich Chemical Company
Hexyl Acrylate, Aldrich Chemical Company
Hydroxyethyl Acrylate, Aldrich Chemical Company
Lauryl Acrylate, Aldrich Chemical Company
Isobornyl Acrylate, Aldrich Chemical Company
Isobutyl Acrylate, Aldrich Chemical Company
t-Butyl Acrylate, Aldrich Chemical Company
Polyethylene (700) Glycol Acrylate, Aldrich Chemical Company
1,4-Diaminobutane, Aldrich Chemical Company

3.1.2.4 Instrumentation

Sievers 280i, Nitric Oxide Analyzer
NOA Firmware Version 3.00

3.1.3 An Experimental Observation of the Reagent in Determining a Nitric Oxide Profile

Although, the NO Analyzer has been utilized to determine the nitric oxide profile of many diazeniumdiolates, it does have some limitations. The diazeniumdiolates made by Michael's addition reaction used either 1,4-diaminobutane (putrescine) or ethylenediamine with the desired acrylate. After a multi-step synthesis, the resulting diazeniumdiolate were analyzed. The problem encountered with these types of nitric oxide donors is solubility in the phosphate, buffered aqueous media. Analysis using one chemiluminiscent method (Nitric Oxide Analyzer) does not give an accurate detection of the total amount of NO in these compounds; additionally a more quantitative analytical method is required for analyzing these materials.

For spectrophotometric determination, the reagent is a cost efficient means to determine total nitric oxide release. In the case of this study, the reagent is a potassium phosphate buffered, neutral, sulfanilic acid and N-(1-naphthyl)ethylenediamine dihydrochloride chemiluminescence reagent. The reagent has been used to determine nitric oxide, nitrite and nitrate concentrations as evident in multiple studies and published articles[29, 66, 67]. According to Ridnour et al [28], the chemiluminescence or spectrophotometric determination of nitric oxide occurs at a wavelength of 496nm with a sensitivity of 1μM as represented by Fig. 3.5. As the azo

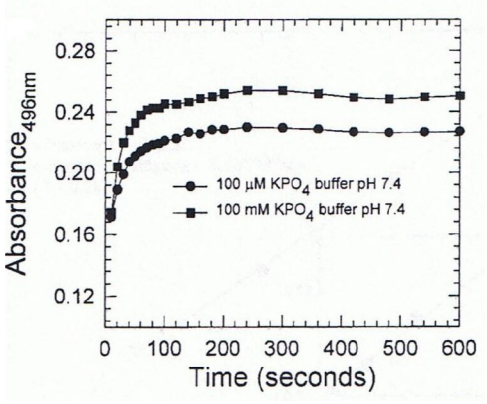

Figure 3.5 Nitric Oxide Profile utilizing Griess Reagent. The release pattern of nitric oxide presented based on data from both 100uM and 100mM KPO_4 solutions at the current physiological conditions. Based on the literature, research data was gathered using the 100mM concentration. Copyright permission has been granted by the publisher.

complex is formed, which is the "…nitric oxide-mediated nitrosative modification of sulfanilic dihydrochloride", an orange color intensifies until all nitric oxide is complexed. In order to determine nitric oxide concentration, a standard curve was calculated using Beer's Law to determine the extinction coefficient as seen in Figure 3.6.

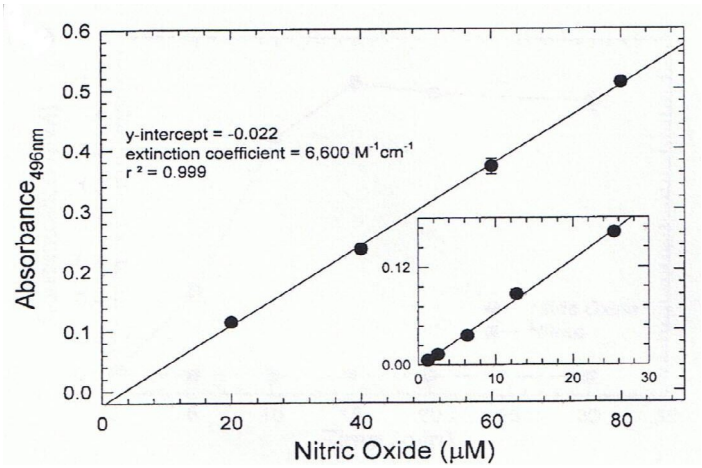

Figure 3.6 Standard Curve of the DEA NO. Using the standard DEA NO at differing conditions, the standard curve was determined from the nitric oxide profiles. Based on the linear regression value, the extinction coefficient value was determined. The lower sensitivity of the Greiss reagent is shown by the inset. Copyright permission has been given by the publisher.

In the case of this experiment, the nitric oxide analyzer's firmware was not used to determine the levels of nitric oxide, but instead a UV/Vis spectrometer measured the absorbance of the solution as the azo complex was formed. The instrument was set at a fixed wavelength of 496nm, the time was set at the maximum of 999min or 16.65 hours and the temperature was standard at 32C. Nims, et al[29], utilized the Griess reagent to determine nitric oxide in physiological solutions, such as phosphate saline buffer. Accordingly, it was determined that the concentration of 17mM sulfanilic acid (SA) and 0.4mM N-(1-naphthyl)ethylenediamine (NEDD) in 100mM phosphate buffer pH to 7.4, was optimal for determination of nitric oxide in release profiles. During Nims, et al experiments, it was resolved that an excess of NEDD act as a

scavenger of nitric oxide and lowered the chances of the azo complex from forming. Figure 3.7 shows the chemical complexation of nitric oxide with the Griess reagent to form the azo compound. Figure 3.8 shows the actual colorimetric change experienced during the experiment.

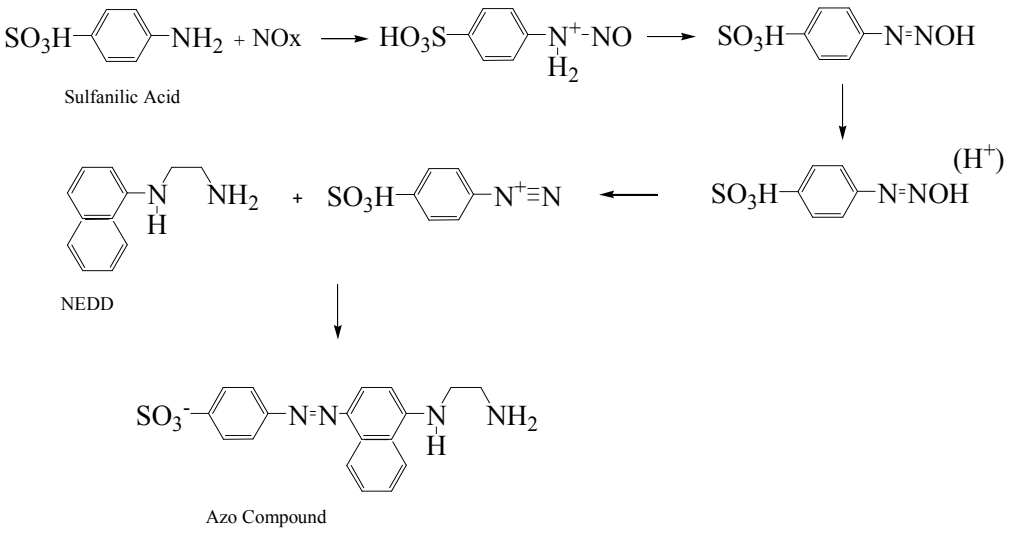

Figure 3.7 Reaction of sulfanilic acid and N-(1-naphthyl)ethylenediamine dihydrochloride. This figure was recreated from Ref .5. pg. 11364. The sulfanilic acid complexes with the nitric oxide, then chemically bonds with NEDD forming the azo compound. The azo compound exhibits the orange color as the azo compound forms.

A

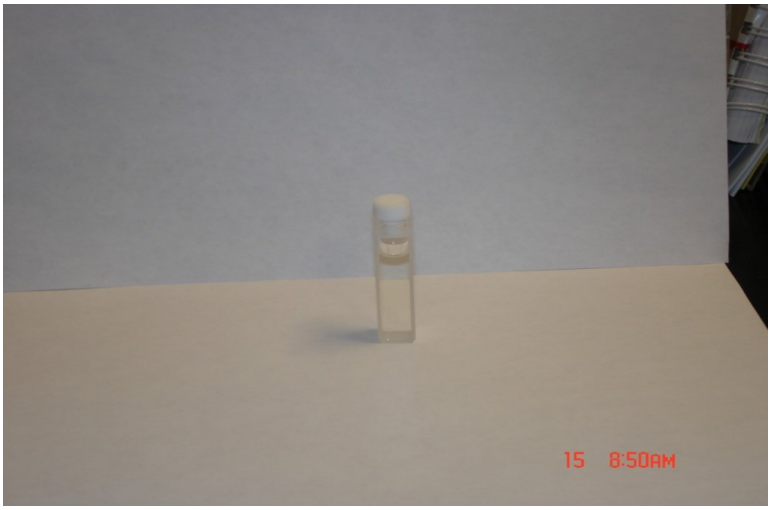

B

Figure 3.8 Reagent reactive states. **A**. Solution of unreacted reagent prior to introduction of diazeniumdiolate material. **B**. Azo complex formed by reaction of reagent and NO producing materials. Note: The UV/Vis cells are capped since NO gas may evolve in the system and should not be released or allowed to escape.

According to figures 3.9 and 3.10, the UV/Vis raw data was gathered and used to calculate the amount of nitric oxide yielded over a predetermined period of time. Finally, the total release of the sample was determined based upon compounded values for the total analysis run time. Nims et al[29, 31] determined that the spectrophotometric analysis and quantitation of nitric oxide exhibited a visual indication of the presence of nitric oxide in the Griess reagent.

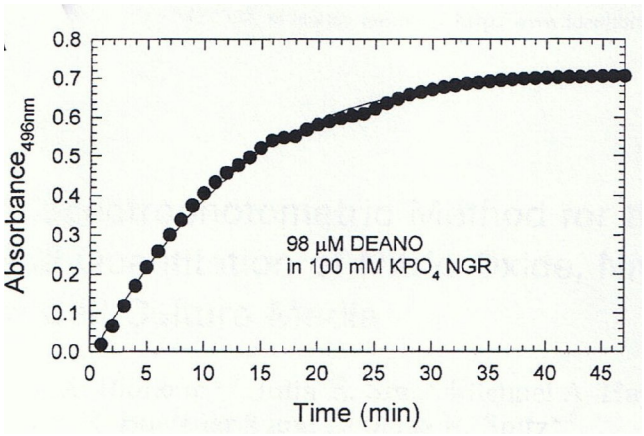

Figure 3.9 Nitric Oxide Release profile of DEA NO. The standard diethylamino nonoate was analyzed in 100mM KPO4 neutral, Greiss reagent at a concentration of 98uM. The sample was one of five concentrations analyzed using the Greiss reagent. Copyright permission has been given by the publisher.

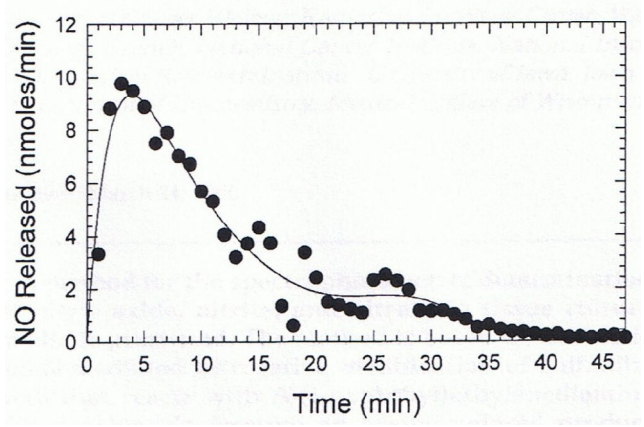

Figure 3.10 Conversion of the DEA NO profile. The standard diethylamino nonoate profile was interpreted to determine the amount of NO released versus time. Accordingly, the profile shows a first order reaction. The release profile confirmed that the Greiss reagent is an effective method for the quantitation of nitric oxide. Copyright permission has been given by the publisher.

Because of the limit of detection (3nmole), this methodology has proven to be the most effective in the determination of nitric oxide, nitrite and nitrate ions which evolve from diazeniumdiolate compounds (NONOates). The maximum extinction coefficient (ε_{max}) calculations can be

determined via the standard curve. According to equation 17, the maximum nitric oxide concentration of the stock solution (98μM) at 496nm utilizing a change in absorbance of 0.24. The volume of the Griess reagent (V_{GR}) and the volume of the stock diazeniumdiolate solution (V_{NO}) are utilized as well.

$$C_{NO} = \Delta A_{496} * V_{GR}/(\varepsilon_{max} * V_{NO}) \quad [17]$$

$$\varepsilon_{max} = (\Delta A_{496} * V_{GR})/(C_{NO} * V_{NO}) \quad [18]$$

Based on the information of the diethylamine nonoate standard curve, the theoretical extinction coefficient (according to equation 18) was noted as ε_{max} of 6600 M^{-1} cm^{-1} utilizing 100mM potassium phosphate buffered solution at a pH of 7.4 for the previous research completed by Ridnour, et al.

3.2 Potentially Reactive Pathway of Nitric Oxide using Nitric Oxide Analyzer

In this section, a connection is suggested between the reactive channel of the nitric oxide analyzer and ozone evolved in the system. As discussed by Samouilov and Zweier[26], the chemiluminescence measurements are gathered utilizing the nitric oxide analyzer as the reaction solution evolves nitric oxide. The carrier gas, helium, moves the nitric oxide released from this reaction solution containing the synthesized diazeniumdiolate to the reaction cell filled with ozone. The excited nitrite was read by the PMT and raw data carried to the amplifier according to the Chemiluminescent Gas Analyzer patent[30]. According to Wink et al[31], there are the possibilities of intermediates created during the reaction of the ozone with nitric oxide. However extensive studies have shown that these intermediates (N_xO_y, ONO_2^-, NO^+), when reacted with iron (III) hexacyanate ($Fe(CN_6)^{-3}$), nitrosonium tetrafluoroborate (BF_4 NO), and 2,2'-azinobis(3-ethylbenzthiazoline-6-sulfonic acid) (ABTS), respectively, do not yield the complexed-intermediate of nitric oxide and oxygen complexation.

3.3 Determination of Polymeric Cross-linking Based on NMR Data

In determining the chemical structures of two cross-linked polymers, multiple instruments and characterization techniques must be employed. Some of the physical properties of these polymers have subjugated a number of avenues for characterization, while others have initiated novel approaches to structural determination. One such application is the identification of the polymer's structure using N^{15} nuclear magnetic resonance (NMR).

During the synthesis of the molecule, a viscous material was formed. Analytical techniques such as roto-evaporation, separatory extraction, etc, were attempted to recover the solvent without the introduction of increased temperature, which leads to deterioration of the molecule, or loss of product. These techniques proved unsuccessful. Therefore, the mixture was removed from the reaction flask and placed in an amber wide mouth jar in refrigerated conditions. As the sample began to solidify during the cooling process, the solvent was removed via pipette. Once the solid was completely formed, it would not hold any solvent.

Due to the low resonance of ^{15}N and the wide range in chemical shift that will needed to be determined in order to isolate a spectrum, the single ^{15}N NMR has proven to be an unsuccessful manner to determine the structure of the diamino polymers and its cross-linking morphology.

The initial review of NMR spectrum for polyethylene glycol diacrylate showed that the acrylate moiety exhibited peaks at 5.8, 6.0 and 6.2 ppm, while the PEG exhibited peaks at 3.5, 3.6 and 4.2 ppm[68]. This spectrum, as seen in figure 3.11, was pertinent to determining the final cross-linked structure of both the polyethylene glycol diaminobutane and polyethylene glycol ethylenediamine polymers. The NMR analyses for the determination of connectivity included heteronuclear single quantum correlation (HSQC), which represented

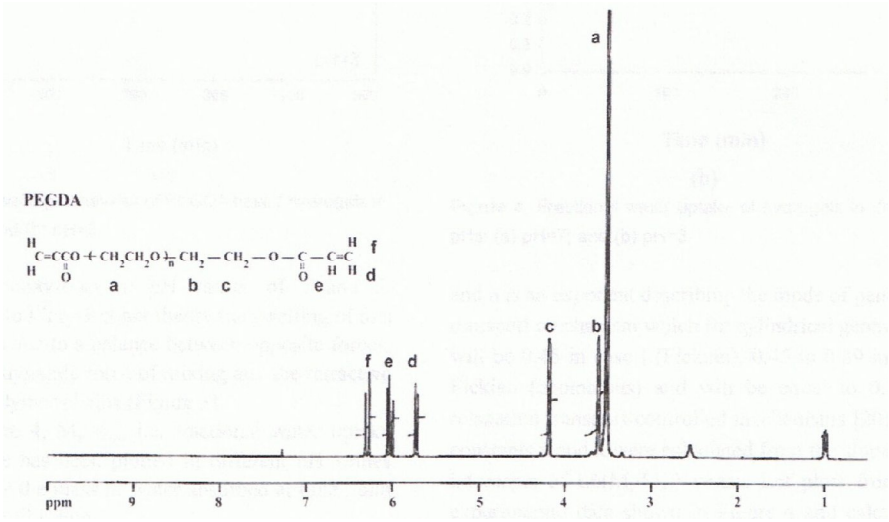

Figure 3.11 NMR Spectrum of polyethylene diacrylate. The structure is broken into two portions: the first was the acrylate moiety in the upfield range at ~6.0 ppm, and the second portion, polyethylene glycol, was represented at ~3.5 and 4.2ppm. Copyright permission has been given by the publisher.

the proton-proton chemical shift of directly connected carbon bonds[69]. The heteronuclear multiple bond correlation (HMBC) NMR analysis determined multi-bond connectivity, over a three bonds distance from one proton to carbon bond[70, 71]. Finally, heteronuclear 2-bond correlation (H2BC) examined the two-bond correlation between carbon-hydrogen bonds and nitrogen-hydrogen bonds[72]. However, as these techniques were applied they did not render significant spectra for the resolution of the final product. Therefore, an ECOSY NMR which determined atom to atom connectivity was employed for characterization of the polymers.

3.3.1 Dynamic Reaction Yielding Amide Cross-linking

It has been determined that increasing the molecular weight of diazeniumdiolates increases the nitric oxide release profile. Reynolds, et al[32] have noted these enhancements have, in some cases, increased the insolubility of the diazeniumdiolate moiety as well. However, Zhou, Annich, Wu and Meyerhoff[33], have documented that the use of poly(ethyleneimine) will create a

water-soluble nitric oxide releasing materials. These water-soluble compounds, once activated, have the potential to release nitric oxide for extended period of time versus the short burst of nitric oxide that many of the well known diazeniumdiolates (DETANO and DEA NO) are known to give. As documented, the total release profile increases from 2.71 μmol/mg to 4.15 μmol/mg as the molecule's functional groups are altered. The molecules ability to incorporate more nitric oxide moieties is encouraged with this structural change. The addition of a polymer to the backbone of the diazeniumdiolate to increase the release profile has been utilized by Smith, et al[34, 35] to expedite wound healing. In these experiments, the types of diazeniumdiolates compared were from the short-burst NONOates to a less soluble polymeric diazeniumdiolate which utilizing topical applications for point of entry. These entities were selected due to the fact that no "…prolonged hypotensive effects" were noted by patients during their use. It was noted that during the experiment, the use of the short-burst diazeniumdiolates had a marked effects on the systolic blood pressure while the polymeric diazeniumdiolate had the same initial effect as the short-burst NONOate, but corrected the decrease in systolic blood pressure within minutes versus numerous hours. The synthesis of a PEG diacrylate NONOate polymer for extension of the current nitric oxide profiles was studied to determine the feasibility of a spun biomaterial versus in-vivo hydrogel application.

It was determined that by increasing the amount of poly(ethylene glycol) (PEG) within a polymer (i.e. an engineered surface), non-specific proteins adsorption is retarded due to its steric stabilization effect by energetic and entropic properties.[36,41] PEG offers biological advantages such as protein-resistivity to prevent restenosis during the introduction of in vivo applications (i.e. tissue engineering, stent introduction, etc) due to lack of changes in the surface of the equipment (stent) during the initial introduction.[37] Secondly, within aqueous surroundings, PEG acts as a spacer to increase cell adhesion which in turn enhances receptor-ligand interactions and increased the hydrophilicity.[38] Also, its conformity to biological environments (inert biological

applications) due to low free energy with aqueous surroundings makes it an ideal polymer for hydrogels.[39, 40] The polyethylene glycol spermeate diazeniumdiolate and polyethylene glycol ethylenediamine diazeniumdiolate both exhibited hydrophilicity in the determination of its solubility. As seen in Tables 3.2 and 3.3, water, sodium hydroxide and sodium methoxide were more effective solvents versus the organic solvents. However, the organic solvents are utilized to modify samples to diazeniumdiolates thus preventing the reduction of nitric oxide in the presence of water as previously stated in chapter 1 (equation 4).

Table 3.2 Solubility data for poly(ethylene glycol) ethylenediamine diazeniumdiolate

Solvent	Solubility
Hexane	Materials turns white on the outside
Chloroform	Material swells
Acetone	Material swells
Diethyl Ether	Material turns white on the outside
Tetrahydrofuran	Material Swells
Water	Dissolved
Sodium Hydroxide	Dissolved
Sodium Methoxide	Dissolved

Table 3.3 Solubility data for poly(ethylene glycol) spermeate diazeniumdiolate

Solvent	Solubility
Hexane	Materials turns white on the outside
Chloroform	Material swells
Acetone	Material swells
Diethyl Ether	Material turns white on the outside
Tetrahydrofuran	Insoluble
Water	Dissolved
Sodium Hydroxide	Dissolved
Sodium Methoxide	Dissolved

In order to determine whether both diazeniumdiolate materials were capable of undergoing the electrospinning process, the materials were dissolved. Utilizing a grounded plate for electrospinning, at a height of 40 centimeters, the materials in Table 3.4 were prepared to determine the optimal conditions for electrospun poly(ethylene glycol) spermeate

diazeniumdiolate polymer. At concentrations of 6% w/w and 12% w/w in chloroform, the modified samples were unable to be electrospun utilizing various spinning cone tips.

Table 3.4 Optimized conditions for electrospun biomaterials utilizing poly(ethylene glycol) ethylenediamine diazeniumdiolate and poly(ethylene glycol) spermeate polymer

Solvent	Modified Material	Percent Concentration (w/w)	Outcome
Tetrahydrofuran	unmodified material	6	Thin, gritty suspension
Chloroform	unmodified material	12	Swollen gel
Tetrahydrofuran	modified material	6	Soluble, can not spin
Chloroform	modified material	12	Soluble, can not spin
Tetrahydrofuran	unmodified material	20	Suspension
Chloroform	unmodified material	20	---
Tetrahydrofuran	modified material	20	---
Chloroform	modified material	20	Soluble, but thin solution

The polymers low viscosity at 6% w/w and 12% w/w was such that the solution's instability prevented the formation of electrospun materials. Modified and unmodified samples were prepared at 20% w/w. At this concentration, the materials formed gels-like particles when placed in a pipette for electro-spinning.

Because of the 12% and 20% polymer solution's inability to electrospin a uniform biomaterial, each of the materials were placed on a glass slide to determine its coating ability. The 12% modified material was plated and gave a grainy consistency, while the 20% modified solution yielded a smooth coating on the glass slide. Each material was air dried and felt tacky to the touch. The goal of this exercise was to determine the materials' possibility as a coating for stents and biomedical devices. Also, an assessment of the release profiles from the reagent determined that the nitric oxide yields were sufficient for both materials to be effective as vasodilators. Thus these materials were possible drugs in the treatment of restenosis which occurs from the initial implantation of a medical device for treatment of arterial plaque. As seen

in Figures 3.12 and 3.13, soluble polymeric diazeniumdiolates are not only effective in releasing nitric oxide from the surface of inert polymers but are more effective if a

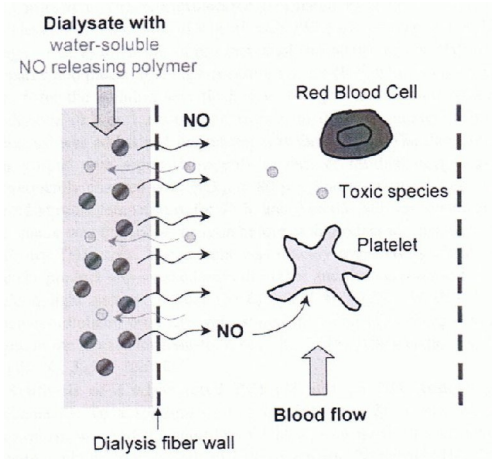

Figure 3.12 Diagram of coated dialysis fibers. As noted, nitric oxide is released through the fiber wall, into the blood flow and retards platelet aggregation via a water-soluble polymer. Copyright permission has been granted by the publisher.

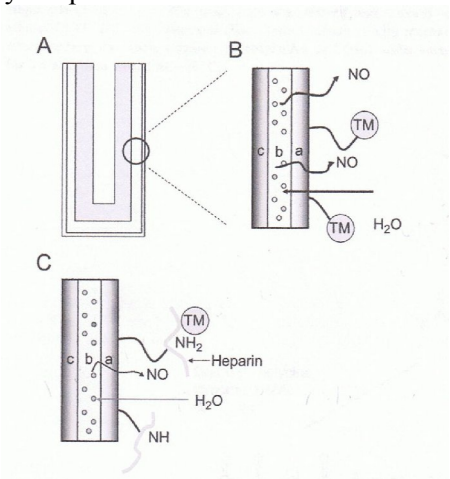

Figure 3.13 A comparison of several stent coatings. Diagram (A) represents a silicone-rubber sleeve for biomedical devices, versus (B) which uses several layers with the diazeniumdiolate encased in the center with thrombomodulin (TM) on the surface to repel platelet aggregation. (C) represents the multilayer material with the diazeniumdiolate encased in the center with both heparin and TM bound to the surface. Copyright permission has been granted by the publisher.

compounded layer has been added to prevent the initial burst of nitric oxide. Instead, the coatings acts as a permeable barrier and by utilizing other medicinal products can further the effectiveness of the diazeniumdiolate polymer.

3.3.2 Outcome of Polymeric Cross-linking

It has been determined that mass spectral analysis afforded the best determination of the polymers end groups and possible structure. The observation of mass spectrometry for the soluble, lipophilic polymeric diazeniumdiolates suggest that there are multiple end groups associated with the polymers. The structure of both compounds will be determined utilizing MS for determination of end groups, while NMR analysis will provide the determination of the connectivity of the compounds.

3.3.3 Determination of Polymeric Structure via Gel Permeation Chromatography

In order to determine the weight distribution of macromolecules, the most widely use technique is Gel Permeation Chromatography (GPC)[48, 49, 50]. For the determination of macromolecule (i.e. proteins, polyurethanes, biodegradable polymer, petroleum materials and etc.) weight distribution, the polymers typically are dissolved in tetrahydrofuran for analysis. Due to the lack of solubility of the polymeric diazeniumdiolate, polyethylene glycol spermeate NONOate and the polyethylene glycol ethylenediamino-NONOate in tetrahydrofuran, GPC analysis was not an available technique.

3.4 Discussion of Results

In the following section, the results of the NOA and Reagent analysis are discussed. The subsequent sections, the results of the determination of the chemical structure of both of the soluble, polymeric diazeniumdiolate are presented and discussed.

3.4.1 The Impact of Nitric Oxide Analyzer versus Griess Reagent

According to figure 3.14, the maximum nitric oxide concentration of the stock solution (490μM) at 496nm utilizing a change in absorbance of 0.426. Based on the information of the diethylamine NONOate standard curve, the extinction coefficient (utilizing equation 18) was calculated as 7824 M^{-1} cm^{-1} versus the theoretical ε_{max} of 6600 M^{-1} cm^{-1} utilizing 100mM

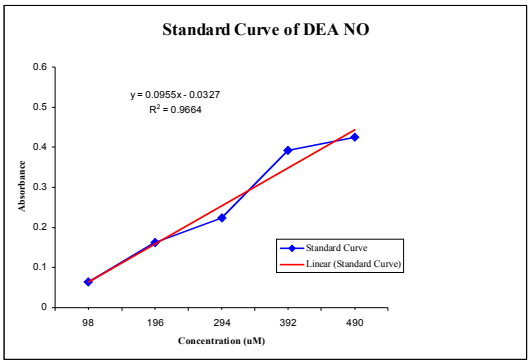

Figure 3.14 Standard Curve of Diethylamine NONOate utilizing the Reagent. This approach was done to determine the linear regression and extinction coefficient of the overall experiment at 496nm, at differing concentrations.

potassium phosphate buffered solution at a pH of 7.4. Therefore, the experimental results mirror the theoretical literature and demonstrate that the compounds of interest have been effectively modified to deliver sufficient amounts of nitric oxide.

Based on figure 3.15, the raw data is gathered via a UV/Vis detector. The interpretation of that data will determine the quantitative value of nitric oxide released by each of the lipophilic, insoluble diazeniumdiolates.

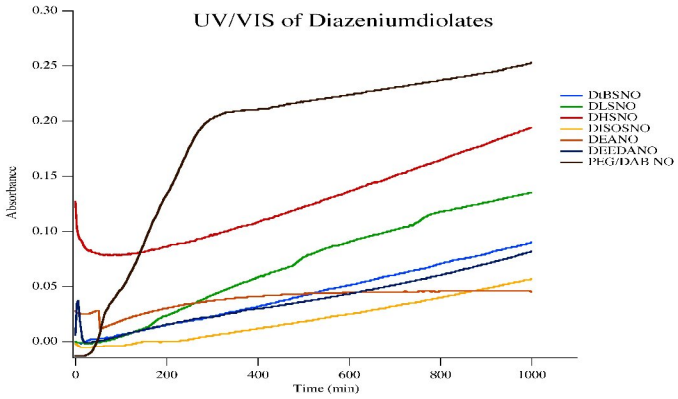

Figure 3.15 Chemiluminescence UV/VIS analyses of lipophilic, insoluble nonoates. The graph represents the raw data for the analysis of diazeniumdiolate utilizing the UV/VIS chemiluminescence, spectrophotometric analysis using reagent.

Figure 3.16 showed the quantitative nitric oxide release values over a period of time. The individual nitric oxide release values for each time point were calculated using beer's law. Figure 3.17 reflected the accumulated release of nitric oxide at each data point over a given period of

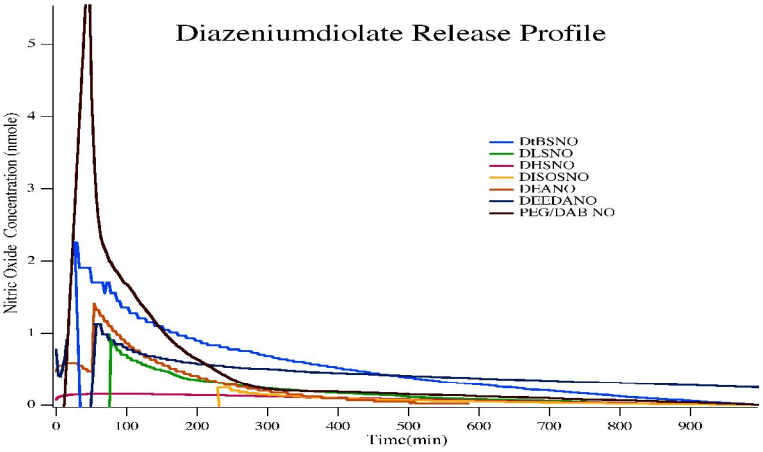

Figure 3.16 Conversion and Quantitation of raw data. The raw data for the analysis of diazeniumdiolate utilizing the UV/VIS chemiluminescence spectrophotometric method has been quantified at each time point to determine the nitric oxide yield over time.

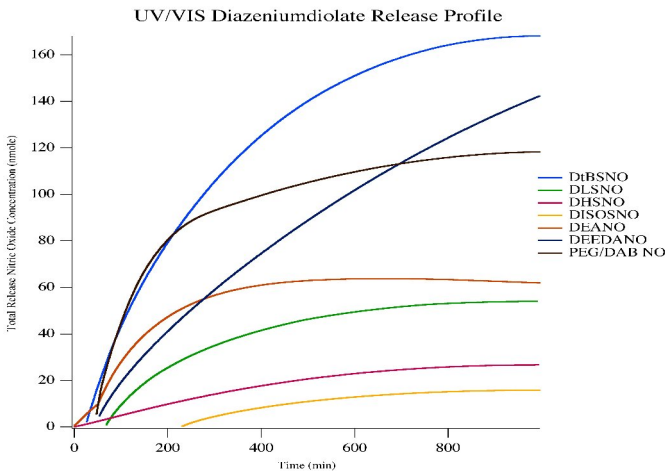

Figure 3.17 Total release nitric oxide profile using Reagent. The total release profile for diazeniumdiolates analyzed via UV/VIS spectrophotometric instrumentation. Each data point represents the sum of the nitric oxide released at that point in time. The samples include the standard of DEA NO as well as the other diazeniumdiolates.

time. The raw data, individual release rate per time point and the total nitric oxide release profile are located in Appendix K.

Based on the data retrieved from the Griess reagent analysis, the quantitative values have proven to be more concentrated than that of the nitric oxide analyzer's analysis. From that data presented in Table 3.5, the Griess reagent was 4 to 25 times more effective at collecting and quantifying nitric oxide versus the NO Analyzer for the smaller molecules.

Table 3.5 Data Acquired via Griess Reagents utilizing UV/Vis analysis

Diazeniumdiolate	Total Nitric Oxide Release (nmol/mg)
DHSNO	26.65
DtBSNO	168.13
DLSNO	53.97
PEG/DAB NO	118.22
DISOSNO	15.79
DEANO	62.01
DEEDANO	142.31

There are several reasons for this: 1. the insoluble materials are not fully digested in the phosphate buffered solution used for NOA, while the reagent slowly digested the materials, 2.

The chamber used in the NOA does not have a PTFE seal to minimize leaks, while the glass cuvette fashioned for analysis when utilizing the reagent has a stoppered seal to prevent the released nitric oxide from escaping and thereby limiting the amount of azo compound formed. Finally while both solutions (phosphate buffered solution and the reagent) allow for dissolution of samples prior to analysis, the NOA sample must be fully soluble for UV analysis in PBS. While the Griess reagent only requires minimal, surface contact with the sample to form the azo compound. This was proven by the fact that the majority of the insoluble compounds were placed on the surface of the solution, at the interface, to yield significant quantitative data.

It was noted that the reagent was prepared by either correcting the pH of the KPO_4 buffer prior to the addition of sulfanilic acid (SA) and NEDD or by correcting the pH to approximately 7.4 using sodium hydroxide (NaOH) once all ingredients (e.g. buffer, SA and NEDD) were added and dissolved. The latter solution had an extended shelf-life of three months.

3.4.2 Determination of Polymeric Diazeniumdiolate Polymer

Based on the previous Michael's addition reactions between the diamine and the numerous acrylates, the proposed repeating, linear structure of the polyethylene glycol (700) diacrylate and 1, 4- diaminobutane is shown in figure 3.18. As seen in the mass spectra of

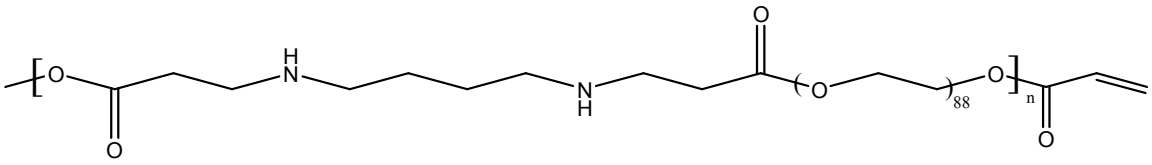

Figure 3.18 Proposed linear structure of polyethylene glycol diacrylate diaminobutane. This structure was synthesized prior to introduction of the cooling process to initiate cross-linking of the molecule. As the product started to solidify, the solvent was removed to prevent degradation due to the acidic environment.

Appendix A, the initial structure of PEG/DAB began with a larger peak around 4500 m/z, but over time the peak decreases as the polymer cross-linking grew, while the peak at 1300 m/z increased in intensity as the polymer cross-linking developed.

The proposed structure was analyzed via mass spectra to determine the end groups (e.g. acrylate, hydroxyl, etc.). Accordingly, this experiment helped to determine the possible linkages within the polymer. Therefore, the determination of the end group began initially with the hypothesis of the possible linear structure of figure 3.18, then calculated the molecular weight of that linear structure (MW=214). The end group was determined by subtraction of the molecular weight of sodium moiety (MW=22.9898) from the first peak of the subgroup. Due to the use of sodium trifluoroacetate in tetrahydrofuran as a solvent, the molecular weight of sodium was subtracted to account for the fact that the sodium salt was formed during the mass spectrometer analysis. Within appendix B, the spectra show each area in which the end group determination has been made. The first end group started at 393.2632 mass to charge (m/z) ratio. The second end group started at 1213.9455 m/z and represented the larger peaks. The third end group started at 1277.9889 m/z, while the fourth end group started at 1267.9574 m/z. Finally, the fifth end group started at 1736.6757 m/z, while the sixth end group started at 1878.8785 m/z.

Based on the calculations, the first end group was determined as the completely hydrolyzed PEG material, H-$(OCH_2CH_2)_{88}O^-$ Na^+ salt, as created by the sodium trifluoroacetate solvent. End group 3 was determined as the partially hydrolyzed polymer with only one of the acrylates catalyzed to a hydroxyl ion and is suggested by figure 3.19. The structure was noted as:

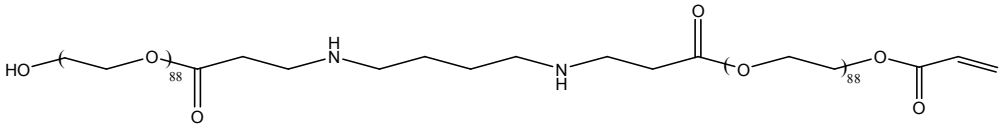

Figure 3.19 Linear structure of polyethylene glycol diacrylate diaminobutane after initial hydrolysis. The structure represents the possible structure of the polymer with one acrylate end group hydrolyzed to the hydroxyl ion.

End group 4 was determined as the completely hydrolyzed polymer with both acrylate moieties reduced to hydroxyl ions. The structure, as seen in figure 3.20, was defined as:

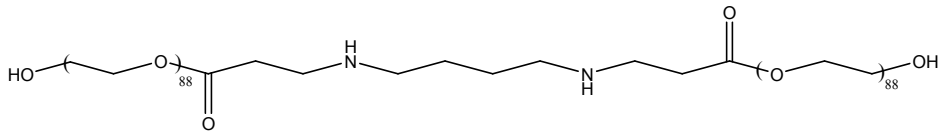

Figure 3.20 Linear structure of polyethylene glycol diacrylate diaminobutane after hydrolysis of polymer. The structure represents the complete hydrolysis of the acrylate end groups to hydroxyl ions.

The structure containing the end groups with complete hydrolysis was confirmed via ^{1}H NMR, as seen in Appendix E. The inner-most methylene groups of the diaminobutyl group have a chemical shift of 1.5ppm, while the methylene groups nearest the amine groups are represented by the 2.5 ppm shift. The polyethylene oxide group is represented by the large multiplet peak at 3.85 ppm. The peak at 4.8 ppm corresponded to the methylene group nearest the oxygen ion of the ester group, while the quartet at 4.3 ppm represented the methylene groups closest to the hydroxyl groups. Also by the lack of peaks in the vicinity of 6.0 ppm, it is confirmed that the acrylate end groups are no longer a concern within the compound.

A review of the NMR spectrum in Appendix F illustrated that all peaks are below 80 ppm. This is due in part to the fact that only nitrogen and oxygen ions have any effect on the carbons of the polymer. The upfield chemical shifts (68-72 ppm) represent the carbon ions in the vicinity of the oxygen ions, while the downfield chemical shifts (25-28 ppm) represent the carbon ions in the vicinity of the nitrogen ions. The absence of the carbonyl group in the spectrum demonstrates that the group is shielded by the large molecule. Based on the data explained above, the NMR spectra in Appendices G and H have the same interpretation given that

ethylenediamine was used as one of the monomers opposed to 1,4-diaminobutane in the previously mentioned polymer.

The ECOSY showed that both polymeric diazeniumdiolates from the initial monomer exhibited connectivity at 3.7 and 4.2 ppm.

CHAPTER IV

TREATMENT OF HPV-POSITIVE VERSUS HPV-NEGATIVE CELLS USING DIAZENIUMDIOLATES

4.1 Determination of Testing Pattern

Human papillomavirus has been linked to low-risk warts such as plantar and butchers warts and high-risk cervical cancer, depending on the virus gene-type. In some cases, there has been research to support treatment of these warts utilizing nitric oxide products.[53] However, there has not been any research of nitric oxide in the treatment of high-risk, HPV-induced cervical cancer cells. Utilizing several cell lines, a study was performed to determine the effect of nitric oxide on HPV-induced, cervical cancer cells.

4.2 Cell-Viability using In-Vitro Testing

The cell lines utilized included HPV negative C33A cells, HPV-16-positive CaSki cells and HPV-18-positive HeLa cells. The cells (stored in a 140°C chamber) were thawed at 37°C, then immediately centrifuged at 2000 rpm to remove the freezing media (Dulbecco's Modified Eagle Medium (DMEM), 5% Fetal Bovine Serum (FBS), and 1% Pen Strep (P/S) containing 5% dimethyl sulfoxide (DMSO), resuspended with growth media (DMEM/FBS and P/S) and stored at 37C in an humidified, incubated atmosphere with 5% CO2/95% room air. Cells were collected after the second passage for testing using the diethylspermeate NONOate (DES NO) standard. The passages were between 3 and 23.

DES NO (~30mg) was initially diluted in 1 mL of DMSO. The initial concentration was diluted to one tenth of the initial concentration with growth media (DMEM/FBS and P/S). The samples were diluted to final concentrations of 10, 50, 100, 300 and 500. The concentration of

DMSO was monitored due to its toxicity to cells. The highest level of DMSO that a cell can tolerate is 0.2% in solution. However with the dilutions of the standards, the 500 μM showed a level of 0.6% DMSO. Therefore, two controls were developed for the study. The first control utilized a concentration of 0.2% DMSO in the growth media without the standard DES NO. The second control utilized DMSO at a concentration of 0.6% without the standard DES NO. This was done to eliminate the option that DMSO at the highest concentration (500 μM) influenced toxicity or bioavailability of the prodrug DES NO. The lowest concentration of DMSO was 0.012% at a concentration of 10 μM DES NO.

The cell lines were trypsinized once to 85-90% confluent in the T75 flask. The trypsin, which is toxic to the cell over an extended period of time, was removed from the cells via centrifuge and replaced with fresh growth media prior to transfer. In order to determine the number of cells available, the cells were counted using a hemacytometer for a total number of cells (Z) times 10^3 per ml as seen in equation 19. The hemacytometer has two grids (X and Y), which are individually counted. The sum of the two grids represents the total number of cells ($Z*10^3$) within a known volume. The equations 20 and 21 were used to determine the amount of sample to deliver to each well.

$$X + Y = Z * 10^3 \text{ /ml} \tag{19}$$

$$(Z*10^3 \text{ /mL})*(x) = 10^5 \text{ cells} \tag{20}$$

$$x = (10^5 \text{ cells})/(Z*10^3 \text{ /mL}) \tag{21}$$

Based on previous research, it was determined that 10^5 cells were optimal for confluence within 24 hours in conditions of 37°C in a humidified, incubated atmosphere with 5% CO2/95% room air utilizing a 12-well plate. After the 24-hour incubation period, the growth media was removed and the previously discussed preparation of the standard was prepared. The sample wells were doped, in duplicate, with each concentration including the two controls (0.2% and 0.6%) and incubated for 24 hours.

4.2.1 Cell Viability using CaSki, C33A and HeLa Cervical Cancer Cell Lines

Several cells lines were utilized to determine the effect of the standard on cervical cancer. The C33A cell line is a HPV-negative induced cancer. This cell line represents approximately 5% of all cervical cancer and has been determined as the mutant cell line. CaSki is a HPV-16-positive cancer cell, meaning that the cell line has been influence by type-16 HPV gene. HeLa is a HPV-18-positive cancer cell, which means that the cell line has been influence by the type-18 HPV gene. Types 16 and 18-induced HPV cells have been linked to approximately 70% of all cervical cancer[54, 55, 56, 57]. Both of these cell lines have been isolated as the wild type for this study.

4.2.2 Determination of Cell Number and Viability

Cell lines were plated in a 12-well tissue culture dish and incubated for 24 hours. The media was removed and replaced with the standard DES NO at differing concentrations. The incubation period for doping of the cells was 24 hours. After which, the drug was removed and cells were washed with 0.5 mL of phosphate buffered saline solution (PBS). The buffer was removed and trypsin was placed in each well until the cells were removed from the plate. The trypsinized solution was centrifuged at 4°C, 2000 rpm for 5 minutes. The trypsin was removed and the cells were resuspended in 0.5mL of PBS. The sample was centrifuged again to remove any trace of trypsin. The solvent was removed and then the cells were resuspended in 0.5 mL PBS. An aliquot of 0.100 mL of the treated cells were placed in a centrifuge tube and mixed with 0.100 mL of trypan blue solution and let to sit for 5 minutes. After the contact time had expired, 10 μL of the solution was placed on either side of the hemacytometer and read via a binocular microscope. A count of the “unstained” (viable) versus the “stained” (nonviable) cells was determined the viable cell percentage[58]. Equation 22 was used to determine the percentage of viable cells:

$$\text{Viable Cell (\%)} = \frac{\text{Total number of viable cells}}{\text{(Sum of viable + non-viable cells)}} * 100 \quad (22)$$

The raw data for the viable cell percentage recovered from the treatment of the three cell lines utilizing DES NO as the prodrug has been placed in Appendix E.

4.2.3 Statistical Analysis of Cell Viability In-Vitro Testing

The one-way ANOVA was used to determine if the mean values for each treatment were significantly different in each cell line. The defined variable design determined the combination of the drug and the DMSO. The order of the variable design is the same as for the variable drug. Table J.2 in Appendix F defines the codes for the variable design.

For each combination of a drug and DMSO, the average proportion of living cells after the treatment was calculated. The variable design is ordered in increasing order of the drug, and demonstrated a general trend for a decrease of the proportion of living cells in higher drug dosage as seen in Table J.4 of Appendix J. For each cell, the number of replications used to obtain the average was reported in the Table J.3 of Appendix J.

4.3 Discussion and Conclusion

The review and analysis of raw data for the determination of availability of human papillomavirus using diethylspermeate NONoate.

4.3.1 Comparison of Cellular Types for Variability Profile

For the determination of the effectiveness of DES NO via the mutant, C33A cell line, there were a total of 41 replications and the F test for the difference in means had a p-value of 0.12. It was concluded that there is no significant difference between the

different combinations of drug and controls containing DMSO. (i.e. between the different levels of the variable design).

However when the wild type, CaSki cell line was utilized, there were a total of 42 replications and the F test for the difference in means had a p-value of 0.01. It was concluded that there is a significant difference between the different combinations of drug and DMSO for the cell line. An examination of the data revealed that the treatments of 5 and 6 (100 and 300 μM) did not differ from one another, but differed in value from all other treatments.

For the wild type HeLa cell line, there were a total of 43 replications and the F test for the difference in means had a p-value smaller than 0.001. It was concluded that there is a significant difference between the different combinations of drug and DMSO.

Figures 4.1 - 4.3 show the effect of DES NO on the mutant and wild type, cell lines. The actual count of each concentration is noted as the viable (alive) cell versus the non-viable (dead) cells. This data was utilized to determine the overall bioavailability of DESNO on the mutant and wild type cell lines. Typically, the effectiveness of drug therapies has been marked as significant once the percent viability of the cell line falls below fifty percent.

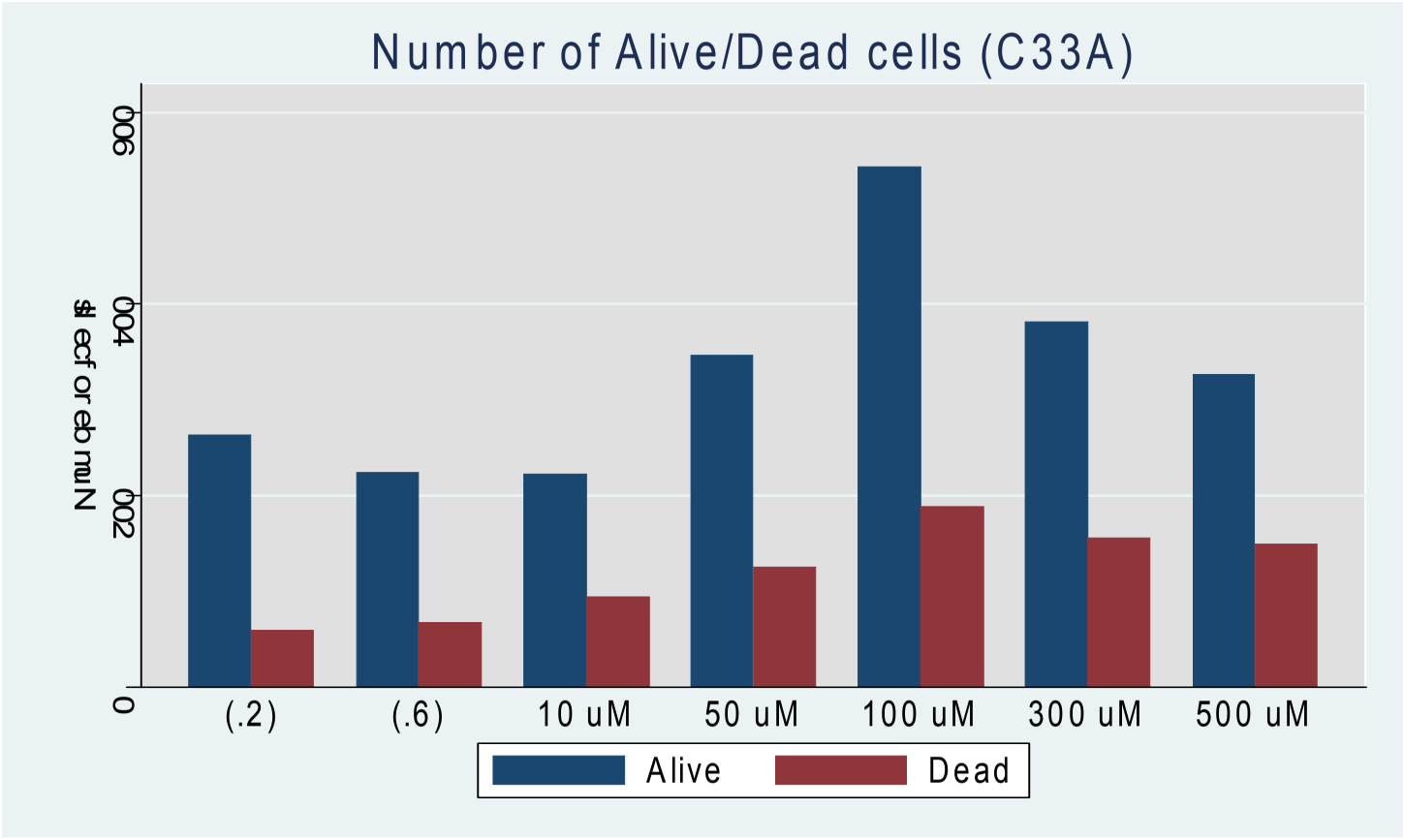

Figure 4.1 Raw data for C33A cell line. Using a hemacytometer, the viable (alive) and non-viable (dead) mutant, C33A cells were counted. The percent viability was determined from this information. The cells were counted 24 hrs after doping with DES NO.

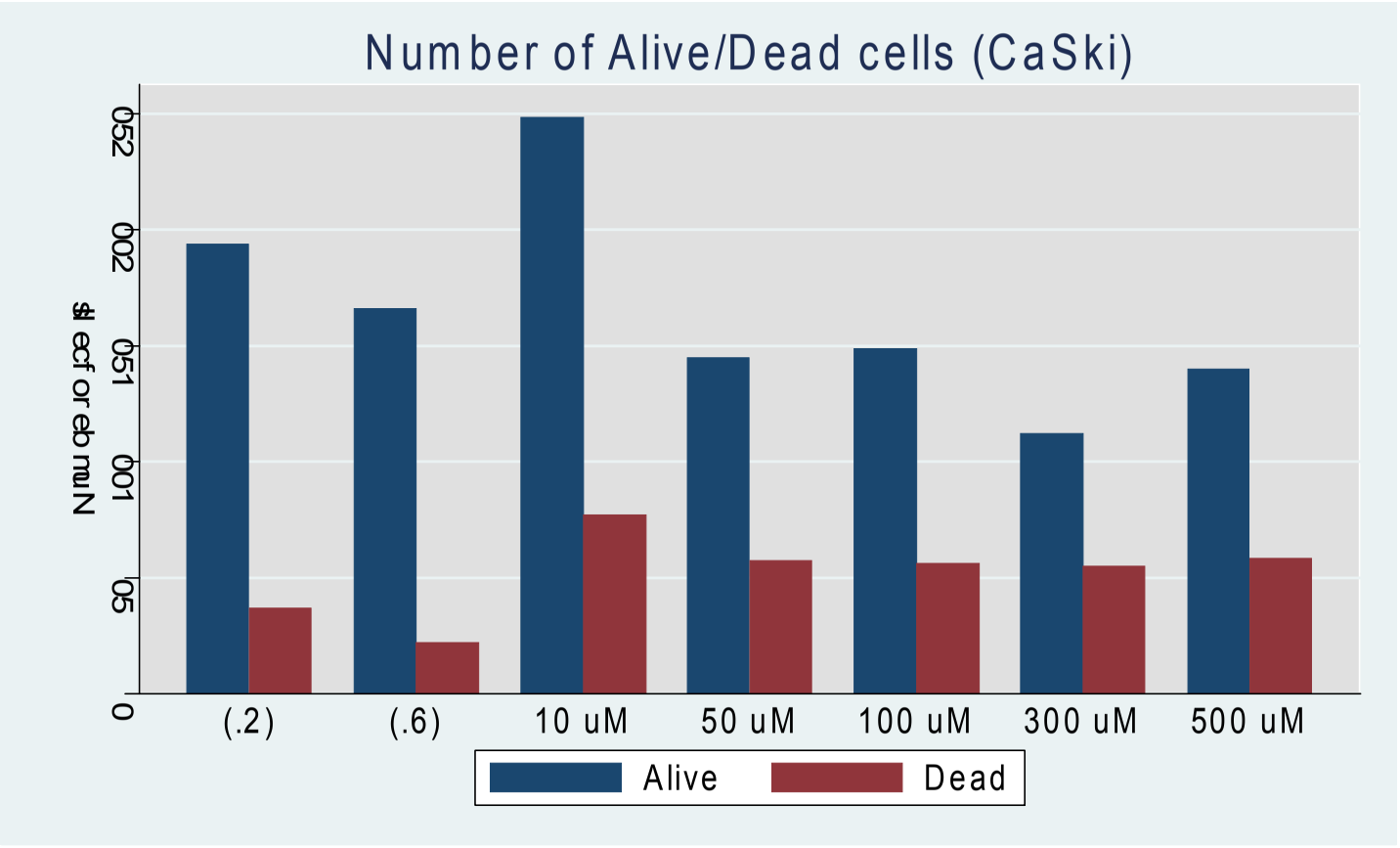

Figure 4.2 Raw data for CaSki cell line. Using a hemacytometer, the viable (alive) and non-viable (dead) wild type, CaSki cells were counted. The percent viability was determined from this information. The cells were counted 24 hrs after doping with DES NO.

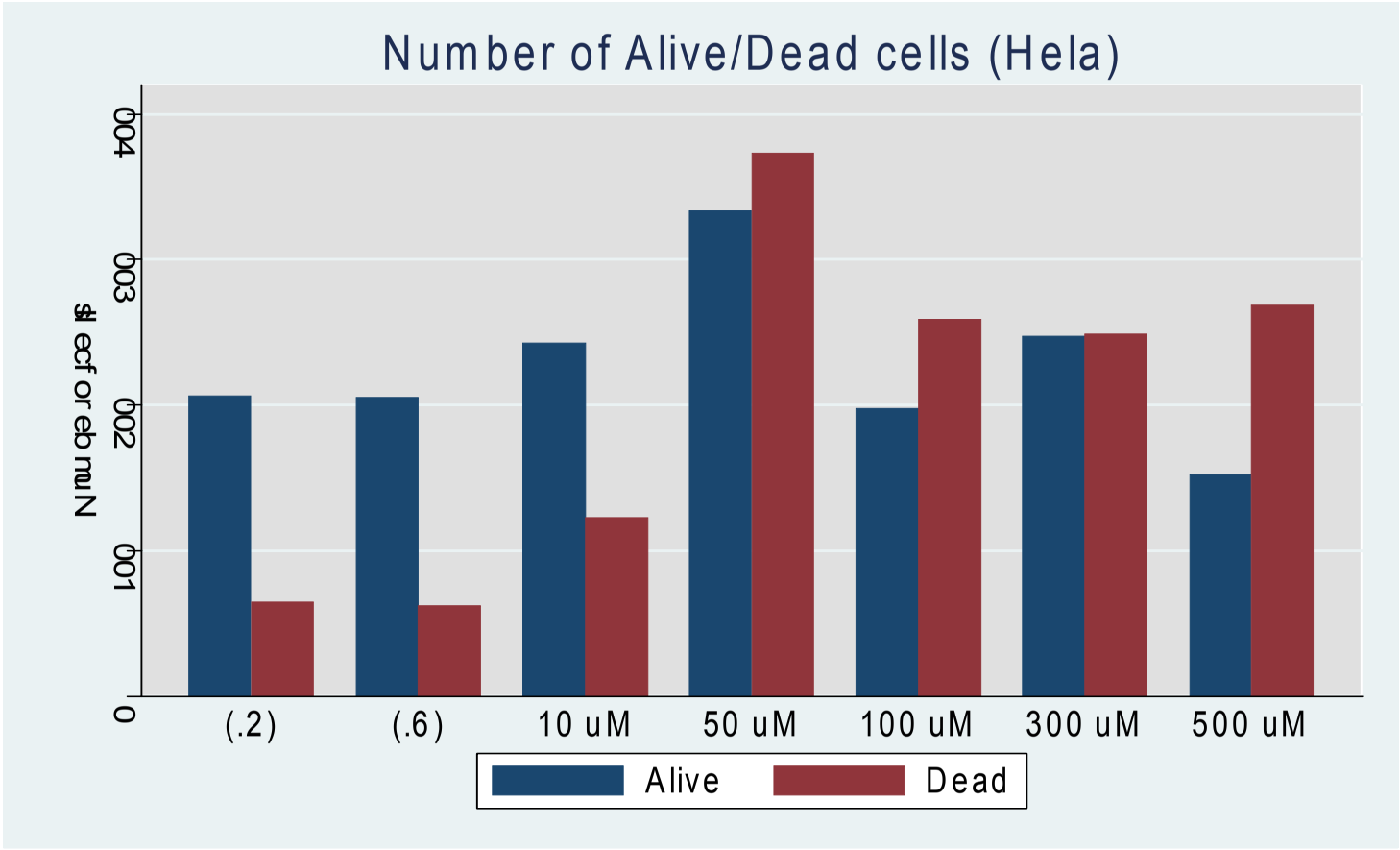

Figure 4.3 Raw data for HeLa cell line. Using a hemacytometer, the viable (alive) and non-viable (dead) wild type, HeLa cells were counted. The percent viability was determined from this information. The cells were counted 24 hrs after doping with DES NO.

Figures 4.4 to 4.6 showed analysis and final evaluation of the raw data into their mean (circle) and a 95% confidence index (bar) at each concentration. The confidence index corresponded to the fact that 95% of the data fell within the range of acceptability, while 5% represented outliers and anomalies. Accordingly, figure 4.4 demonstrated that the mutant cell line C33A is not affected by the therapeutic nature of NO. The data reveled that the mutant, non-HPV induced cell line (C33A) availability yielded no significant response to the drug at differing concentrations. The range of the drug's effectiveness was noted as 69% - 76%.

Figure 4.5 illustrated the effect that the NO drug would have on HPV. The wild type cells (CaSki) were not responsive and tended to follow the same trend as the mutant cell line (C33A). The range of the effect noted against the cell line was 70% - 76%. This analysis did take into account the effect of the DMSO on the cells. It was determined that DMSO had little effect on the group. An F-test for the difference in treatments concluded no significant difference between the drug combinations of concentrations 10 to 300 μM and the final concentration of 500 μM.

While in figure 4.6, the wild type HeLa cell line (the HPV induced cell line) exhibited a positive effect from contact with NO. The HeLa cell's availability fell below the 50% range at the 100uM concentration. The availability of the cell line ranged from 36% to 67%. Based on the data, NO was effective in leading to apoptosis of the cell. A F-test analysis showed significant difference between controls and the final concentration of 500 μM.

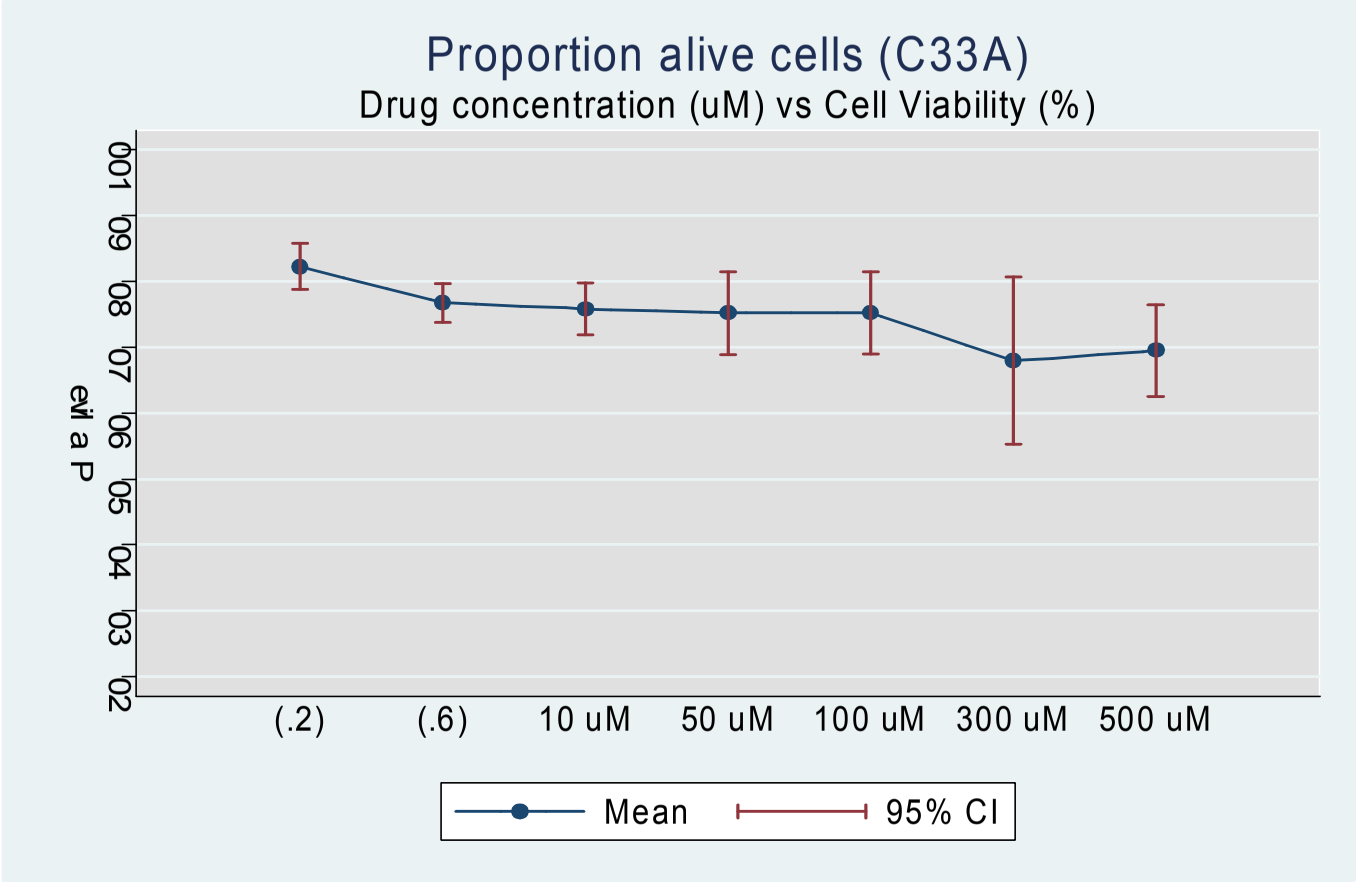

Figure 4.4 Bioavailability of C33A cell line. The graph reflects the effect of DESNO on C33A cell line at differing concentrations. The control concentrations were spiked with DMSO at 0.2% and 0.6% to determine the toxicity of highest DMSO concentration at 500 µM doping. The 95% confidence interval shows the range of the data from the experiment.

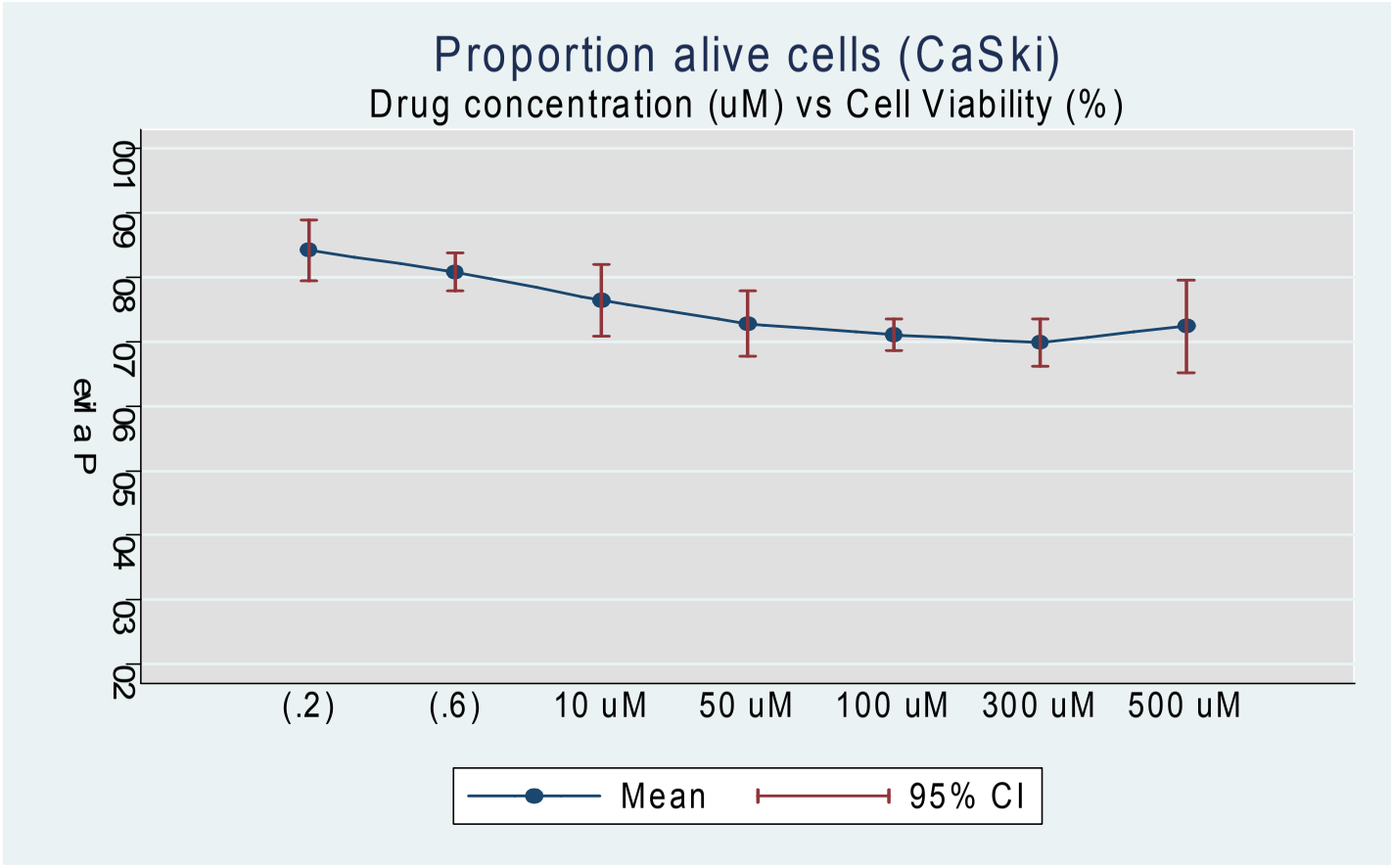

Figure 4.5 Bioavailability of CaSki cell line. The graph reflects the effect of DESNO on CaSki cell line at differing concentrations. The control concentrations were spiked with DMSO at 0.2% and 0.6% to determine the toxicity of highest DMSO concentration at 500 µM doping. The 95% confidence interval shows the range of the data from the experiment.

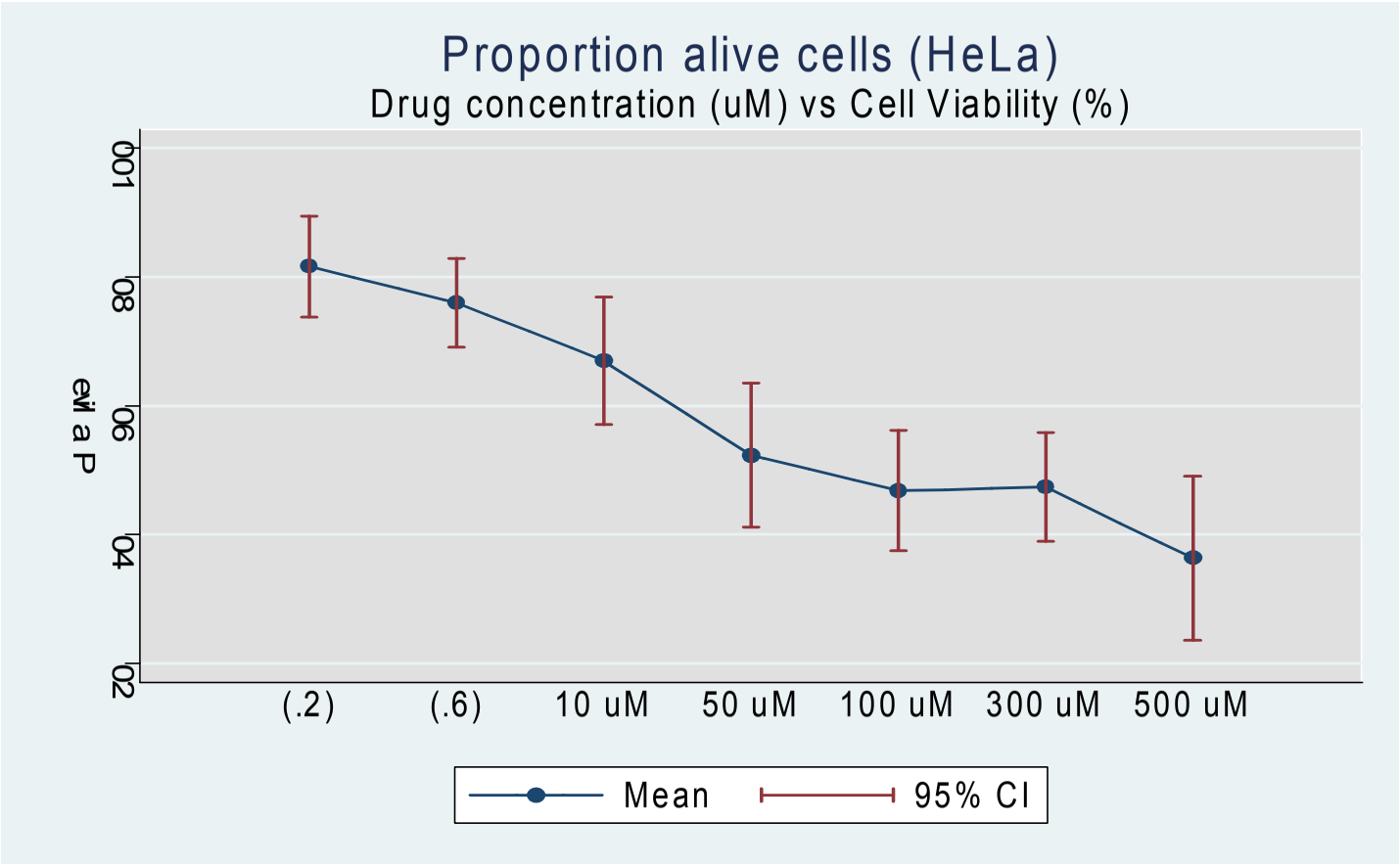

Figure 4.6 Bioavailability of HeLa cell line. The graph reflects the effect of DESNO on HeLa cell line at differing concentrations. The control concentrations were spiked with DMSO at 0.2% and 0.6% to determine the toxicity of highest DMSO concentration at 500 µM doping. The 95% confidence interval shows the range of the data from the experiment.

Due to the differing effects on the two wild type cell lines, the experiment was inconclusive. There are two reasons for this occurrence: 1) Studies have shown that the interaction of nitric oxide can promote carcinogenesis in cervical cancer intraepithelial neoplasia[59, 60] as well as hinder carcinogenesis and 2) research has shown that the induction of nitric oxide has the possibility to activate phosphatidylinositol-3-kinase (PI3K), protein kinase B (PKB is known as AKT) and eNOS along the Ras pathway to maintain tumor growth[61, 62].

In the first case: reactive oxygen species (ROSs) such as hydrogen peroxide (H_2O_2), hydroxyl radicals (OH^-), etc. can lead to DNA damage. In particular, this damage has shown increased levels of 8-hydroxy-2'-dexyguanosine (8-OHdG), where C8 of guanine moiety is oxidized and has been found mainly in the cervical cells according to Romano, et al[60]. With the addition of nitric oxide to ROS, there are increased opportunities for carcinogenesis, since nitric oxide has been known to mediate 8-nitroguanine, an indicator for nitrative DNA damage. Additionally, nitric oxide is known to have managed oxidative DNA damage.

Researchers such as Cooke, et al[63], have shown that the oxidative DNA damage of guanine by ROS was measured in considerable amounts in patients suffering from gynecological cancers. By introducing DES NO to the C33A cell line, a small amount of nitric oxide would not lead to apoptosis, but instead promoted mutagenesis of the cell. This theory of introducing nitric oxide levels and influencing oxidative injury has been substantiated by Anggard's research of nitric oxide's role in mediating and promoting oxidative injury[64]. As noted in the study by Cooke, et al, and Romano, et al, the oxidative guanine product influenced cervical cancer, but was not localized in HPV-induced cancer cells, thus theorizing that only C33A cell lines (mutant) would have a negative effect from any therapeutic use of nitric oxide. However, this does not explain the two wild type cell lines.

In the HPV-induced, wild type cell lines of CaSki (type 16) and HeLa (type 18), there are a myriad of systems that are in place to maintain the mutagenic process of cell life. In particular,

researchers have explored both E6 and E7 conditions which have promoted, cumulatively, the initiation and maintenance of cancer in the cervical epithelial cells.

However, there has been a recent study of Ras/PI3K/AKT activation that leads to cell survival[61, 62, 65]. In the presence of eNOS and nitric oxide, Lim et al proved that the Ras-activated PI3K/AKT/eNOS pathway lead to tumorigenesis. This pathway supports that apoptosis can either be hindered or induced by the promotion of the capase 9 in the pathway. Capase 9 is known to promote cellular death by regulating permeability of the cellular membrane to cytochrome C and other factors. There are numerous triggers for the activation of capase-9, but the trigger for activation of capase 9 in the wild-type cell lines is not fully understood. However, further investigation is warranted to determine the mechanism by which it is activated. Figure 4.7 shows the pathway of Ras induced anti-apoptosis activity.

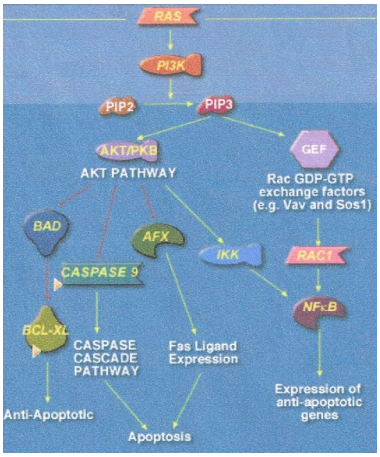

Figure 4.7 Pathway of Ras induced anti-apoptosis. The graph reflects the effect of Ras on the cessation of apoptosis. With the activation of Ras, PI3K is activated and either leads to the AKT pathway or GEF pathway. Both pathways lead to anti-apoptotic events, unless capase 9 commences and mediates cell death. Copyright permission has been granted by the publisher.

CHAPTER V

SUMMARY

The use of the Griess reagent versus the nitric oxide analyzer for the analysis of lipophilic, insoluble diazeniumdiolates has proven to yield a more quantitative measurement of nitric oxide release profiles. While the nitric oxide analyzer does provide an opportunity to analyze diazeniumdiolate utilizing the electronic detector, the NOA has flaws. First, the instrument requires a hands-on approach. Secondly, the reaction chamber does not provide the best seal for total quantitative analysis of released nitric oxide. For this reason, the Griess reagent offers more opportunities to analyze diazeniumdiolates. Besides the soluble diazeniumdiolates, the Griess reagent has been proven to quantify insoluble, lipophilic diazeniumdiolates without dissolving them in solution prior to analysis. The Griess reagent does not require the hands-on approach as the NOA, which makes the Griess reagent the more compatible approach for future analysis.

From the standpoint of the characterization of the polymeric diazeniumdiolates, it proved more cumbersome than initially considered. Due to the fact that the material developed slowly and continuously over time, spectra analysis confirmed that the transformation of the initially viscous material to the cross-linked polymer did occur. The final structure was speculated as a long chain polymer with cross-linking at that continued to allow the material to be modified. Based on H^1 and C^{13} NMR and mass spectral analysis, the final shift for the polymer pointed towards the complete hydrolysis of the acrylate to form either a hydroxyl (–OH) group or a hydrogen molecule (-H). The hydroxyl end-group shows that the cross-linking not only occurs

with the acrylate, but that it is possible for cross-linking to occur by the hydroxyl group, thus producing a more hydrophilic material. The conclusion is that the polymer continues to change over a period of time to increase its hydrophilic nature, while at the same time increasing its ability to bind more nitric oxide.

The study of the effect of nitric oxide on HPV-induced, cervical cancer cells proved more evasive than the answer to the original hypothesis. The effects of nitric oxide on the mutant non-HPV induced cervical cancer cells and the wild-type HVP-induced (type 16) CaSki cells versus the wild-type HPV-induced (type 18) HeLa cells showed that the nitric oxide did not effect the human papillomavirus, but some effect was experienced to cause apoptosis. Based on the current literature, the RAS/PI3K/AKT interaction with nitric oxide is the most probable culprit to investigate for future research. This is based on the fact that RAS, when activated, promotes cellular survival in epithelial cells utilizing nitric oxide.

Suggestions for future work:

(i) The use of capase-9 in a study with the wild-type HPV-induced and mutant non-HPV-induced cell lines to determine if apoptosis was influenced in both of the wild-types. If cell death was noted, then it would prove that nitric oxide does not affect the human papillomavirus, but instead triggers apoptosis via normal well documented channels. Also the examination should determine the mechanism by which nitric oxide triggers the activation of capase-9.

(ii) The physical properties of the diazeniumdiolate polymers, PEG diaminobutane and PEG ethylenediamine, should be explored for other opportunities to influence wound healing. Currently, the compounds have been characterized and a nitric oxide profile has been rendered. Medicinal applications are possible, however animal, efficacy and safety studies are need to determine future uses.

REFERENCES

[1] Kristyn S. Bohl and Jennifer L. West; Biomaterials, Nitric Oxide-generating polymers reduce platelet adhesion and smooth muscle cell proliferation, **21**, 2273-2278, (2000)

[2] Sinisa Miketic, Joerg Carlsson, Ulrich Tebbe; American Heart Journal, Randomized comparison of J&J Crown stent versus NIR stent after routine coronary angioplasty, **142** (5), e8, (2001).

[3] Larry K. Keefer, Annual Review Pharmacological Toxicology, Progress Toward Clinical Application of The Nitric Oxide-Releasing Diazeniumdiolates, **43**, 585-607, (2003).

[4] JL Hill-West; SM Chowdhury; MJ Slepian; JA Hubbel; Proc Natl Acad Sci, USA, Inhibition of thrombosis and intimal thickening after ballon injury by in situ photopolymerization of thin hydrogel barriers, **91,** 5967-5971, (1994).

[5] JH Ip, V. Fuster, D. Israel, L Badimon, J. Badimon, JH Chesebro; Journal of the College of Cardiology, The role of platelets, thrombin and hyperplasia in restenosis after coronary angioplasty, **17**, 77B-88B, (1991).

[6] K. Seedorf; T. Oltersdorf; G. Krammer; and W. Rowekamp; The European Molecular Biology Organization Journal, Identification of early proteins of the human papillomaviruses type 16 (HPV16) and type 18 (HPV 18) in cervical carcinoma cells, **6(1),** 139-144, (1987).

[7] W-Y Au; E.S. Ma; T-L. Lee; S-Y. Ha; A. T. Fung; Lie, Albert K.W.; and Kwong, Yok-Lam; British Journal of Haemtology, Successful treatment of thrombotic microangiopathy after haematopoietic stem cell transplantation with rituximab, **137**, 475-478, 2007.

[8] Joseph A. Bauer; Weisun Rao; Daniel J. Smith; Wound Repair and Regeneration, Evaluation of linear polyethyleneimine/nitric oxide adduct on wound repair: therapy versus toxicity, **6**, 569-577 (1998).

[9] Sabrina Fritzen; Angelika Schmitt; Katharina Koth; Claudia Sommer; Klaus-Peter Lesch; and Andreas Reif; Molecular and Cellular Neuroscience, Neuronal nitric oxide synthase (NOS-1) knockout increases the survival rate of neural cells in the hippocampus independently of BDNF, **35**, 261-271 (2007).

[10] Roberta Scatena; Expert Opinion on therapeutic patents, New nitric oxide-releasing polymers for implantable devices, **17** (11), 1397-1400, 2007.

[11] J.A. Hrabie; J.R. Klose; D.A. Wink; and L.K. Keefer; J. Organic Chemistry, New Nitric Oxide-Releasing Zwitterions Derived from Polyamines, **58** (6), 1472-1476, (1993).

[12] Pawel Parzuchowski; Megan Frost; and Mark E. MeyerhoffE; Journal of American Chemical Society, Synthesis and Characterization of polymethylacrylated-based nitric oxide donors, **124**, 12182-12191, (2002).

[13] Joseph S.Beckham; Nitric Oxide: Principles and Actions; The Physiological and Pathological Chemistry of Nitric Oxide, edited by Jack Lancanster, Jr., pp. 7, (1996).

[14] Antonius C.F. Gorren; Bernd Mayer; Nitric Oxide: Basic Research and Clinical Application; The role of Tetrahydrobiopterin in Nitric Oxide Synthesis, NATO Science Series, (Edited by Ryszard J Gryglewski and Pietro Minuz), 27-34, (2001).

[15] D.J. Struehr; S. Adak; J. Santolini; C.C. Wei; Z. Wang; Nitric Oxide: Basic Research and Clinical Application; Mechanism of Oxygen Activation in the NO Synthases, and a Kinetic Model for Catalysis; NATO Science Series, (Edied by Ryszard J Gryglewski and Pietro Minuz), 23-26, (2001) .

[16] Aurora Seminara; Joshua S. Krumenacker; Ferid Murad; Nitric Oxide: Basic Research and Clinical Application; *Signal Transduction with Nitric Oxide, Guanylyl Cyclase and Cyclic Guanosine Monophospate*; NATO Science Series, (Edied by Ryszard J Gryglewski and Pietro Minuz), 5-22, (2001) .

[17] Jack Lancaster, Jr.; and Dennis J. Stuehr, Nitric Oxide: Principles and Actions, The Intracellular Reactions of Nitric Oxide in the Immune System and Its Enzymatic Synthesis, (edited b Jack Lancaster, Jr.139-175 (1996).

[18] Joseph Beckman; Nitric Oxide: Principles and Actions, Physiological and Pathological Chemistry of Nitric Oxide, (edited b Jack Lancaster, Jr.), 1-82 (1996).

[19] J. S. Stamler, D.I. Simon, J. A. Osborne, M. E Mullins, O. Jaraki, T. Michel, D.J. Singel, and J. Loscalzo, Proceedings of the National Acadamy of Sciences, S-Nitrosylation of proteins with nitric oxide: Synthesis and characterization of biologically active compounds, USA, **89**, 444-448, (1992b).

[20] D. Wink, K. Kasprzak, C. Maragos, R. Elespuru, M. Misra, T. Dunams, T. Cebula, W. Koch, A. Andrews, J. Allen, and Larry Keefer, Science, DNA deaminating ability and genotoxicity of nitric oxide and its progenitors, **254**, 1001-1003, (1991).

[21] D. A. Wink, J. F. Darbyshire, R. W. Nims, J. E. Saavedra, and P. .C. Ford, Chemical Research in Toxicology, Reactions of the bioregulatory agent nitric oxide in oxygenated aqueous media: Determination of the kinetics for oxidation and nitrosation by intermediates generated in the NO/O_2 reaction, **6**, 23-27 (1993).

[22] R. O. Ragsdale, Developments in Inorganic Nitrogen Chemistry, Reactions of nitrogen (II) oxide, Elsevier, Amsterdam, (1973).

[23] HHHW Schmidt, T. D. Warner, U. Forstermann, F. Murad, Molecular Pharmocology, Regulation and subcellular location of nitric oxide synthase in RAW 264.7 macrophages. **41**, 615-664 (1992).

[24] Weisun Rao, Linear Polyethyleneimine and Spermic Acid Derivatives as Carriers for Controlled Nitric Oxide Delivery, The University of Akron, (1998).

[25] Larry K Keefer, Annual Review of Pharmacological Toxicology, Progress Toward Clinical Application of the Nitric Oxide-Releasing Diazeniumdiolates, **43**, 585-607 (2003).

[26] A. Samouilov and J. Sweier, Analytical Biochemistry, *Development of* Chemiluminescence-Based Methods for Specific Quantitation of Nitrosylated Thiols, **258**, 322-330, (1998).

[27] J. F. Ewing and D. R. Janero, Free Radical Biology and Medicine, Specific S-Nitrosothiol (Thionitrite) Quantification as Solution Nitrite after Vanadium (III) Reduction and Ozone Chemilunescent Detection, **25** (4/5), 621-628 (1985).

[28] Lisa A. Ridnour, Julia Sim, Michael A. Hayward, David A. Wink, Sean M Martin, Garry R. Buettner, and Douglas Spitz, Analytical Biochemistry, Spectrophotometric Method for the Direct Detection and Quantiation of Nitric Oxide, Nitrite and Nitrate in Cell Culture Media, **281** (2), 223-229, (2000).

[29] Raymond W. Nims, John F. Darbyshire, Joseph E. Saavedra, Danae Christodoulou, Ingeborg Hanbauer, George W. Cox, Matthew B. Grisham, Franciose Laval, John A. Cook, Murali C. Krishna, and David Wink, Methods: A Companion to Methods in Enzymology, Colorimetric Methods for the Determination of Nitric Oxide Concentration in Neutral Aqueous Solution, **7**, 48-54 (1995).

[30] Kurt Weckstrom; Patent US2002/0137227 A1, Chemiluminescent Gas Analyzer, (2002).

[31] David A. Wink; Raymond W. Nims; John F. Darbyshire; Danae Christodoulou, Ingeborg Hanbauer, George W. Cox; Francoise Laval; Jacques Laval; John A. Cook; Murali C. Krishna; William G. DeGraff; and James B. Mitchell; Chemical Research of Toxicology, Reaction Kinetics for Nitrosation of Cysteine and Glutathoine in Aerobic Nitric Oxide Solutions at Neutral pH. Insights into the Fate and Physiological Effects of Intermediates Generated in the NO/O_2 Reaction. **7**, 519-525, (1994).

[32] Melissa M. Reynolds; Joseph A. Hrabie; Bong K.Oh; Jeffrey K. Politis; Michael L. Citro; Larry K. Keefer; and Mark E. Meyerhoff; Biomacromolecules, Nitric Oxide Releasing Polyurethanes with Covalently Linked Diazeniumdiolates Secondary Amines, **7** (3), 987-994, (2006).

[33] Zhengrong Zhou; Gail M. Annich; Yidou Wu; and Mark E. Meyerhoff; Biomacromolecules, Water-soluble Poly(ethylenimine)-Based nitric oxide Donors: Preparation, Characterization, and Potential Application in Hemodialysis, **7** (9), 2565-2574, (2006).

[34] Joseph A. Bauer; Weisun Rao; and Daniel J Smith; Wound Repair and Regeneration, Evaluation of linear polyethyleneimine/nitric oxide adduct on wound repair: therapy versus toxicity, **6**, 569-577 (1998).

[35] Mohammad Shabani; Sharon K. Pulfer; Jeffrey P. Bulgrin; and Daniel J Smith; Wound Repair and Regeneration, Enhancement of wound repair with a topically applied nitric oxide-releasing polyme*r*, **4**, 353-362 (1996).

[36] A.S. Lea; J.D. Andrade; V. Hlady; Colloids and Surfaces. A: Physicochemical Engineering Aspects, Compression of polyethylene glycol chains grafted onto silicon nitride surface as measured by scanning force microscopy, **93**, 349-357 (1997).

[37] Stephanie Lopina; George Wu; Edward Merrill; Linda Griffinth-Cima; Biomaterials, Hepatocyte culture on carbohydrate-modified star polyethylene oxide hydrogels, **17** (6), 559-569 (1996).

[38] Robert Langer and Joseph P. Vacanti, Science, *Tissue Engeering*, **260** (5110), 920-926 (1993).

[39] M. Amiji and K. Park, Journal of Biomaterial Science, Polymer Edition, Surface modification of polymeric biomaterials with poly(ethylene oxide), albumin and heparin for reduces thrombogenicity, **4** (3), 217-234 (1993).

[40] D.K. Han; K.D. Park; G.H.Ryu; U.Y. Kim; B.G. Min; and Y.H. Kim; Journal of Biomedical Materials Research PartB: Applied Biomaterials, Plasma protein adsorption to sulfonated poly(ethylene oxide)-grafted polyurethane surface, **30** (1), 23-30 (1996).

[41] D.K. Han; S.Y. Jeong; Y.H. Kim; B.G. Min; and H.I. Cho; Journal of Biomedical Materials Research PartB: Applied Biomaterials, Negative cilia concept for thromboresistance: synergistic effect of PEO and sulfonate groups grafted onto polyurethane*s*, **25** (5), 561-575 (1991).

[42] Biyun Wu; Bruce Gerlitz; Brian W. Grinnell and Mark E. Meyerhoff; Biomaterials Polymeric coatings that mimic the endothelium: Combining ntiric oxide release with surface-bound active thrombomodulin and heparin, **28**, 4047-4055 (2007).

[*43*] D.J. Stueher; N.S. Kwon; M.F. Weise; and C.F. Nathan; Protocol of the National Academy of Science USA, Purification and characterization of the cytokine-induced macrophage nitric oxide synthase: An FAD- and FMN-containing flavoprotein, ***88****, 7773-7777, (1991)*.

[44] R.M. Palmer; A.G. Ferrige; S. Moncada; Nature, Nitric oxide release accounts for the biological activity of endothelium-derived relaxing fact*r*, **327**, 524-526, (1987).

[45] C. Nathan; The Federation of American Society of Experimental Biology (FASEB) Journal, Nitric oxide as a secretory product of mammalian cells, **6**, 3051-3064, (1992).

[46] Donald M Lloyd-Jones and Kenneth D. Bloch; Annual Review of Medicine, The Vascular Biology of Nitric Oxide and its Role in Atherogenesis, **47**, 365-375, (1996).

[47] Jack Lancaster, Jr.; and JosephS. Beckman; Nitric Oxide: Principles and Actions, The Physiological and Pathological Chemistry of Nitric Oxide, (edited by Jack Lancaster, Jr.1-71 (1996).

[48] W.W. Yau; J.J. Kirkland; D.D. Bly; Modern Size Exclusion Liquid Chromatography, Wiley, New York, 476 (1979).

[49] Rongxin Su; Wei Qi; Zhimin He; Fengmin Jin; and Hongjiang Ge; Journal of Macromolecular Science, Part B: Physics, Flow Rate and Concentration-dependent Effects of Molecular Dynamics on Elution Behaviors of Flexible Polymers in Gel Permeation Chromatography: A Multi-angle Laser Light Scattering Study, **45**, 699-708 (2006).

[50] Guilherme Marson; Journal of Chemical Education, Principles of gel permeation chromatography: interactive software, **83**(10), 1567-1568 (2006).

[51] Benjamin Hemmens and Bernd Mayer, Methods in Molecular Biology: Nitric Oxide Protocols, Enzymology of Nitric Oxide Synthases (Edited by: Michael A. Titheradge) Humana Press Inc., **100**, 1-32 (1998).

[52] G.K. Turner; Bioluminescence and Chemiluminescence: Instruments and Applications; Measurement of light from chemical biochemical reations (Edited by K. Van Dyke), CRC Press, Boca Raton, FL, 43-87 (1985).

[53] Tors Peters; Cosmetic Treatment with Nitric Oxide, Device for Performing said Treatment and Manufacturing Methods, International Publication Number WO 2006/100154 A1, (PCT/EP2006/050884), (2006).

[54] R.M. Richart; Cancer, Causes and Management of cervical intraepithelial Neoplasia, **60** (8), 1951-1959 (1987).

[55] C.P. Crum; H. Ikenberg; R.M. Richart; L. Gissman; New England Journal of Medicine, Human Papillomavirus type 16 and early cervical neoplasia, **310** (14), 880-883, (1984).

[56] F.X. Bosch; M.M. Manos; N. Mun□oz; M. Sherman; A.M. Jansen; J. Peto; J.H. Schiffman; V. Moreno; R. Kurman; and K.V. Shah; Journal of the National Cancer Institute, Prevalence of human papillomavirus in cervical cancer: A worldwide perspective, **87**, 796-802 (1995).

[57] N. Muñoz; F.X. Bosch; S. deSanjose; R. Herrero; X. Castellsague; K.V. Shah; P.J.Snijdrs; and C.J. Meijer; New England Journal of Medicine, Epidemiological classification of human papillomavirus types associated with cervical cancer, **348** (6), 518-527, (2003).

[58] John E. Coligan; Ada M. Kruisbeek; David H. Margulies; Ethan M. Shevach; and Warren Strober; Current Protocols in Immunology, Trypan Blue Exclusion Test of Cell Viability (1997).

[59] Yusuke Hiraku; Tsutomu Tabata; Ning Ma; Mariko Murata; Xiohui Ding and Shosuke Kawanishi; Cancer Science, Nitrative and Oxidative DNA Damage in Cervical Intraepithelial Neoplasia Associated with Human Papilloma Virus Infection, **98** (7), 964-972 (2007).

[60] G. Romano; A. Sgambato; R. Mancini; G. Capelli; M. R. Giovagnoli; G. Flamini; A. Boninsegna; A. Vecchione and A. Cittadini; Carcinogenesis, 8-Hydroxy-2'-deoxyguanosine in Cervical Cells: Correlation with Grade of Dysplasia and Human Papillomavirus Infection, **21** (6), 1143-1147 (2000).

[61] K-H Lim; B. Ancrile; D. Kashatus and C. Counter; Nature (Letters), Tumour Maintenance is Mediated by eNOS, **452** (3), 646-650 (2008).

[62] A. B.Vojtek and C. J. Der; The Journal of Biological Chemistry, Increasing Complexity of Ras Signaling Pathway, **273** (32), 19925-19928 (1998).

[63] M. S. Cooke; M.D. Evans; M. Dizdaroglu and J. Lunec, The Federation of American Society of Experimental Biology (FASEB) Journal, Oxidative DNA damage: Mechanisms, Mutation, and Disease, **17** (6), 1195-1214 (2003).

[64] E. Anggard; The Lancet, Nitric Oxide: Mediator, Murderer, and Medicine, **343**, 1199-1206 (1994).

[65] M. P. Hayes; D. Sinha; K.S. Russuell; M.Collinge; D. Fulton; M. Morales-Ruiz; W. C. Sessa and J. R. Bender; Circulation Research, Membrane Estrogen Receptor Engagement Activates Endothelial Nitric Oxide Synthase via the PI3K-Kinase-AKT Pathway in Human Endothelial Cells, **22**, 667-682 (2000).

[66] L.C. Green; D. A. Wagner; J. Glogowski; P. L. Skipper; J. S. Wishnok and S. R. Tannenbaum; Analytical Biochemistry, Analysis of Nitrate, Nitrite and [N^{15}] Nitrate in Biological Fluids **126**, 131-138 (1982).

[67] M. Feelisch; E.A. Noack; European Journal of Pharmacology, Correlation between Nitric Oxide Formation during Degradation of Organic Nitrates and Activation of Guanylate Cyclase **139**, 19-30 (1987).

[68] M. Imani; S. Sharifi; H. Mirzadeh and F. Ziaee; Iranian Polymer Journal, Monitoring of Polyethylene Glycol-Diacrylate-based Hydrogel Formation by Real Time NMR Spectroscopy **16** (1), 13-20 (2007).

[69] J. Decatur; http://www.columbia.edu/cu/chemistry/groups/nmr/HSQC.pdf (2007).

[70] N. T. Nyberg and O.W. Sorensen; Magnetic Resonance in Chemistry, Multiplicity-edited Broadband HMBC NMR Spectra, **44**, 451-454 (2006).

[71] M-E. Dumas; C. Canlet; F. Andre; J. Vercauteren and A. Paris; Analytical Chemistry, Metabonomic Assessment of Physiological Disruption Using ^{1}H-^{13}C HMBC-NMR Spectroscopy Combined with Pattern Recognition Procedures Performed on Filtered Variables, **74** (10), 2261-2273 (2002).

[72] B.O. Petersen; E. Vinogradov; W. Kay; P. Wurtz; N.T. Nyberg, J.Ø.Duus and O.W. Sorensen; Carbohydrate Research, H2BC: A New Technique for Analysis of Complex Carbohydrates, **341**, 550-556 (2006).

[73] L. Badimon; J. Martinez-Gonzalez; V. Llorente-Cortes; C. Rodriguez and T. Padro; Current Molecular Medicine, Cell Biology and Lipoproteins in Atherosclerosis, **6**, 439-456, (2006).

[74] R. Nesto; Diabetic Medicine, C-Reactive Protein, Its Role inInflammation, Type 2 Diabetes and Cardiovascular Disease, and the Effects of Insulin-Sensitizing Treatment with Thiazolidinediones, **21** (7), 810-817 (2004).

[75] K. Huber and G. Maurer; Adjunctive Infusion of Antithrombin III during Percutaneous Transluminal Coronary Angioplasty, European Heart Journal **18**, 362-363 (1997).

[76] R. Kharbanda and R.J. MacAllister; Current Medicinal Chemistry- Immunology, Endocrinology and Metabolic Agents, The Atherosclerosis Time-Line an the Role of the Endothelium, **5** (1), 47-52 (2005).

[77] H.C. McGill, Jr; J.P. Strong; Annuals of the New York Academic of Science, **149**, 923(1968).

[78] D. McGrowder; D. Tagoobirsingh; and P. Brown; International Journal of Pharmacology, Therapeutic Uses of Nitric Oxide-Donating Drugs in the Treatment fo Cardiovascular Diseases, **2** (4), 366-373 (2006).

[79] S. Doucet; M. Schalij; M. C.M. Vrolix; D. Hilton; O, P. Chenu; D. DeBruyne; W. Udayachalerm; A. Seth; L. Bilodeau; J. Reiber; F. Harel; and J. Lesperance; Circulation: Journal of the American Heart Association, Stent Placement to Prevent Restenosis After Angioplasty in Small Coronary Arteries, **104**, 2029-2033 (2001).

[80] J. Rodes; G. Cotes; J. Lesperance; M. G. Bourassa; S. Doucet; L. Bilodeau; O.F. Bertrand; F. Harel; R. Gallo; and J-C. Tardif; Circulation: Journal of the American Heart

Association, Prevention of Restenosis After Angioplasty in Small Coronary Arteries with Probucol, **97**, 429-436 (1998).

[81] J.F. Kocsis; G. Llanos; and E. Holmer; Journal of Long-Term Effects of Medical Implants, Heparin-Coated Stents, **10** (1-2), 19-45 (2000).

[82] J. Loscalzo; Circulation: Journal of the American Heart Association, Folate and Nitrate-Induced Endothelial Dysfunction, **104**, 1086-1088 (2001).

[83] C. Llechi; G. Andrioli; S. Gaino; R. Tomassoli; V. Zuliani; R. Ortolani; M. Degan; G. Benoni; A. Lechi and P. Minuz; Thrombosis Haemostasis, The Anti-Platelet Effects of a New Nitroderivative of Acetylsalicilic Acid: An In-Vitro Study of Inhibition on the Early Phase of Platelet Activation and on Thromboxane A_2 production, **76**, 791-198 (1996).

[84] B. Voetsch; R. C. Jin and J. Loscalzo; Histochemistry of Cell Biology, Nitric Oxide Insufficiency and Atherothrombosis, **122**, 353-367 (2004); J. Loscalzo and G. Welch; Progressive Cardiovascular Disease, Nitric oxide and its role in the cardiovascular system, **38**, 87-104 (1995); J. Loscalzo; Circulation Research, Nitric Oxide Insufficiency, Platelet Activation and Arterial Thrombosis, **88**, 756-762 (2001b).

[85] P. Minuz; S. Gaino; V. Zuliani; R. Tommasolf; A. Lechi; C. Lechi Santonastaso; Nitric Oxide: Basic Research and Clinical Applications, Oxidized Lipids and Platelet Activation: Interaction with Nitric Oxide, (edited by R.J. Gryglewski and P. Minuz), 100-107 (2001).

[86] L. Cominacini; A. Fratta Pasini; U. Garbin; A. Rigoni; A. Davoli; V. LoCascio; A. Pastorino; Nitric Oxide: Basic Research and Clinical Applications, Effect of Oxidized LDL on Nitrotyrosines Production in Endothelial Cells; (edited by R.J. Gryglewski and P. Minuz),108-116 (2001).

[87] D.M. Lloyd-Jones and K.D. Bloch; Annual Review of Medicine, The Vascular Biology of Nitric Oxide and its Role in Atherogenesis, **47**, 365-375 (1996).

[88] C. Nathan and Q. Xie; Cell, Nitric Oxide: Roles, Tolls, Controls, **78**, 915-918 (1994).

[89] S. Miketic; J. Carlsson; and U. Tebbe; American Heart Journal, Randomized Comparison of J&J Crown Stent versus NIR Stent after Routine Coronary Angioplasty, **142** (5), E8 (2001).

[90] W.R. Gombotz; W. Guanghui; T.A. Horbett; and A.S. Hoffman; Journal of Biomedical Materials Research. Part B, Applied Biomaterials, Protein Adsorption to poly(ethylene oxide) surfaces, **25** (12), 1547-1562 (1991).

[91] S.M. Anderson; Clinical Microbiology Newsletter, Human Papillomavirus and Cervical Cancer, **24** (15), 113-118 (2002); K.R. Beutner; The American Journal of Medicine, Human Papillomavirus and Human Disease, **102** (5A), 9-15 (1997).

[92] W.C. Phelps; and K.A. Alexander; Annals of Internal Medicine, Antiviral Therapy for Human Papillomaviruses: Rationale and Prospects, **123**(5), 368-382 (1995).

[93] P.M. Howley; Transactions of the American Clinical and Climatological Association, Warts, Cancer and Ubiquitlation: Lessons from the Papillomaviruses, **117**, 113-127 (2006).

[94] K. Munger; A. Baldwin; K. M. Edwards; H. Hayakawa; C. L. Nguyen; M. Owens; M. Grace and K.W. Huh; Journal of Virology, Mechanisms of Human Papillomavirus-Induced Oncogenesis, **78** (21), 11451-11460 (2004).

[95] L. G. Koss; Human Pathology, Human Papillomavirus - Passenger, Driver or Both? **29** (4), 309-310 (1998).

[96] D. R. Lowy and J. T. Schiller; The Journal of Clinical Investigation, Prophylactic Human Papillomavirus Vaccines, **116** (5), 1167-1173 (2006).

[97] C.P. Crum; Modern Pathology, Contemporary Theories of Cervical Carcinogenesis: The Virus, The Host, and the Stem Cell, **13** (3),243-251 (2000).

[98] A.C. Armstrong and R.E. Hawkins; The British Journal of Radiology, Vaccines in Oncology: Background and Clinical Potential, **74**, 991-1002(2001).

[99] M. Frisch; Danish Medical Bulletin, On The Etiology of Anal Squamous Carcinoma, **49**, 194-209 (2002).

[100] M.L. Gillison and K.V. Shah; Journal of the National Cancer Institute Monograph, Chapter 9: Role of Mucosal Human Papillomavirus in Nongenital Cancers, **31**, 57-65 (2003).

[101] M. Schiffman and S.K. Kjaer; Journal of the National Cancer Institute Monograph, Chapter 2: Natural History of Anogenital Human Papillomavirus Infection and Neoplasia, **31**, 14-19 (2003).

[102] Center for Disease Control and Prevention, Morbidity and Mortality Weekly Report, Sexually Transmitted Diseases Treatment Guidelines 2002, **51,** RR-6 (2002).

[103] A.T. Lorincz; R. Reid; A.B. Jenson; M.D. Greenberg; W. Lancaster; R.J. Kurman; Obstetrics and Gynecoloy, Human papillomavirus infection of the cervix: relative risk associations of 15 common anogenital types, **79** (3), 328-337 (1992).

[104] H. Hunter Handsfield; The American Journal of Medicine, Clinical Presentation and Natural Course of Anogenital Warts, **102** (5A), 16-20 (1997).

[105] P.D. Indman; Colposcopy and Gynecologic Laser Surgery, Cone Biopsy of the Cervix with the Cabon Dioxide Laser: Report of 101 Cases in an Office Setting, **3**, 205 (1987).

[106] T. Peters; The Cosmetic Treatment with Nitric Oxide, Device for Performing said Treatment and Manufacturing Method Therefor,WO2006/100154 A1, PCT/EP2006/050884 (2006).

[107] 1). D.R. Lowy and EJ Androphy;In: Fitzpatrick's Dermatology in General Medicine, Warts.(5th Edition, McGraw Hill, New York), 2484-2497; 2).W.M. Pringle and D.C. Helms; Achives of Dermatology, Treatment of Plantar Warts by Blunt Dissection, **108** (1), 79-82 (1973).

[108] L. Lubich, O. V. Boyarkin, R. D. F. Settle, D. S. Perry, and R. T. Rizzo, Faraday Discussions **1995,102**, 167 (1996).

[109] R.B. Silverman; The Organic Chemistry of Drug Design and Drug Action, 2nd Edition, 2004, pg. 298-302.

APPENDICES

APPENDIX A

MASS SPECTROMETRY SPECTRA OF POLYETYHLENE GLYCOL

DIAMINOBUTANE POLYMER

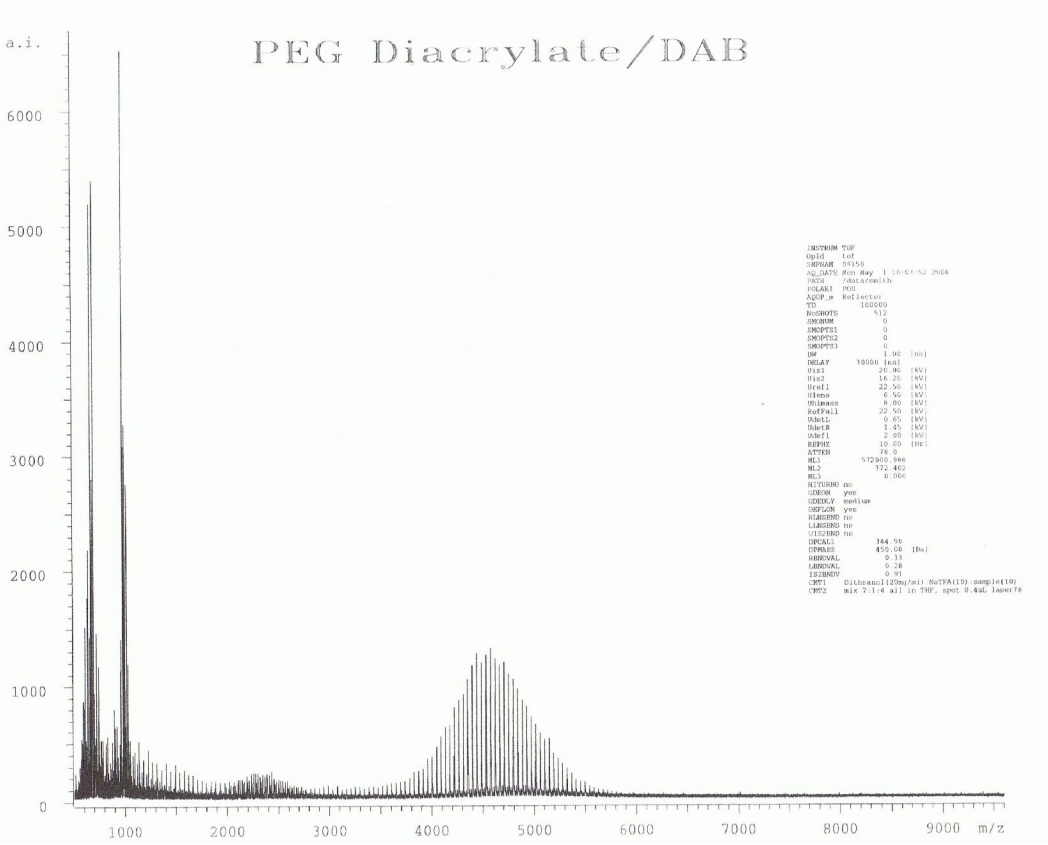

Mass Spectrum of PEG Diacrylate Diaminobutane taken at 3 months.

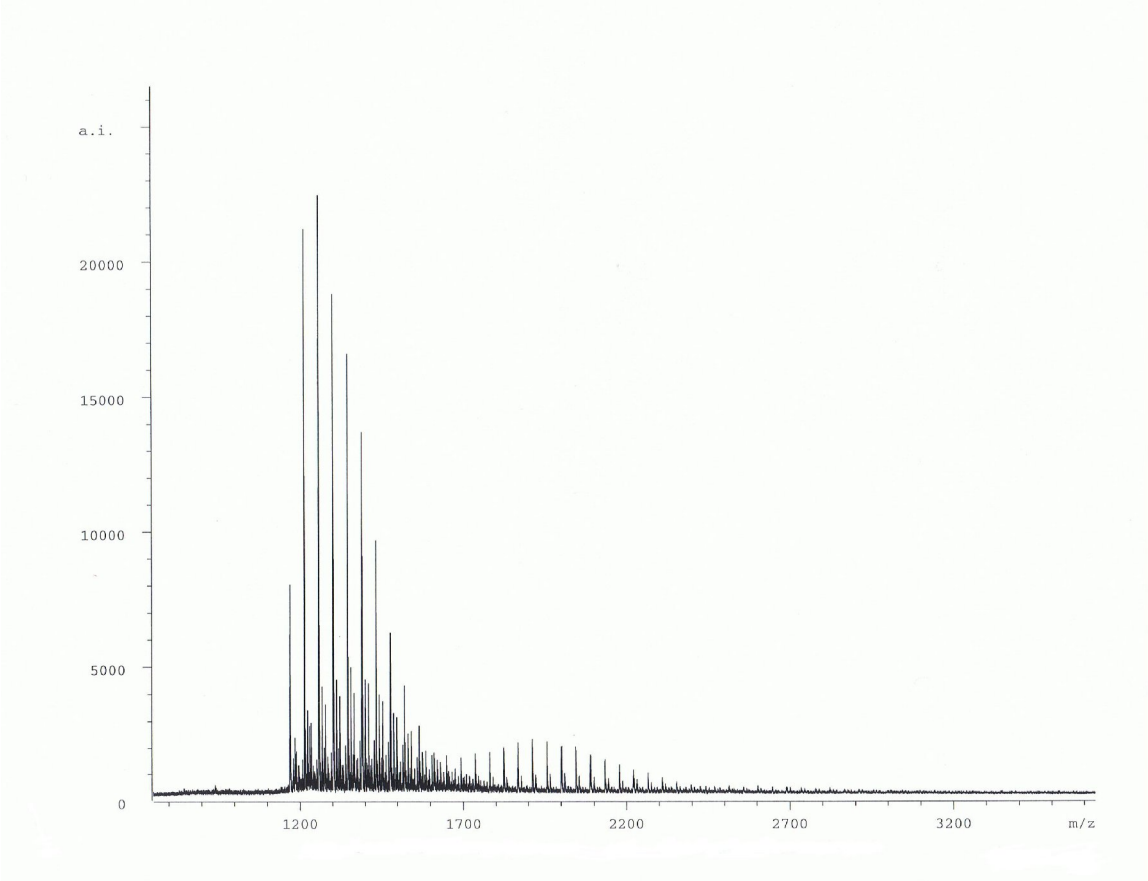

Mass spectrum of PEG Diacrylate Diaminobutane at 24 months.

APPENDIX B

MASS SPECTROMETRY FOR THE DETERMINATION OF END GROUPS WITHIN POLYETHYLENE GLYCOL DIAMINOBUTANE POLYMER

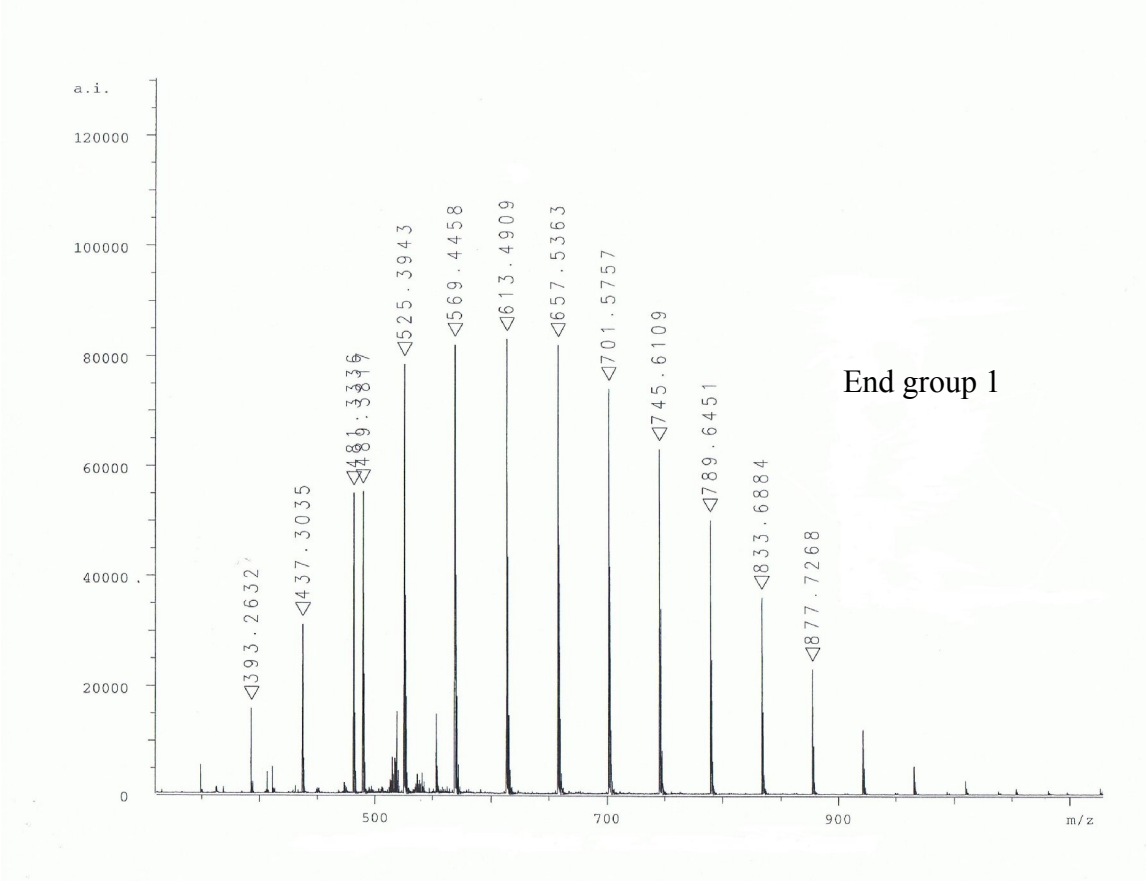

Mass Spectra of PEG Diacrylate Diaminobutane at magnified mass to charge ratios, used to determine the end groups for the polymer at 24 month timepoint. This spectrum represents end group 1.

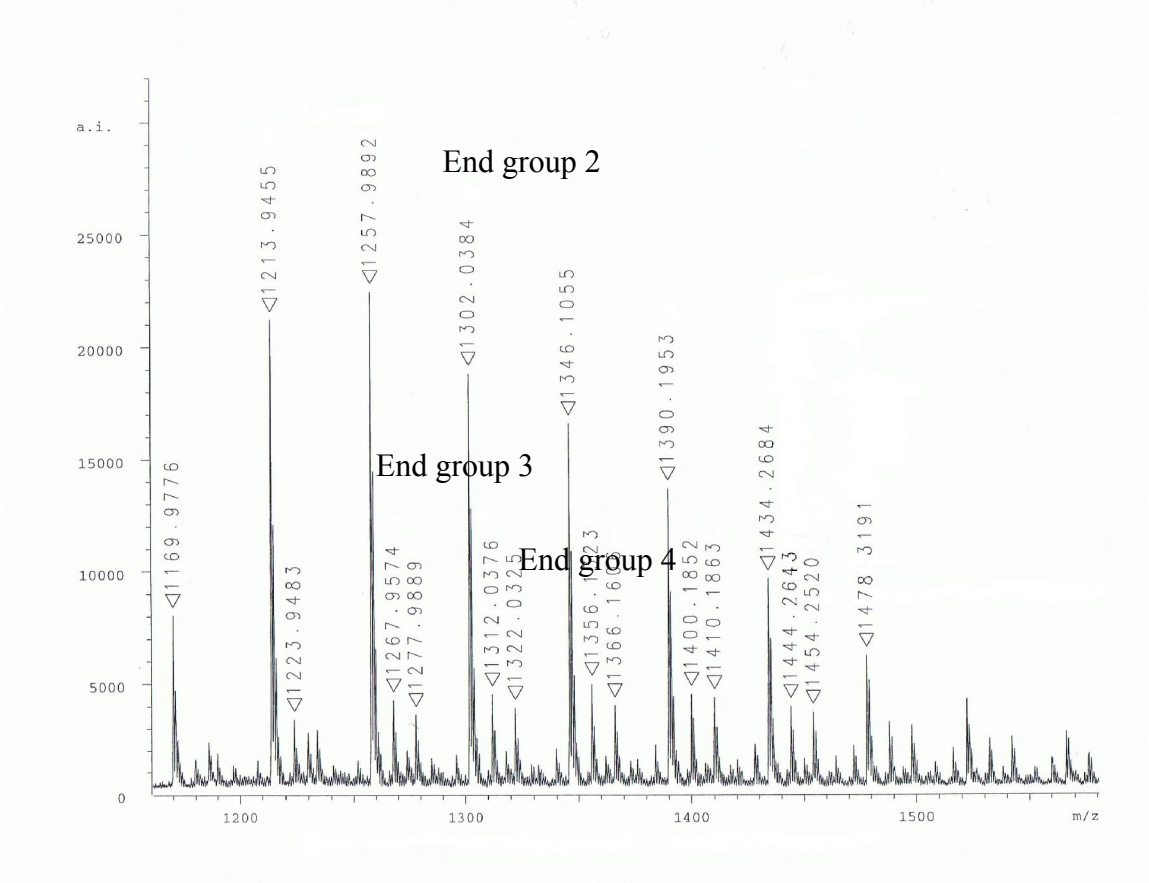

Mass Spectra of PEG Diacrylate Diaminobutane at magnified mass to charge ratios, used to determine the end groups for the polymer at 24 month timepoint. This spectrum represents end groups 2, 3 and 4.

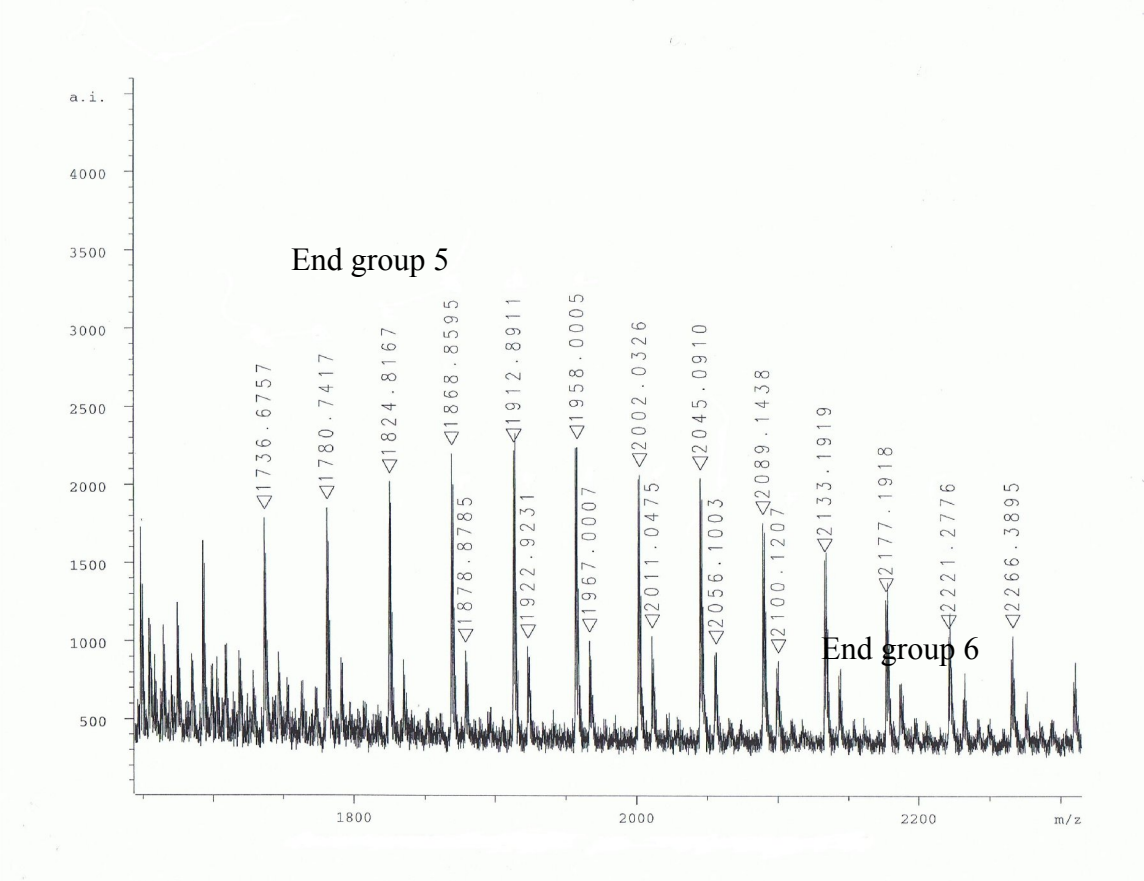

Mass Spectra of PEG Diacrylate Diaminobutane at magnified mass to charge ratios, used to determine the end groups for the polymer at 24 month timepoint. This spectrum represents end groups 5 and 6.

APPENDIX C

MASS SPECTROMETRY SPECTRA OF POLYETYHLENE GLYCOL

ETHYLDIAMINE POLYMER

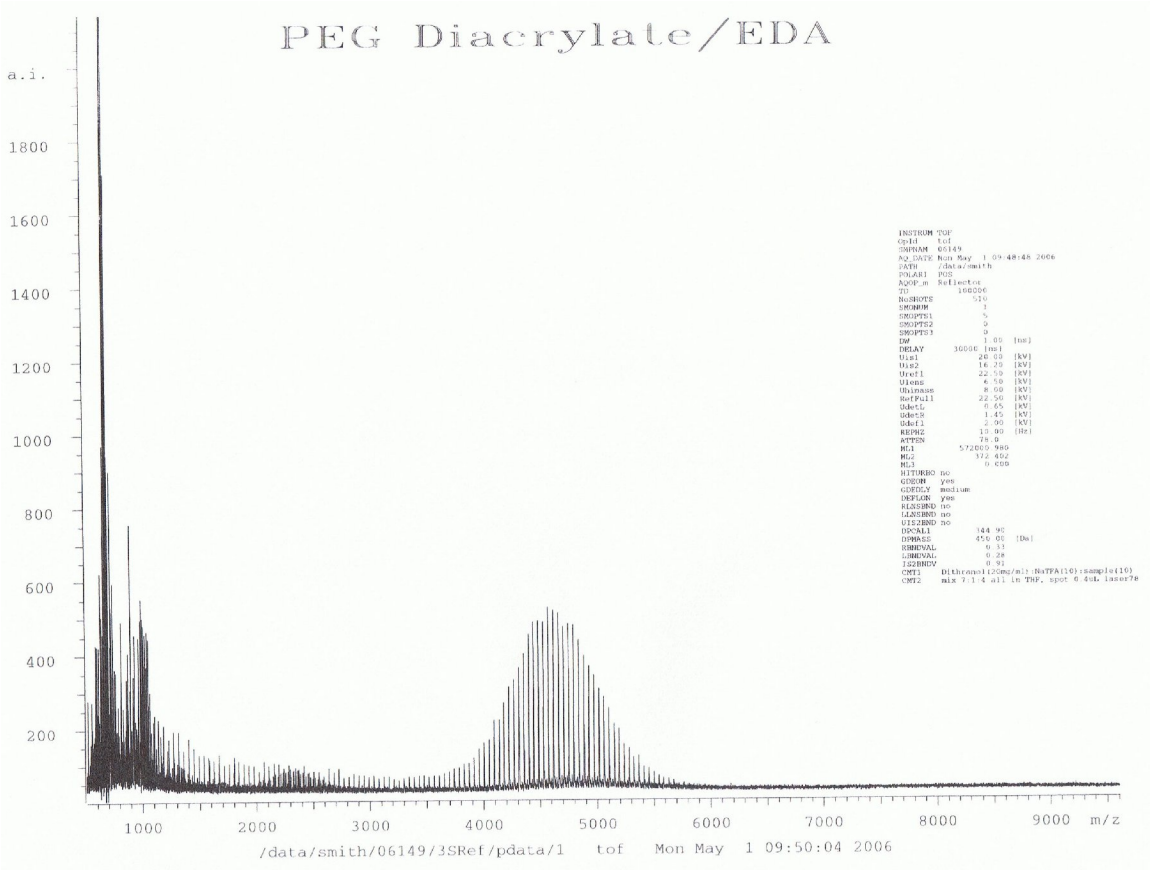

Mass Spectrum of PEG Diacrylate Ethylenediamine taken at 3 months.

APPENDIX D

MASS SPECTROMETRY SPECTRA FOR THE DETERMINATION OF END GROUPS WITHIN POLYETHYLENE GLYCOL ETHYLDIAMINE POLYMER

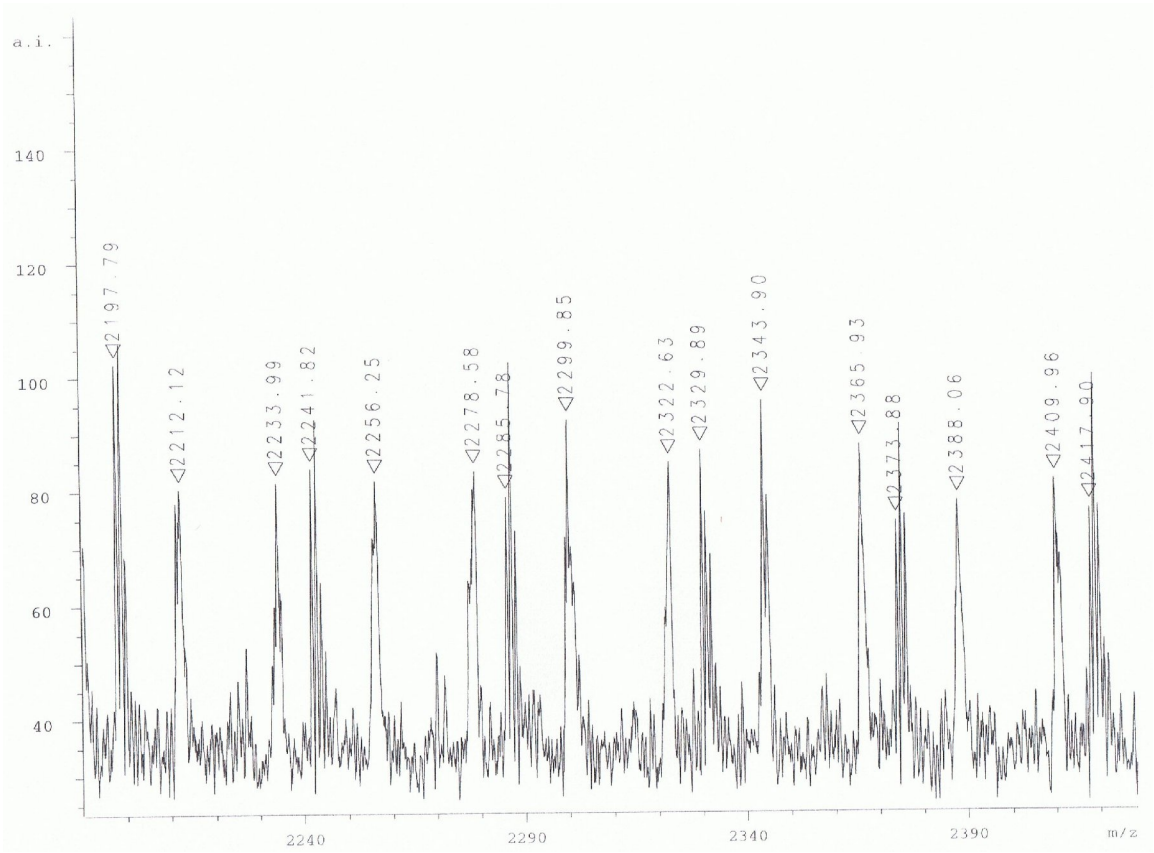

APPENDIX E

H1 NMR SPECTRUM OF POLYETHYLENE DIAMINOBUTANE NONOATE

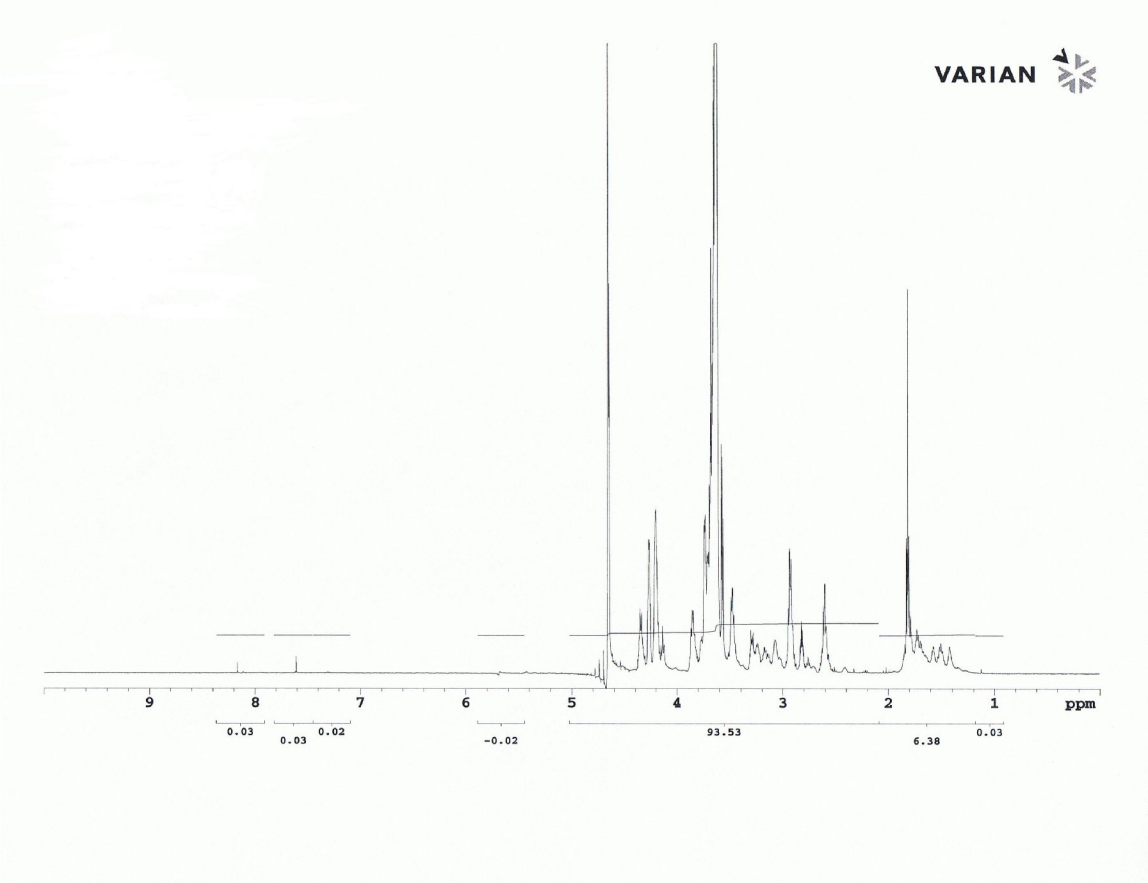

APPENDIX F

C13 NMR SPECTRUM OF POLYEHTYLENE DIAMINOBUTANE NONOATE

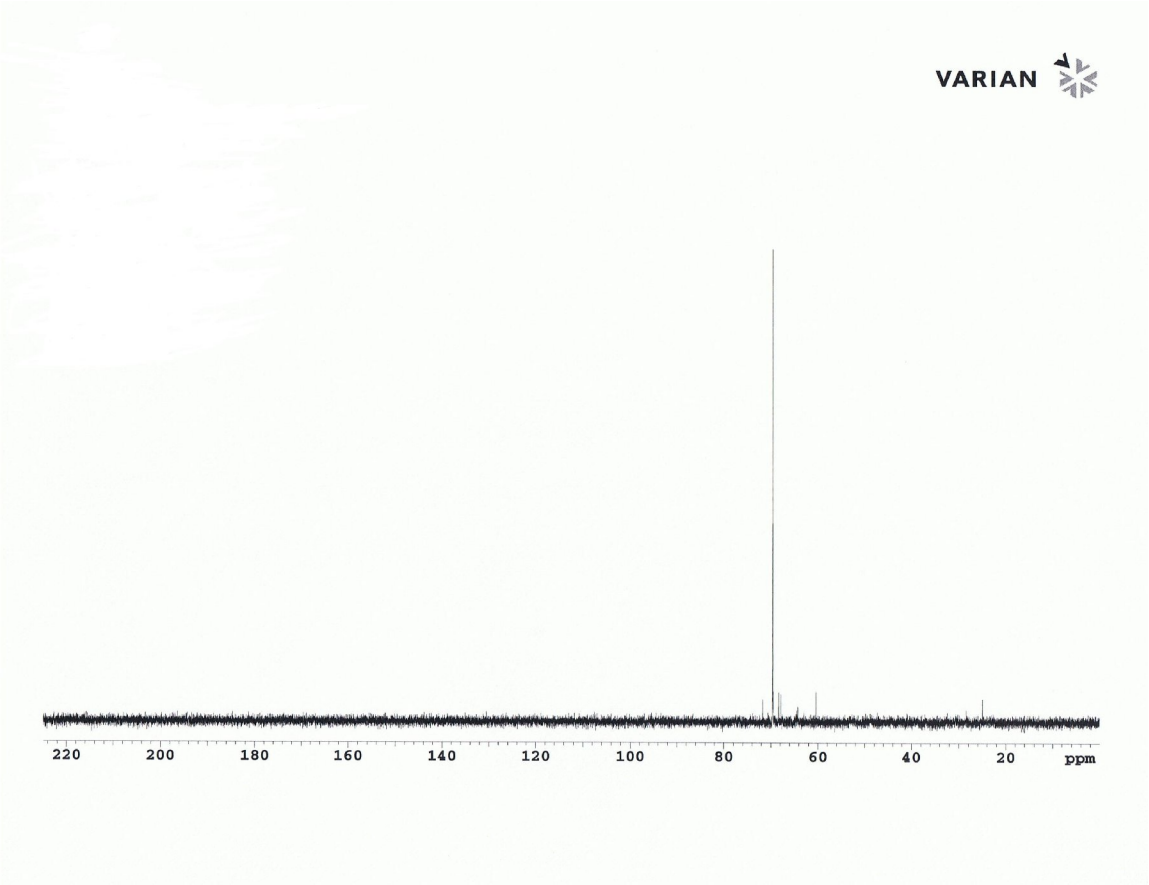

APPENDIX G

H1 NMR SPECTRUM OF POLYETHYLENE ETHYLDIAMINE NONOATE

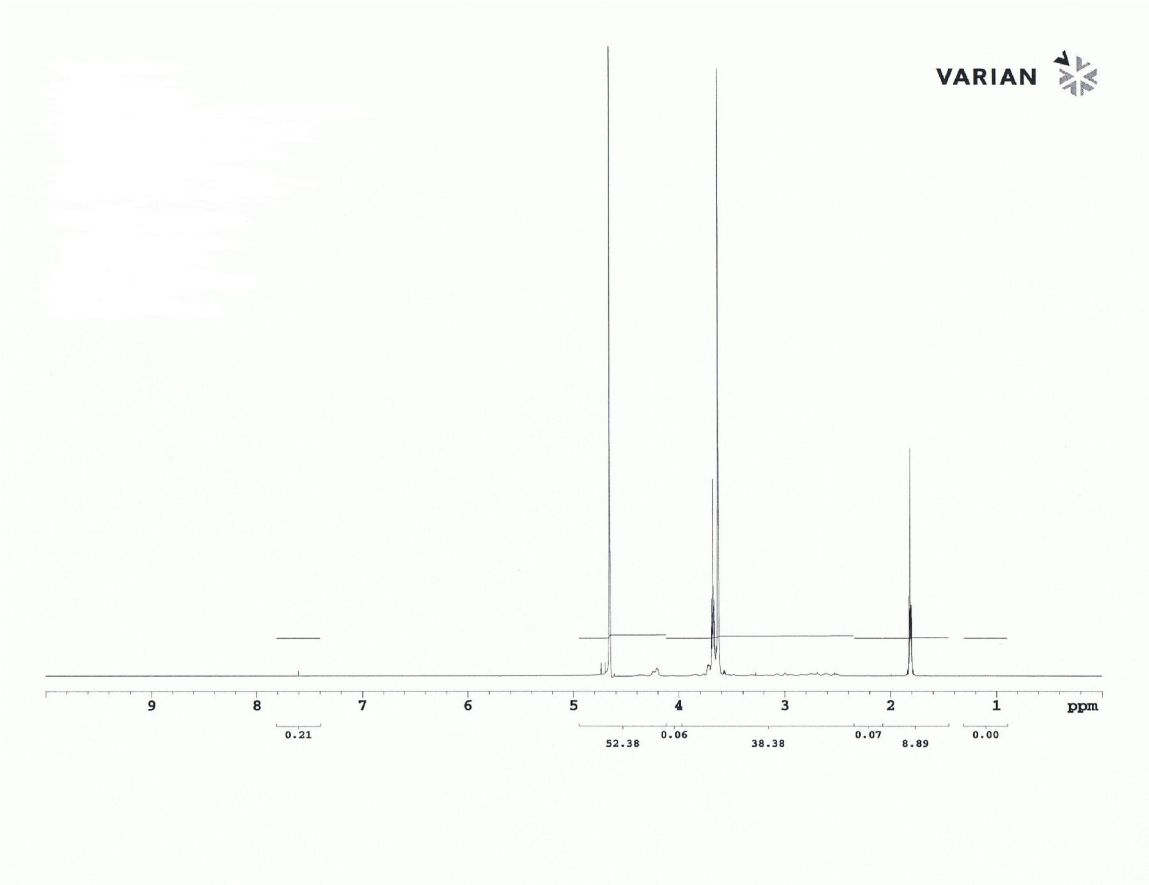

APPENDIX H

C13 NMR SPECTRUM OF POLYETHYLENE ETHYLDIAMINE NONOATE

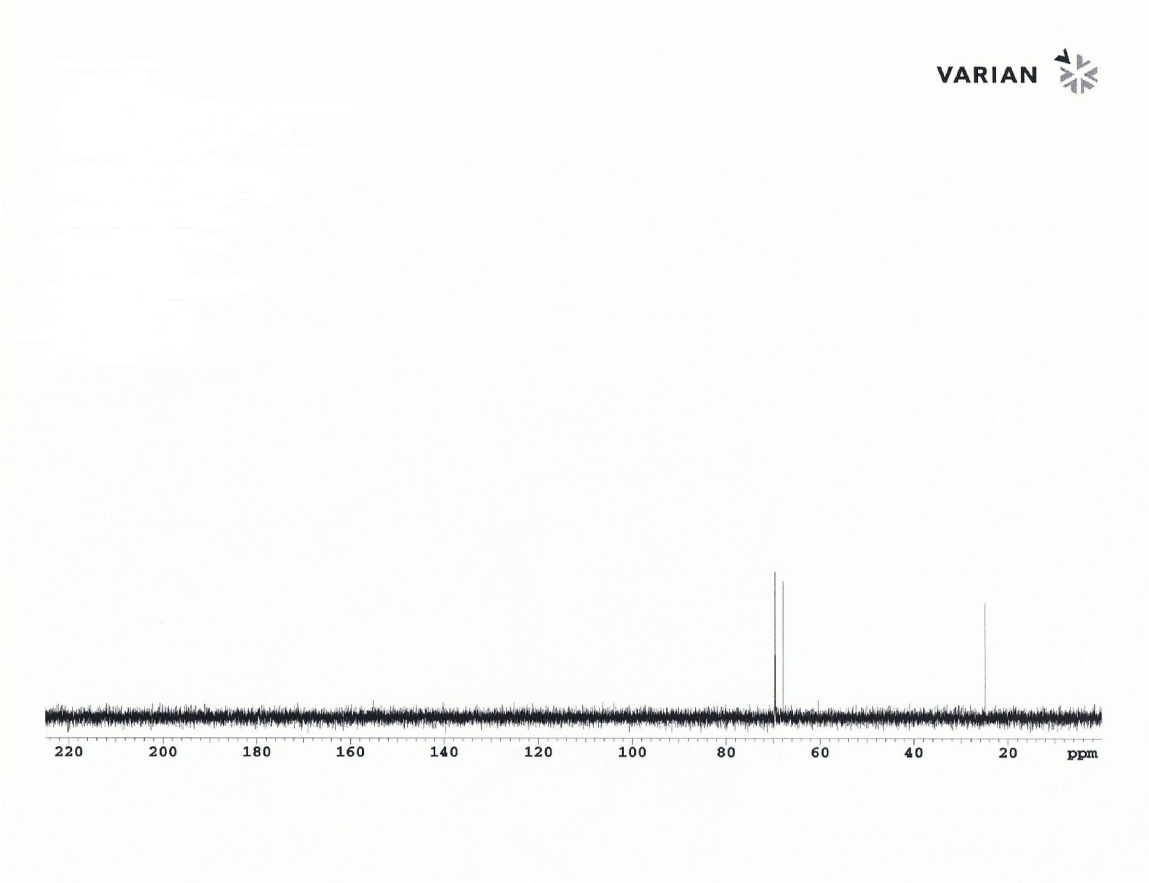

APPENDIX I

RAW DATA FOR THE BIOAVAILABILITY OF CANCER CELLS
UTILIZING DIETHYLSPERMATE NONOATE

Raw data collected over several months utilizing cervical cancer cell lines HeLa (H), CaSki (Ca) and C33A (C33).

Table I1. Cell line data set with the drug and DMSO concentration to determine p-Alive value

	(a)	(b)	(C)	(d)
Cell Line	**DMSO**	**Drug**	**Replicate**	**P-Alive**
C33	0.2	0	1	83.3
C33	0.2	0	2	84.6
C33	0.2	0	3	83.1
C33	0.2	0	4	80.7
C33	0.2	0	5	74.6
C33	0.2	0	6	87.3
C33	0.6	0	1	80.3
C33	0.6	0	2	75.4
C33	0.6	0	3	77.9
C33	0.6	0	4	73.3
C33	0.6	500	1	82.4
C33	0.6	500	2	78.3
C33	0.6	500	3	66.3
C33	0.6	500	4	61.9
C33	0.6	500	5	65.9
C33	0.6	500	6	62.1
C33	0.36	300	1	81.7
C33	0.36	300	2	78.1
C33	0.36	300	3	79.9
C33	0.36	300	4	39.9
C33	0.36	300	5	63
C33	0.36	300	6	65
C33	0.12	100	1	77.9
C33	0.12	100	2	83.5
C33	0.12	100	3	75
C33	0.12	100	4	81.2
C33	0.12	100	5	61.6
C33	0.12	100	6	72

RAW DATA FOR THE BIOAVAILABILITY OF CANCER CELLS
UTILIZING DIETHYLSPERMATE NONOATE (continued)

C33	0.12	100	6	72
C33	0.06	50	1	75.3
C33	0.06	50	2	85.7
C33	0.06	50	3	78.7
C33	0.06	50	4	78.8
C33	0.06	50	5	63.8
C33	0.06	50	6	68.7
C33	0.012	10	1	70
C33	0.012	10	2	76.9
C33	0.012	10	3	76.9
C33	0.012	10	4	86.3
C33	0.012	10	5	73.7
C33	0.012	10	6	75.6
C33	0.012	10	7	71.3
Ca	0.2	0	1	89.2
Ca	0.2	0	2	85.3
Ca	0.2	0	3	89.4
Ca	0.2	0	4	83.6
Ca	0.2	0	5	73.2
Ca	0.2	0	6	84.6
Ca	0.6	0	1	81.6
Ca	0.6	0	2	83.2
Ca	0.6	0	3	80
Ca	0.6	0	4	85.8
Ca	0.6	0	5	75
Ca	0.6	0	6	79.3
Ca	0.6	500	1	63.4
Ca	0.6	500	2	75
Ca	0.6	500	3	73.7
Ca	0.6	500	4	86.3
Ca	0.6	500	5	61.7
Ca	0.6	500	6	74.4
Ca	0.36	300	1	62.3
Ca	0.36	300	2	72.3
Ca	0.36	300	3	71.4
Ca	0.36	300	4	67.7
Ca	0.36	300	5	69.7
Ca	0.36	300	6	75.7
Ca	0.12	100	1	71.3
Ca	0.12	100	2	69.9
Ca	0.12	100	3	67.6
Ca	0.12	100	4	70.8
Ca	0.12	100	5	76.8
Ca	0.12	100	6	70

RAW DATA FOR THE BIOAVAILABILITY OF CANCER CELLS
UTILIZING DIETHYLSPERMATE NONOATE (continued)

Ca	0.06	50	1	67.2
Ca	0.06	50	2	64.7
Ca	0.06	50	3	77.4
Ca	0.06	50	4	81.7
Ca	0.06	50	5	71.4
Ca	0.06	50	6	74.3
Ca	0.012	10	1	77.9
Ca	0.012	10	2	84.8
Ca	0.012	10	3	73
Ca	0.012	10	4	78.5
Ca	0.012	10	5	64.6
Ca	0.012	10	6	79.9
H	0.2	0	1	96.9
H	0.2	0	2	78.2
H	0.2	0	3	72
H	0.2	0	4	75.9
H	0.2	0	5	90.6
H	0.2	0	6	76.1
H	0.6	0	1	79.1
H	0.6	0	2	74.6
H	0.6	0	3	87.3
H	0.6	0	4	63
H	0.6	0	5	70.2
H	0.6	0	6	81.6
H	0.6	500	1	30
H	0.6	500	2	9.4
H	0.6	500	3	39.5
H	0.6	500	4	57.4
H	0.6	500	5	42.1
H	0.6	500	6	39.6
H	0.36	300	1	57.6
H	0.36	300	2	33.2
H	0.36	300	3	60.7
H	0.36	300	4	40
H	0.36	300	5	35.7
H	0.36	300	6	58.1
H	0.36	300	7	46.4
H	0.12	100	1	48.3
H	0.12	100	2	26.4
H	0.12	100	3	52.1
H	0.12	100	4	43.1
H	0.12	100	5	61.7
H	0.12	100	6	49.4

RAW DATA FOR THE BIOAVAILABILITY OF CANCER CELLS
UTILIZING DIETHYLSPERMATE NONOATE (continued)

H	0.06	50	1	56.3
H	0.06	50	2	39.5
H	0.06	50	3	52.7
H	0.06	50	4	32.4
H	0.06	50	5	66.2
H	0.06	50	6	66.8
H	0.012	10	1	78
H	0.012	10	2	50
H	0.012	10	3	71.1
H	0.012	10	4	58.3
H	0.012	10	5	82.6
H	0.012	10	6	62

APPENDIX J

STATISTICAL REPORT OF THE CELL BIOAVAILABILITY ANALYSIS

Variables: DMSO, drug, cell line, P_alive , replication

The variable dmsoX1000 equals 1000 times of DMSO concentration. There are 7 combinations of the drug and the DMSO. The frequencies for each combination are presented in the table J.1 below.

Table J.1 Testing Grid used for the Determination of a Testing Plan

	dmsoX1000						
Drug	12	60	120	200	360	600	Total
0	0	0	0	18	0	16	34
10	19	0	0	0	0	0	19
50	0	18	0	0	0	0	18
100	0	0	18	0	0	0	18
300	0	0	0	0	19	0	19
500	0	0	0	0	0	18	18
Total	19	18	18	18	19	34	126

We define a variable design, determined of the combination of the drug and the DMSO. The order of the variable design is the same as for the variable drug. Table J.2 below defines the codes for the variable design.

Table J.2 Concentration of DMSO within each Drug Preparation

Design	**Drug**	**dmsoX1000**
1	0	200
2	0	600
3	10	12
4	50	60
5	100	120
6	300	360
7	500	600

Table J.3 shows the frequencies for the replication for each combination of drug and DMSO. They are presented in terms of the variable design, since it uniquely identifies the combination, and the three cell lines. All combinations are replicated 6 times, with the following 3 exceptions: one combination is replicated 4 times, and two are replicated 7 times.

Table J.3 Complete Testing Schematic for each Cell Line at the differing concentrations

	Design							
Cell Line	**1**	**2**	**3**	**4**	**5**	**6**	**7**	**Total**
C33	**6**	**4**	**7**	**6**	**6**	**6**	**6**	**41**
Ca	**6**	**6**	**6**	**6**	**6**	**6**	**6**	**42**
H	**6**	**6**	**6**	**6**	**6**	**7**	**6**	**43**
Total	**18**	**16**	**19**	**18**	**18**	**19**	**18**	**126**

Next, for each combination of a drug and DMSO, we calculate the average proportion of alive cells after the treatment. The variable design is ordered in increasing order of the drug, and we can see a general trend for a decrease of the proportion of alive in higher drug dosage as seen in Table J.4. For each cell, the number of replication used to obtain the average is reported in the Table J.3 above.

.

Table J.4 The Average Proportion of Alive Cells Per Concentrations for each Cell Line

	Design						
Cell Line	1	2	3	4	5	6	**7**
C33	82.27	76.73	75.81	75.17	75.20	67.93	69.48
Ca	84.22	80.82	76.45	72.78	71.07	69.85	72.42
H	81.62	75.97	67.00	52.32	46.83	47.39	36.33
Total	**82.70**	**77.97**	**73.23**	**66.76**	**64.37**	**60.97**	**59.41**

Next, we will use one-way ANOVA to determine if the mean values for each treatment are significantly different in each cell line separately.

Cell line = C33
There are total of 41 replications and the F test for the difference in means has a p-value of .12. We conclude that there is no significant difference between the different

combinations of drug and DMSO. (i.e. between the different levels of the variable design).

Cell line = Ca
There are total of 42 replications and the F test for the difference in means has a p-value of 0.01. We conclude that there is significant difference between the different combinations of drug and DMSO.

Cell line = H
There are total of 43 replications and the F test for the difference in means has a p-value smaller than 0.001. We conclude that there is significant difference between the different combinations of drug and DMSO.

We have concluded significant differences between the combinations of drug and DMSO in the cell lines Ca and H. Next, we will look more closely which treatments are different From the treatment in design=7.

The ANOVA analysis suggests that the combinations of treatments in designs {6,5,4,3} are not significantly different from the design 7. The two treatments in designs {1,2} are significantly different from design 7. The designs 1 and 2 correspond to the drug concentration of 0.

Cell line = Ca
Similar analysis reveals that the treatments defined as design=7 is not significantly different from the treatments in designs {6,5}, but is different from the other treatments.

APPENDIX K

RAW DATA FROM NOA AND UV/VIS ANALYSIS OF DIAZENIUMDIOLATES

Table K1. NOA NO Release Profile Data for Dihexyl spermeate Nonoate

NOA NO Release Profile	
DHSNO (nmole)	Time
0.0015	5.0000
0.0022	15.0000
0.0056	30.0000
0.0074	45.0000
0.0098	60.0000
0.0118	75.0000
0.0139	90.0000
0.0152	105.0000
0.0163	120.0000
0.0171	135.0000
0.0179	150.0000
0.0188	165.0000
0.0198	180.0000
0.0216	195.0000
0.0245	210.0000
0.0304	225.0000
0.0416	240.0000
0.0586	255.0000
0.0928	270.0000
0.1386	285.0000
0.1892	300.0000
0.2550	315.0000
0.3325	330.0000
0.4141	345.0000
0.4969	360.0000
0.5854	375.0000
0.6812	390.0000
0.7594	405.0000
0.8538	420.0000
0.9129	435.0000
0.9629	450.0000
1.0035	465.0000

Table K.2 NOA NO Release Profile of Diazeniumdiolates

NOA Diazeniumdiolate Profile						
Time	DTBSNO	DLSNO	PEG/DABNO	DISOSNO	DtBSNO	DMSNO
5.00000	0.00042	0.00140	0.00032	0.00142	0.00028	0.00002
15.00000	0.00073	0.00265	0.00038	0.00146	0.00029	0.00033
30.00000	0.00103	0.00400	0.00077	0.00153	0.00029	0.00047
45.00000	0.00146	0.00608	0.00116	0.00161	0.00030	0.00058
60.00000	0.00174	0.00809	0.00167		0.00030	0.00069
75.00000	0.00192	0.01139	0.00224		0.00030	0.00072
90.00000	0.00219	0.01378	0.00284		0.00030	0.00084
105.00000	0.00242	0.01684	0.00342		0.00030	0.00095
120.00000	0.00264	0.01981	0.00411		0.00031	0.00106
135.00000	0.00288	0.02271	0.00484		0.00032	0.00117
150.00000	0.00310	0.02622	0.00557		0.00033	0.00128
165.00000	0.00328	0.02958	0.00626		0.00034	0.00140
180.00000	0.00343	0.03264	0.00705		0.00040	0.00148
195.00000	0.00364	0.03812	0.00770		0.00043	
210.00000	0.00386	0.04018	0.00847		0.00044	
225.00000	0.00406	0.04183	0.00915		0.00046	
240.00000	0.00426	0.04337	0.00997		0.00047	
255.00000	0.00445	0.04421	0.01063		0.00048	
270.00000	0.00465	0.04508	0.01153		0.00058	
285.00000	0.00487	0.04588	0.01237		0.00066	
300.00000	0.00509	0.04648	0.01334		0.00071	
315.00000	0.00523	0.04699	0.01424			
330.00000	0.00541	0.04748	0.01526			
345.00000	0.00559	0.04789	0.01629			
360.00000	0.00582	0.04820	0.01722			
375.00000	0.00600	0.04879	0.01812			
390.00000	0.00617	0.04922	0.01918			
405.00000	0.00632		0.02036			
420.00000	0.00651		0.02147			
435.00000	0.00671		0.02282			
450.00000	0.00691		0.02413			
465.00000	0.00711		0.02566			
480.00000			0.02725			
495.00000			0.02885			
510.00000			0.03062			
525.00000			0.03227			

Table K.3 Absorbance Data for Diazeniumdiolates utilizing Greiss Reagent

Raw Data for Diazeniumdiolatesfrom UV/VIS analysis of Greiss Reagent							
Time (min)	DTBSNO	DLSNO	DHSNO	DISOSNO	DEANO	DEEDANO	PEG/DABNO
0	-0.002	0.000	0.127	-0.002	0.028	0.006	-0.014
3	-0.001	-0.001	0.103	-0.003	0.026	0.034	-0.014
6	-0.001	-0.001	0.097	-0.004	0.026	0.037	-0.014
9	-0.001	-0.001	0.093	-0.005	0.026	0.022	-0.014
12	-0.002	-0.001	0.092	-0.006	0.025	0.011	-0.014
15	-0.001	-0.001	0.090	-0.006	0.025	0.003	-0.014
18	-0.001	-0.001	0.087	-0.006	0.025	0.000	-0.014
21	0.000	-0.002	0.085	-0.006	0.025	-0.001	-0.014
24	0.000	-0.002	0.084	-0.006	0.025	-0.001	-0.013
27	0.001	-0.002	0.083	-0.006	0.025	-0.001	-0.013
30	0.001	-0.001	0.082	-0.006	0.025	-0.001	-0.012
33	0.002	-0.002	0.083	-0.006	0.026	-0.001	-0.011
36	0.002	-0.002	0.081	-0.006	0.026	-0.001	-0.010
39	0.002	-0.001	0.081	-0.005	0.027	0.000	-0.008
42	0.002	-0.001	0.081	-0.005	0.027	0.000	-0.005
45	0.002	-0.001	0.080	-0.005	0.028	0.000	-0.002
48	0.002	-0.001	0.080	-0.005	0.028	0.000	0.001
51	0.003	-0.001	0.080	-0.005	0.028	0.000	0.004
54	0.003	-0.001	0.079	-0.005	0.011	0.001	0.008
57	0.003	0.000	0.079	-0.005	0.012	0.001	0.014
60	0.003	0.000	0.079	-0.005	0.012	0.001	0.019
63	0.003	0.000	0.078	-0.004	0.013	0.001	0.024
66	0.003	0.000	0.079	-0.004	0.013	0.002	0.027
69	0.004	0.001	0.079	-0.004	0.014	0.002	0.029
72	0.003	0.001	0.078	-0.004	0.014	0.002	0.031
75	0.003	0.001	0.079	-0.004	0.015	0.003	0.034
78	0.004	0.002	0.078	-0.004	0.015	0.003	0.035
81	0.004	0.002	0.078	-0.004	0.016	0.003	0.037
84	0.004	0.002	0.079	-0.004	0.016	0.004	0.039
87	0.005	0.003	0.079	-0.004	0.017	0.004	0.040
90	0.005	0.003	0.079	-0.004	0.017	0.004	0.042
93	0.006	0.004	0.078	-0.004	0.018	0.004	0.044
96	0.006	0.004	0.079	-0.004	0.018	0.005	0.046
99	0.006	0.004	0.078	-0.004	0.019	0.005	0.047
102	0.006	0.005	0.079	-0.004	0.019	0.006	0.048
105	0.007	0.005	0.079	-0.004	0.020	0.006	0.050
108	0.007	0.006	0.079	-0.004	0.020	0.006	0.052
111	0.007	0.006	0.079	-0.003	0.021	0.007	0.054
114	0.007	0.006	0.079	-0.003	0.021	0.007	0.057
117	0.008	0.007	0.080	-0.003	0.021	0.007	0.059
120	0.008	0.007	0.079	-0.003	0.022	0.008	0.062

Table K.3 Absorbance Data for Diazeniumdiolates utilizing Greiss Reagent (continued)

123	0.008	0.008	0.080	-0.003	0.022	0.008	0.064
126	0.008	0.008	0.080	-0.002	0.023	0.008	0.066
129	0.009	0.009	0.080	-0.002	0.023	0.009	0.069
132	0.009	0.009	0.080	-0.002	0.023	0.009	0.071
135	0.009	0.010	0.080	-0.001	0.024	0.009	0.074
138	0.009	0.010	0.081	-0.001	0.024	0.009	0.077
141	0.010	0.011	0.081	-0.001	0.024	0.010	0.080
144	0.010	0.011	0.081	-0.001	0.025	0.010	0.083
147	0.010	0.011	0.081	0.000	0.025	0.010	0.086
150	0.010	0.012	0.081	0.000	0.025	0.011	0.088
153	0.011	0.012	0.082	0.000	0.026	0.011	0.092
156	0.011	0.013	0.082	0.000	0.026	0.011	0.095
159	0.011	0.013	0.082	0.000	0.026	0.012	0.098
162	0.012	0.014	0.083	0.000	0.027	0.012	0.101
165	0.012	0.015	0.083	0.000	0.027	0.012	0.104
168	0.012	0.016	0.084	0.000	0.027	0.012	0.107
171	0.012	0.017	0.083	0.000	0.028	0.013	0.110
174	0.013	0.018	0.084	0.000	0.028	0.013	0.112
177	0.013	0.019	0.084	0.000	0.028	0.013	0.114
180	0.013	0.020	0.084	0.000	0.028	0.014	0.117
183	0.013	0.021	0.084	0.000	0.029	0.014	0.120
186	0.014	0.021	0.085	-0.001	0.029	0.014	0.123
189	0.014	0.022	0.085	0.000	0.029	0.014	0.125
192	0.014	0.023	0.086	0.000	0.030	0.015	0.128
195	0.014	0.023	0.086	0.000	0.030	0.015	0.130
198	0.015	0.023	0.086	0.000	0.030	0.015	0.132
201	0.015	0.024	0.086	0.000	0.030	0.016	0.134
204	0.015	0.024	0.087	0.000	0.031	0.016	0.136
207	0.016	0.025	0.087	0.000	0.031	0.016	0.138
210	0.016	0.025	0.088	0.000	0.031	0.016	0.141
213	0.016	0.026	0.088	0.000	0.031	0.016	0.143
216	0.017	0.026	0.088	0.000	0.032	0.017	0.146
219	0.017	0.027	0.088	0.000	0.032	0.017	0.148
222	0.017	0.027	0.088	0.000	0.032	0.017	0.151
225	0.017	0.028	0.089	0.000	0.032	0.018	0.154
228	0.017	0.029	0.089	0.000	0.033	0.018	0.157
231	0.017	0.029	0.089	0.001	0.033	0.018	0.159
234	0.018	0.030	0.089	0.001	0.033	0.018	0.162
237	0.018	0.030	0.089	0.001	0.033	0.018	0.165
240	0.018	0.031	0.089	0.001	0.034	0.019	0.167
243	0.018	0.031	0.090	0.001	0.034	0.019	0.170
246	0.019	0.032	0.090	0.001	0.034	0.019	0.173
249	0.019	0.032	0.090	0.002	0.034	0.019	0.176
252	0.019	0.033	0.091	0.002	0.034	0.020	0.178
255	0.019	0.034	0.091	0.002	0.034	0.020	0.180

Table K.3 Absorbance Data for Diazeniumdiolates utilizing Greiss Reagent (continued)

258	0.019	0.034	0.091	0.002	0.035	0.020	0.183
261	0.020	0.035	0.091	0.003	0.035	0.021	0.185
264	0.020	0.035	0.092	0.003	0.035	0.021	0.187
267	0.020	0.036	0.093	0.003	0.035	0.021	0.189
270	0.020	0.037	0.093	0.003	0.035	0.021	0.191
273	0.020	0.037	0.093	0.004	0.036	0.021	0.192
276	0.020	0.038	0.093	0.004	0.036	0.022	0.194
279	0.021	0.038	0.094	0.004	0.036	0.022	0.195
282	0.021	0.039	0.094	0.004	0.036	0.022	0.197
285	0.021	0.039	0.095	0.004	0.036	0.022	0.198
288	0.022	0.040	0.095	0.005	0.037	0.022	0.199
291	0.022	0.041	0.095	0.005	0.037	0.022	0.200
294	0.022	0.041	0.096	0.005	0.037	0.022	0.201
297	0.023	0.042	0.097	0.005	0.037	0.022	0.202
300	0.023	0.042	0.096	0.005	0.037	0.022	0.202
303	0.023	0.043	0.097	0.006	0.037	0.023	0.203
306	0.023	0.043	0.098	0.006	0.038	0.023	0.204
309	0.024	0.044	0.097	0.006	0.038	0.023	0.204
312	0.024	0.044	0.098	0.006	0.038	0.023	0.205
315	0.024	0.045	0.098	0.006	0.038	0.023	0.205
318	0.025	0.045	0.099	0.007	0.038	0.024	0.206
321	0.025	0.046	0.099	0.007	0.038	0.024	0.206
324	0.025	0.046	0.099	0.007	0.038	0.024	0.207
327	0.025	0.047	0.100	0.007	0.038	0.025	0.207
330	0.026	0.047	0.100	0.007	0.039	0.025	0.208
333	0.026	0.048	0.100	0.007	0.039	0.025	0.208
336	0.026	0.048	0.101	0.007	0.039	0.025	0.208
339	0.027	0.049	0.101	0.008	0.039	0.026	0.208
342	0.027	0.049	0.102	0.008	0.039	0.026	0.208
345	0.027	0.050	0.102	0.008	0.039	0.026	0.208
348	0.027	0.050	0.102	0.008	0.039	0.026	0.209
351	0.027	0.051	0.103	0.009	0.040	0.026	0.209
354	0.028	0.051	0.103	0.009	0.040	0.027	0.209
357	0.028	0.052	0.104	0.009	0.040	0.027	0.209
360	0.028	0.052	0.104	0.009	0.040	0.027	0.209
363	0.029	0.053	0.104	0.009	0.040	0.028	0.209
366	0.029	0.053	0.105	0.010	0.040	0.028	0.210
369	0.029	0.054	0.105	0.010	0.040	0.028	0.209
372	0.029	0.054	0.105	0.010	0.040	0.028	0.210
375	0.030	0.054	0.105	0.010	0.040	0.029	0.210
378	0.030	0.055	0.106	0.010	0.041	0.029	0.210
381	0.030	0.055	0.106	0.010	0.041	0.029	0.210
384	0.030	0.056	0.106	0.011	0.041	0.029	0.210
387	0.031	0.056	0.106	0.011	0.041	0.029	0.210
390	0.031	0.057	0.107	0.011	0.041	0.029	0.210

Table K.3 Absorbance Data for Diazeniumdiolates utilizing Greiss Reagent (continued)

393	0.031	0.057	0.107	0.011	0.041	0.030	0.210
396	0.031	0.058	0.108	0.011	0.041	0.030	0.210
399	0.032	0.058	0.108	0.012	0.041	0.030	0.210
402	0.032	0.059	0.109	0.012	0.041	0.030	0.211
405	0.032	0.059	0.109	0.012	0.041	0.030	0.211
408	0.033	0.060	0.110	0.012	0.041	0.030	0.211
411	0.033	0.059	0.110	0.012	0.041	0.030	0.211
414	0.033	0.060	0.111	0.013	0.042	0.031	0.211
417	0.033	0.061	0.111	0.013	0.042	0.031	0.211
420	0.034	0.061	0.111	0.013	0.042	0.031	0.211
423	0.034	0.061	0.111	0.013	0.042	0.031	0.211
426	0.034	0.062	0.112	0.013	0.042	0.031	0.212
429	0.035	0.063	0.112	0.013	0.042	0.031	0.212
432	0.035	0.063	0.112	0.014	0.042	0.032	0.213
435	0.035	0.063	0.113	0.014	0.042	0.032	0.213
438	0.035	0.064	0.114	0.014	0.042	0.032	0.213
441	0.036	0.064	0.114	0.014	0.042	0.032	0.213
444	0.036	0.064	0.114	0.014	0.042	0.032	0.213
447	0.037	0.065	0.115	0.015	0.042	0.033	0.214
450	0.037	0.065	0.115	0.015	0.042	0.033	0.214
453	0.037	0.066	0.116	0.015	0.043	0.033	0.214
456	0.037	0.066	0.116	0.015	0.043	0.033	0.214
459	0.038	0.066	0.116	0.016	0.043	0.033	0.215
462	0.038	0.067	0.117	0.016	0.043	0.034	0.215
465	0.038	0.067	0.117	0.016	0.043	0.034	0.216
468	0.038	0.068	0.118	0.016	0.043	0.034	0.215
471	0.039	0.068	0.118	0.016	0.043	0.034	0.216
474	0.039	0.068	0.119	0.016	0.043	0.034	0.216
477	0.040	0.069	0.119	0.017	0.043	0.035	0.216
480	0.040	0.070	0.119	0.017	0.043	0.035	0.216
483	0.040	0.071	0.120	0.017	0.043	0.035	0.216
486	0.040	0.072	0.120	0.017	0.043	0.035	0.217
489	0.041	0.073	0.121	0.018	0.043	0.036	0.217
492	0.041	0.074	0.121	0.018	0.043	0.036	0.217
495	0.041	0.075	0.121	0.018	0.043	0.036	0.218
498	0.042	0.076	0.122	0.018	0.043	0.036	0.217
501	0.042	0.077	0.122	0.018	0.043	0.036	0.218
504	0.042	0.077	0.123	0.018	0.044	0.037	0.218
507	0.042	0.078	0.123	0.019	0.043	0.037	0.218
510	0.043	0.079	0.123	0.019	0.044	0.037	0.218
513	0.043	0.079	0.124	0.019	0.044	0.037	0.218
516	0.043	0.079	0.124	0.019	0.044	0.037	0.219
519	0.044	0.080	0.124	0.019	0.044	0.038	0.219
522	0.044	0.080	0.125	0.020	0.044	0.038	0.219
525	0.044	0.081	0.125	0.020	0.044	0.038	0.219

Table K.3 Absorbance Data for Diazeniumdiolates utilizing Greiss Reagent (continued)

528	0.045	0.081	0.126	0.020	0.044	0.038	0.219
531	0.045	0.082	0.126	0.020	0.044	0.038	0.220
534	0.045	0.082	0.126	0.021	0.044	0.039	0.220
537	0.046	0.083	0.127	0.021	0.044	0.039	0.220
540	0.046	0.083	0.128	0.021	0.044	0.039	0.220
543	0.046	0.084	0.128	0.021	0.044	0.039	0.220
546	0.047	0.084	0.129	0.021	0.044	0.039	0.220
549	0.047	0.085	0.129	0.022	0.044	0.040	0.221
552	0.047	0.085	0.129	0.022	0.044	0.040	0.221
555	0.048	0.085	0.130	0.022	0.044	0.040	0.221
558	0.048	0.086	0.130	0.022	0.044	0.040	0.221
561	0.048	0.086	0.131	0.023	0.044	0.041	0.221
564	0.048	0.087	0.131	0.023	0.044	0.041	0.222
567	0.048	0.087	0.131	0.023	0.044	0.041	0.222
570	0.049	0.087	0.132	0.023	0.044	0.041	0.222
573	0.049	0.087	0.132	0.023	0.044	0.041	0.222
576	0.049	0.087	0.133	0.024	0.044	0.042	0.222
579	0.049	0.088	0.133	0.024	0.044	0.042	0.222
582	0.050	0.088	0.133	0.024	0.044	0.042	0.223
585	0.050	0.088	0.134	0.024	0.044	0.042	0.223
588	0.050	0.089	0.134	0.024	0.045	0.043	0.223
591	0.050	0.089	0.135	0.024	0.044	0.043	0.223
594	0.051	0.089	0.135	0.025	0.045	0.043	0.223
597	0.051	0.090	0.136	0.025	0.045	0.043	0.224
600	0.051	0.090	0.136	0.025	0.045	0.043	0.224
603	0.051	0.091	0.137	0.025	0.045	0.044	0.224
606	0.052	0.091	0.137	0.025	0.045	0.044	0.224
609	0.052	0.091	0.137	0.025	0.045	0.044	0.224
612	0.052	0.092	0.138	0.026	0.045	0.044	0.225
615	0.052	0.092	0.138	0.026	0.045	0.045	0.225
618	0.053	0.093	0.139	0.026	0.045	0.045	0.225
621	0.053	0.093	0.139	0.026	0.045	0.045	0.225
624	0.053	0.093	0.140	0.026	0.045	0.045	0.225
627	0.054	0.094	0.140	0.027	0.045	0.046	0.225
630	0.054	0.094	0.141	0.027	0.045	0.046	0.226
633	0.054	0.094	0.141	0.027	0.045	0.046	0.226
636	0.055	0.095	0.141	0.027	0.045	0.046	0.226
639	0.055	0.095	0.142	0.028	0.045	0.047	0.227
642	0.055	0.095	0.143	0.028	0.045	0.047	0.227
645	0.055	0.096	0.143	0.028	0.045	0.047	0.227
648	0.056	0.096	0.143	0.028	0.045	0.047	0.227
651	0.056	0.096	0.144	0.029	0.045	0.047	0.227
654	0.056	0.097	0.144	0.029	0.045	0.048	0.227
657	0.057	0.097	0.145	0.029	0.045	0.048	0.228
660	0.057	0.097	0.144	0.029	0.045	0.048	0.228

Table K.3 Absorbance Data for Diazeniumdiolates utilizing Greiss Reagent (continued)

663	0.057	0.097	0.145	0.029	0.045	0.048	0.228
666	0.058	0.098	0.145	0.030	0.045	0.049	0.228
669	0.058	0.098	0.145	0.030	0.045	0.049	0.228
672	0.058	0.098	0.146	0.030	0.045	0.049	0.229
675	0.059	0.099	0.146	0.030	0.045	0.049	0.229
678	0.059	0.099	0.147	0.030	0.045	0.050	0.229
681	0.059	0.099	0.147	0.031	0.045	0.050	0.229
684	0.059	0.100	0.148	0.031	0.045	0.050	0.229
687	0.060	0.100	0.148	0.031	0.045	0.050	0.230
690	0.060	0.100	0.149	0.032	0.045	0.051	0.230
693	0.060	0.101	0.149	0.032	0.045	0.051	0.230
696	0.060	0.101	0.150	0.032	0.045	0.051	0.230
699	0.060	0.101	0.150	0.032	0.045	0.051	0.230
702	0.061	0.102	0.151	0.032	0.045	0.052	0.231
705	0.061	0.102	0.151	0.033	0.045	0.052	0.231
708	0.061	0.102	0.152	0.033	0.045	0.052	0.231
711	0.062	0.103	0.152	0.033	0.045	0.052	0.231
714	0.062	0.103	0.152	0.033	0.045	0.053	0.231
717	0.062	0.103	0.153	0.034	0.045	0.053	0.231
720	0.062	0.104	0.153	0.034	0.045	0.053	0.232
723	0.063	0.104	0.153	0.034	0.046	0.053	0.232
726	0.063	0.104	0.154	0.034	0.045	0.054	0.232
729	0.063	0.104	0.155	0.034	0.045	0.054	0.232
732	0.064	0.105	0.155	0.035	0.045	0.054	0.233
735	0.064	0.106	0.155	0.035	0.045	0.055	0.233
738	0.064	0.105	0.156	0.035	0.045	0.055	0.233
741	0.064	0.106	0.156	0.035	0.045	0.055	0.233
744	0.065	0.107	0.157	0.035	0.045	0.055	0.233
747	0.065	0.108	0.157	0.036	0.045	0.056	0.234
750	0.065	0.108	0.158	0.036	0.045	0.056	0.234
753	0.065	0.109	0.158	0.036	0.046	0.056	0.234
756	0.066	0.110	0.159	0.036	0.046	0.056	0.234
759	0.066	0.111	0.159	0.037	0.046	0.057	0.234
762	0.066	0.112	0.159	0.037	0.045	0.057	0.235
765	0.066	0.113	0.160	0.037	0.046	0.057	0.235
768	0.067	0.113	0.160	0.038	0.046	0.057	0.235
771	0.067	0.114	0.161	0.038	0.046	0.058	0.235
774	0.067	0.115	0.161	0.038	0.046	0.058	0.235
777	0.068	0.115	0.161	0.038	0.046	0.058	0.236
780	0.068	0.116	0.162	0.038	0.045	0.059	0.236
783	0.068	0.116	0.162	0.039	0.046	0.059	0.236
786	0.069	0.116	0.163	0.039	0.046	0.059	0.236
789	0.069	0.117	0.163	0.039	0.045	0.059	0.236
792	0.070	0.117	0.163	0.039	0.045	0.060	0.236
795	0.070	0.117	0.164	0.040	0.045	0.060	0.237

Table K.3 Absorbance Data for Diazeniumdiolates utilizing Greiss Reagent (continued)

798	0.070	0.118	0.164	0.040	0.046	0.060	0.237
801	0.071	0.118	0.165	0.040	0.046	0.060	0.237
804	0.071	0.118	0.165	0.040	0.046	0.061	0.237
807	0.071	0.118	0.166	0.041	0.046	0.061	0.238
810	0.072	0.119	0.166	0.041	0.046	0.061	0.238
813	0.072	0.119	0.167	0.041	0.046	0.062	0.238
816	0.072	0.119	0.167	0.041	0.046	0.062	0.238
819	0.072	0.119	0.168	0.042	0.046	0.062	0.238
822	0.073	0.119	0.168	0.042	0.046	0.062	0.238
825	0.073	0.120	0.169	0.042	0.046	0.063	0.239
828	0.074	0.120	0.169	0.042	0.046	0.063	0.239
831	0.074	0.120	0.170	0.042	0.046	0.063	0.239
834	0.074	0.121	0.170	0.043	0.046	0.064	0.239
837	0.074	0.121	0.170	0.043	0.046	0.064	0.240
840	0.075	0.121	0.171	0.043	0.046	0.064	0.240
843	0.075	0.121	0.171	0.044	0.046	0.065	0.240
846	0.075	0.121	0.172	0.044	0.046	0.065	0.240
849	0.075	0.122	0.172	0.044	0.046	0.065	0.240
852	0.075	0.122	0.173	0.044	0.046	0.066	0.240
855	0.076	0.122	0.173	0.045	0.046	0.066	0.241
858	0.076	0.123	0.174	0.045	0.046	0.066	0.241
861	0.076	0.123	0.174	0.045	0.046	0.066	0.241
864	0.076	0.123	0.174	0.045	0.046	0.067	0.241
867	0.077	0.123	0.175	0.046	0.046	0.067	0.241
870	0.077	0.124	0.175	0.046	0.046	0.067	0.242
873	0.077	0.124	0.176	0.046	0.046	0.068	0.242
876	0.077	0.124	0.176	0.046	0.046	0.068	0.242
879	0.078	0.124	0.176	0.046	0.046	0.068	0.242
882	0.078	0.124	0.177	0.047	0.046	0.069	0.243
885	0.078	0.125	0.177	0.047	0.046	0.069	0.243
888	0.078	0.125	0.177	0.047	0.046	0.069	0.243
891	0.079	0.125	0.178	0.047	0.046	0.070	0.243
894	0.079	0.126	0.178	0.048	0.046	0.070	0.243
897	0.079	0.126	0.179	0.048	0.046	0.070	0.244
900	0.080	0.126	0.179	0.048	0.046	0.070	0.244
903	0.080	0.126	0.180	0.048	0.046	0.071	0.244
906	0.080	0.127	0.180	0.049	0.046	0.071	0.244
909	0.081	0.127	0.181	0.049	0.046	0.071	0.244
912	0.081	0.127	0.181	0.049	0.046	0.072	0.244
915	0.082	0.127	0.182	0.049	0.046	0.072	0.245
918	0.082	0.128	0.182	0.050	0.046	0.072	0.245
921	0.082	0.128	0.183	0.050	0.046	0.073	0.245
924	0.083	0.128	0.183	0.050	0.046	0.073	0.245
927	0.083	0.129	0.184	0.050	0.046	0.073	0.246
930	0.083	0.129	0.184	0.051	0.046	0.074	0.246

Table K.3 Absorbance Data for Diazeniumdiolates utilizing Greiss Reagent (continued)

933	0.083	0.129	0.184	0.051	0.046	0.074	0.246
936	0.084	0.129	0.185	0.051	0.046	0.074	0.246
939	0.084	0.130	0.185	0.052	0.046	0.075	0.247
942	0.084	0.130	0.186	0.052	0.046	0.075	0.247
945	0.085	0.130	0.186	0.052	0.046	0.075	0.248
948	0.085	0.131	0.187	0.052	0.046	0.076	0.248
951	0.085	0.131	0.187	0.053	0.046	0.076	0.248
954	0.085	0.131	0.187	0.053	0.046	0.076	0.248
957	0.086	0.131	0.188	0.053	0.046	0.077	0.249
960	0.086	0.132	0.188	0.053	0.046	0.077	0.249
963	0.086	0.132	0.189	0.054	0.046	0.077	0.249
966	0.086	0.132	0.189	0.054	0.046	0.078	0.249
969	0.087	0.132	0.189	0.054	0.046	0.078	0.250
972	0.087	0.133	0.190	0.054	0.046	0.079	0.250
975	0.087	0.133	0.191	0.055	0.046	0.079	0.250
978	0.088	0.133	0.191	0.055	0.046	0.079	0.250
981	0.088	0.134	0.191	0.055	0.046	0.080	0.251
984	0.088	0.134	0.192	0.056	0.046	0.080	0.251
987	0.088	0.134	0.192	0.056	0.046	0.080	0.251
990	0.089	0.134	0.193	0.056	0.046	0.081	0.252
993	0.089	0.135	0.193	0.056	0.046	0.081	0.252
996	0.089	0.135	0.194	0.056	0.046	0.081	0.252
999	0.090	0.135	0.194	0.057	0.045	0.082	0.253

APPENDIX L

RELEASE PROFILE FROM GREISS REAGENT ANALYSIS OF DIAZENIUMDIOLATES

Table L.1 Release Profile of Diazeniumdiolates using Greiss Reagent

Diazeniumdiolate Release Profile for Greiss Reagent Analysis							
Time (min)	DTBSNO	DLSNO	DSSNO	DISOSNO	DEANO	DEEDANO	PEG/DABNO
0	2.250	0.981	0.072	0.241	0.474	1.126	5.533
3	2.250	0.981	0.107	0.241	0.549	1.126	4.147
6	1.903	0.981	0.117	0.241	0.549	1.126	3.454
9	1.903	0.842	0.125	0.241	0.549	1.126	2.894
12	1.903	0.842	0.126	0.241	0.588	0.988	2.589
15	1.903	0.842	0.130	0.241	0.588	0.988	2.355
18	1.903	0.761	0.136	0.199	0.588	0.988	2.238
21	1.903	0.761	0.140	0.199	0.588	0.907	2.166
24	1.701	0.704	0.142	0.199	0.588	0.907	2.099
27	1.701	0.704	0.144	0.199	0.588	0.907	2.007
30	1.701	0.704	0.146	0.175	0.588	0.849	1.978
33	1.701	0.659	0.144	0.175	0.549	0.849	1.922
36	1.701	0.659	0.148	0.175	0.549	0.849	1.870
39	1.701	0.623	0.148	0.175	0.511	0.849	1.845
42	1.557	0.623	0.148	0.158	0.511	0.804	1.796
45	1.701	0.623	0.150	0.158	0.474	0.804	1.749
48	1.701	0.592	0.150	0.158	0.474	0.768	1.705
51	1.557	0.592	0.150	0.158	0.474	0.768	1.683
54	1.557	0.565	0.152	0.158	1.409	0.768	1.662
57	1.557	0.565	0.152	0.145	1.322	0.737	1.621
60	1.445	0.542	0.152	0.145	1.322	0.737	1.582
63	1.445	0.542	0.154	0.145	1.242	0.737	1.544
66	1.354	0.521	0.152	0.145	1.242	0.710	1.490
69	1.354	0.521	0.152	0.145	1.168	0.710	1.456
72	1.354	0.501	0.154	0.134	1.168	0.710	1.406
75	1.354	0.501	0.152	0.134	1.099	0.687	1.375
78	1.277	0.501	0.154	0.134	1.099	0.687	1.344
81	1.277	0.484	0.154	0.134	1.034	0.687	1.299
84	1.277	0.484	0.152	0.134	1.034	0.687	1.271
87	1.277	0.468	0.152	0.125	0.973	0.666	1.229
90	1.210	0.468	0.152	0.125	0.973	0.666	1.190
93	1.210	0.453	0.154	0.125	0.916	0.666	1.151
96	1.210	0.439	0.152	0.125	0.916	0.647	1.115
99	1.210	0.427	0.154	0.125	0.862	0.647	1.079

RELEASE PROFILE FROM GREISS REAGENT ANALYSIS OF DIAZENIUMDIOLATES
(continued)

102	1.151	0.414	0.152	0.125	0.862	0.647	1.056
105	1.151	0.403	0.152	0.125	0.811	0.629	1.012
108	1.151	0.392	0.152	0.117	0.811	0.629	0.980
111	1.151	0.382	0.152	0.117	0.762	0.629	0.948
114	1.099	0.372	0.152	0.117	0.762	0.629	0.918
117	1.099	0.372	0.150	0.117	0.762	0.613	0.889
120	1.099	0.363	0.152	0.110	0.716	0.613	0.861
123	1.099	0.354	0.150	0.110	0.716	0.613	0.833
126	1.051	0.354	0.150	0.110	0.671	0.598	0.815
129	1.051	0.354	0.150	0.110	0.671	0.598	0.797
132	1.051	0.345	0.150	0.110	0.671	0.598	0.771
135	1.007	0.345	0.150	0.104	0.629	0.598	0.746
138	1.007	0.337	0.148	0.104	0.629	0.585	0.721
141	1.007	0.337	0.148	0.104	0.629	0.585	0.705
144	1.007	0.329	0.148	0.104	0.588	0.585	0.681
147	0.967	0.329	0.148	0.104	0.588	0.572	0.666
150	0.967	0.322	0.148	0.104	0.588	0.572	0.651
153	0.967	0.322	0.146	0.098	0.549	0.572	0.636
156	0.967	0.315	0.146	0.098	0.549	0.572	0.621
159	0.930	0.308	0.146	0.098	0.549	0.572	0.606
162	0.930	0.308	0.144	0.098	0.511	0.560	0.585
165	0.930	0.301	0.144	0.098	0.511	0.560	0.571
168	0.930	0.301	0.142	0.093	0.511	0.560	0.550
171	0.896	0.294	0.144	0.093	0.474	0.548	0.536
174	0.896	0.294	0.142	0.093	0.474	0.548	0.516
177	0.896	0.288	0.142	0.093	0.474	0.548	0.496
180	0.864	0.288	0.142	0.093	0.474	0.548	0.477
183	0.864	0.282	0.142	0.088	0.439	0.548	0.464
186	0.864	0.276	0.140	0.088	0.439	0.537	0.446
189	0.833	0.276	0.140	0.088	0.439	0.537	0.427
192	0.833	0.270	0.138	0.088	0.405	0.537	0.415
195	0.833	0.270	0.138	0.088	0.405	0.537	0.398
198	0.833	0.264	0.138	0.088	0.405	0.527	0.380
201	0.833	0.259	0.138	0.084	0.405	0.527	0.363
204	0.833	0.259	0.136	0.084	0.373	0.527	0.352
207	0.805	0.254	0.136	0.084	0.373	0.517	0.340
210	0.805	0.254	0.134	0.084	0.373	0.517	0.324
213	0.805	0.248	0.134	0.084	0.373	0.517	0.313
216	0.805	0.248	0.134	0.079	0.341	0.517	0.302
219	0.778	0.243	0.134	0.079	0.341	0.517	0.292
222	0.778	0.238	0.134	0.079	0.341	0.508	0.281
225	0.778	0.238	0.132	0.079	0.341	0.508	0.276
228	0.778	0.234	0.132	0.076	0.310	0.508	0.266
231	0.778	0.234	0.132	0.076	0.310	0.508	0.260
234	0.752	0.229	0.132	0.076	0.310	0.508	0.250

RELEASE PROFILE FROM GREISS REAGENT ANALYSIS OF DIAZENIUMDIOLATES
(continued)

237	0.752	0.229	0.132	0.076	0.310	0.508	0.245
240	0.752	0.224	0.132	0.076	0.280	0.508	0.240
243	0.752	0.224	0.130	0.076	0.280	0.508	0.235
246	0.752	0.220	0.130	0.072	0.280	0.508	0.230
249	0.752	0.220	0.130	0.072	0.280	0.499	0.225
252	0.728	0.215	0.128	0.072	0.280	0.499	0.225
255	0.728	0.215	0.128	0.072	0.280	0.499	0.220
258	0.728	0.211	0.128	0.069	0.251	0.499	0.215
261	0.704	0.211	0.128	0.069	0.251	0.499	0.215
264	0.704	0.207	0.126	0.069	0.251	0.491	0.210
267	0.704	0.207	0.125	0.069	0.251	0.491	0.210
270	0.682	0.203	0.125	0.069	0.251	0.491	0.206
273	0.682	0.203	0.125	0.069	0.223	0.482	0.206
276	0.682	0.199	0.125	0.065	0.223	0.482	0.201
279	0.682	0.199	0.123	0.065	0.223	0.482	0.201
282	0.661	0.195	0.123	0.065	0.223	0.482	0.196
285	0.661	0.195	0.121	0.065	0.223	0.475	0.196
288	0.661	0.191	0.121	0.065	0.196	0.475	0.196
291	0.640	0.191	0.121	0.062	0.196	0.475	0.196
294	0.640	0.187	0.119	0.062	0.196	0.475	0.196
297	0.640	0.187	0.117	0.062	0.196	0.475	0.196
300	0.640	0.183	0.119	0.062	0.196	0.467	0.191
303	0.621	0.183	0.117	0.059	0.196	0.467	0.191
306	0.621	0.183	0.116	0.059	0.169	0.467	0.191
309	0.621	0.180	0.117	0.059	0.169	0.460	0.191
312	0.602	0.180	0.116	0.059	0.169	0.460	0.191
315	0.602	0.176	0.116	0.059	0.169	0.460	0.191
318	0.602	0.176	0.114	0.057	0.169	0.460	0.186
321	0.602	0.172	0.114	0.057	0.169	0.453	0.191
324	0.602	0.172	0.114	0.057	0.169	0.453	0.186
327	0.584	0.169	0.112	0.057	0.169	0.453	0.186
330	0.584	0.169	0.112	0.054	0.143	0.453	0.186
333	0.584	0.166	0.112	0.054	0.143	0.453	0.186
336	0.566	0.166	0.111	0.054	0.143	0.453	0.186
339	0.566	0.162	0.111	0.054	0.143	0.446	0.186
342	0.566	0.166	0.109	0.054	0.143	0.446	0.186
345	0.566	0.162	0.109	0.051	0.143	0.446	0.186
348	0.549	0.159	0.109	0.051	0.143	0.446	0.186
351	0.549	0.159	0.107	0.051	0.118	0.446	0.186
354	0.549	0.159	0.107	0.051	0.118	0.446	0.182
357	0.549	0.156	0.106	0.051	0.118	0.446	0.182
360	0.533	0.152	0.106	0.051	0.118	0.439	0.182
363	0.533	0.152	0.106	0.049	0.118	0.439	0.182
366	0.533	0.152	0.104	0.049	0.118	0.439	0.182
369	0.533	0.149	0.104	0.049	0.118	0.439	0.182

RELEASE PROFILE FROM GREISS REAGENT ANALYSIS OF DIAZENIUMDIOLATES
(continued)

372	0.517	0.149	0.104	0.049	0.118	0.439	0.182
375	0.517	0.149	0.104	0.049	0.118	0.439	0.182
378	0.517	0.146	0.102	0.049	0.093	0.433	0.177
381	0.502	0.146	0.102	0.047	0.093	0.433	0.177
384	0.502	0.143	0.102	0.047	0.093	0.433	0.172
387	0.502	0.143	0.102	0.047	0.093	0.433	0.172
390	0.502	0.143	0.101	0.047	0.093	0.433	0.172
393	0.487	0.140	0.101	0.047	0.093	0.427	0.172
396	0.487	0.140	0.099	0.044	0.093	0.427	0.172
399	0.487	0.137	0.099	0.044	0.093	0.427	0.167
402	0.472	0.137	0.098	0.044	0.093	0.427	0.167
405	0.472	0.137	0.098	0.044	0.093	0.427	0.167
408	0.472	0.134	0.096	0.042	0.093	0.421	0.167
411	0.472	0.131	0.096	0.042	0.093	0.421	0.163
414	0.458	0.129	0.095	0.042	0.069	0.421	0.163
417	0.458	0.126	0.095	0.042	0.069	0.421	0.158
420	0.444	0.123	0.095	0.040	0.069	0.421	0.163
423	0.444	0.120	0.095	0.040	0.069	0.415	0.158
426	0.444	0.118	0.093	0.040	0.069	0.415	0.158
429	0.444	0.115	0.093	0.040	0.069	0.415	0.158
432	0.431	0.112	0.093	0.040	0.069	0.415	0.158
435	0.431	0.112	0.092	0.038	0.069	0.410	0.158
438	0.431	0.110	0.090	0.038	0.069	0.410	0.153
441	0.431	0.107	0.090	0.038	0.069	0.410	0.153
444	0.418	0.107	0.090	0.038	0.069	0.410	0.153
447	0.418	0.107	0.089	0.038	0.069	0.410	0.149
450	0.405	0.105	0.089	0.036	0.069	0.404	0.153
453	0.405	0.105	0.087	0.036	0.045	0.404	0.149
456	0.405	0.102	0.087	0.036	0.045	0.404	0.149
459	0.405	0.102	0.087	0.034	0.045	0.404	0.149
462	0.393	0.100	0.086	0.034	0.045	0.404	0.149
465	0.393	0.100	0.086	0.034	0.045	0.399	0.149
468	0.393	0.097	0.084	0.034	0.045	0.399	0.144
471	0.381	0.097	0.084	0.034	0.045	0.399	0.144
474	0.381	0.095	0.083	0.033	0.045	0.399	0.144
477	0.381	0.095	0.083	0.033	0.045	0.399	0.144
480	0.381	0.093	0.083	0.033	0.045	0.394	0.144
483	0.369	0.093	0.081	0.033	0.045	0.394	0.140
486	0.369	0.093	0.081	0.031	0.045	0.394	0.140
489	0.369	0.090	0.080	0.031	0.045	0.394	0.140
492	0.358	0.090	0.080	0.031	0.045	0.394	0.140
495	0.358	0.088	0.080	0.031	0.045	0.388	0.140
498	0.358	0.088	0.079	0.031	0.045	0.388	0.140
501	0.347	0.088	0.079	0.029	0.045	0.388	0.135
504	0.347	0.088	0.077	0.029	0.022	0.388	0.135

RELEASE PROFILE FROM GREISS REAGENT ANALYSIS OF DIAZENIUMDIOLATES
(continued)

507	0.347	0.088	0.077	0.029	0.045	0.384	0.135
510	0.336	0.086	0.077	0.029	0.022	0.384	0.135
513	0.336	0.086	0.076	0.029	0.022	0.384	0.135
516	0.336	0.086	0.076	0.027	0.022	0.384	0.131
519	0.325	0.083	0.076	0.027	0.022	0.384	0.131
522	0.325	0.083	0.074	0.027	0.022	0.379	0.131
525	0.325	0.083	0.074	0.027	0.022	0.379	0.131
528	0.314	0.081	0.073	0.026	0.022	0.379	0.131
531	0.314	0.081	0.073	0.026	0.022	0.379	0.131
534	0.314	0.079	0.073	0.026	0.022	0.374	0.126
537	0.314	0.079	0.072	0.024	0.022	0.374	0.126
540	0.314	0.079	0.070	0.024	0.022	0.374	0.126
543	0.304	0.077	0.070	0.024	0.022	0.374	0.126
546	0.304	0.077	0.069	0.024	0.022	0.374	0.126
549	0.304	0.075	0.069	0.024	0.022	0.369	0.122
552	0.304	0.075	0.069	0.023	0.022	0.369	0.122
555	0.294	0.075	0.068	0.023	0.022	0.369	0.122
558	0.294	0.072	0.068	0.023	0.022	0.369	0.122
561	0.294	0.072	0.067	0.023	0.022	0.365	0.122
564	0.294	0.072	0.067	0.021	0.022	0.365	0.117
567	0.284	0.070	0.067	0.021	0.022	0.365	0.117
570	0.284	0.070	0.065	0.021	0.022	0.365	0.117
573	0.284	0.070	0.065	0.021	0.022	0.361	0.117
576	0.284	0.068	0.064	0.020	0.022	0.361	0.117
579	0.274	0.068	0.064	0.020	0.022	0.361	0.117
582	0.274	0.068	0.064	0.020	0.022	0.361	0.113
585	0.274	0.066	0.063	0.020	0.022	0.356	0.113
588	0.274	0.066	0.063	0.018		0.356	0.113
591	0.265	0.066	0.061	0.018		0.356	0.108
594	0.265	0.066	0.061	0.018		0.356	0.108
597	0.265	0.064	0.060	0.018		0.356	0.108
600	0.255	0.064	0.060	0.018		0.352	0.108
603	0.255	0.064	0.059	0.017		0.352	0.108
606	0.255	0.062	0.059	0.017		0.352	0.108
609	0.246	0.062	0.059	0.017		0.352	0.104
612	0.246	0.062	0.058	0.015		0.348	0.104
615	0.246	0.060	0.058	0.015		0.348	0.104
618	0.246	0.060	0.057	0.015		0.348	0.104
621	0.237	0.060	0.057	0.015		0.348	0.104
624	0.237	0.058	0.055	0.014		0.344	0.100
627	0.237	0.058	0.055	0.014		0.344	0.100
630	0.228	0.058	0.054	0.014		0.344	0.100
633	0.228	0.056	0.054	0.014		0.344	0.100
636	0.228	0.056	0.054	0.013		0.340	0.100
639	0.220	0.056	0.053	0.013		0.340	0.095

RELEASE PROFILE FROM GREISS REAGENT ANALYSIS OF DIAZENIUMDIOLATES
(continued)

642	0.220	0.054	0.052	0.013		0.340	0.095
645	0.220	0.054	0.052	0.013		0.340	0.095
648	0.211	0.054	0.052	0.013		0.336	0.095
651	0.211	0.052	0.051	0.011		0.336	0.095
654	0.211	0.052	0.051	0.011		0.336	0.091
657	0.211	0.052	0.049	0.011		0.336	0.091
660	0.203	0.052	0.051	0.011		0.332	0.091
663	0.203	0.050	0.049	0.010		0.332	0.091
666	0.203	0.048	0.049	0.010		0.332	0.091
669	0.203	0.050	0.049	0.010		0.332	0.091
672	0.203	0.048	0.048	0.010		0.328	0.087
675	0.194	0.046	0.048	0.009		0.328	0.087
678	0.194	0.045	0.047	0.009		0.328	0.087
681	0.194	0.045	0.047	0.009		0.325	0.087
684	0.186	0.043	0.046	0.009		0.325	0.082
687	0.186	0.041	0.046	0.008		0.325	0.082
690	0.186	0.039	0.045	0.008		0.325	0.082
693	0.186	0.037	0.045	0.008		0.321	0.082
696	0.178	0.036	0.044	0.008		0.321	0.082
699	0.178	0.036	0.044	0.007		0.321	0.078
702	0.178	0.034	0.042	0.007		0.321	0.078
705	0.170	0.032	0.042	0.007		0.318	0.078
708	0.170	0.032	0.041	0.005		0.318	0.078
711	0.170	0.030	0.041	0.005		0.318	0.078
714	0.170	0.030	0.041	0.005		0.318	0.074
717	0.163	0.030	0.040	0.005		0.314	0.074
720	0.163	0.029	0.040	0.004		0.314	0.074
723	0.163	0.029	0.040	0.004		0.314	0.074
726	0.163	0.029	0.039	0.004		0.311	0.074
729	0.155	0.027	0.038	0.004		0.311	0.070
732	0.155	0.027	0.038	0.003		0.311	0.070
735	0.155	0.027	0.038	0.003		0.311	0.070
738	0.155	0.027	0.037	0.003		0.307	0.070
741	0.148	0.025	0.037	0.003		0.307	0.070
744	0.148	0.025	0.036	0.002		0.307	0.070
747	0.148	0.025	0.036	0.002		0.307	0.065
750	0.140	0.025	0.035	0.002		0.304	0.065
753	0.140	0.025	0.035	0.001		0.304	0.065
756	0.140	0.024	0.034	0.001		0.304	0.065
759	0.133	0.024	0.034	0.001		0.301	0.061
762	0.133	0.024	0.034	0.001		0.301	0.061
765	0.126	0.022	0.033	0.001		0.301	0.061
768	0.126	0.022	0.033			0.301	0.061
771	0.126	0.022	0.032			0.298	0.061
774	0.119	0.022	0.032			0.298	0.061

RELEASE PROFILE FROM GREISS REAGENT ANALYSIS OF DIAZENIUMDIOLATES
(continued)

777	0.119	0.022	0.032			0.298	0.057
780	0.119	0.020	0.031			0.294	0.057
783	0.112	0.020	0.031			0.294	0.057
786	0.112	0.020	0.030			0.294	0.057
789	0.112	0.019	0.030			0.291	0.053
792	0.112	0.019	0.030			0.291	0.053
795	0.105	0.019	0.028			0.291	0.053
798	0.105	0.019	0.028			0.288	0.053
801	0.098	0.017	0.027			0.288	0.053
804	0.098	0.017	0.027			0.288	0.053
807	0.098	0.017	0.026			0.288	0.049
810	0.098	0.017	0.026			0.285	0.049
813	0.091	0.017	0.025			0.285	0.049
816	0.091	0.015	0.025			0.285	0.049
819	0.091	0.015	0.024			0.282	0.049
822	0.091	0.015	0.024			0.282	0.044
825	0.091	0.014	0.023			0.282	0.044
828	0.085	0.014	0.023			0.279	0.044
831	0.085	0.014	0.022			0.279	0.044
834	0.085	0.014	0.022			0.279	0.040
837	0.085	0.012	0.022			0.277	0.040
840	0.078	0.012	0.021			0.277	0.040
843	0.078	0.012	0.021			0.277	0.040
846	0.078	0.012	0.020			0.277	0.040
849	0.078	0.011	0.020			0.274	0.036
852	0.072	0.011	0.019			0.274	0.036
855	0.072	0.011	0.019			0.274	0.036
858	0.072	0.009	0.018			0.271	0.036
861	0.072	0.009	0.018			0.271	0.036
864	0.065	0.009	0.018			0.271	0.036
867	0.065	0.009	0.017			0.268	0.032
870	0.065	0.008	0.017			0.268	0.032
873	0.059	0.008	0.017			0.268	0.032
876	0.059	0.008	0.017			0.265	0.032
879	0.059	0.006	0.017			0.265	0.028
882	0.053	0.006	0.016			0.265	0.028
885	0.053	0.006	0.016			0.263	0.028
888	0.047	0.006	0.016			0.263	0.028
891	0.047	0.004	0.015			0.263	0.024
894	0.047	0.004	0.015			0.260	0.024
897	0.040	0.004	0.014			0.260	0.020
900	0.040	0.004	0.014			0.260	0.020
903	0.040	0.003	0.013			0.257	0.020
906	0.040	0.003	0.013			0.257	0.020
909	0.034	0.003	0.012			0.257	0.016

RELEASE PROFILE FROM GREISS REAGENT ANALYSIS OF DIAZENIUMDIOLATES
(continued)

912	0.034	0.001	0.012			0.255	0.016
915	0.034	0.001	0.011			0.255	0.016
918	0.029	0.001	0.011			0.252	0.016
921	0.029	0.001	0.010			0.252	0.012
924	0.029		0.010			0.252	0.012
927	0.029		0.009			0.250	0.012
930	0.023		0.009			0.250	0.012
933	0.023		0.009			0.250	0.008
936	0.023		0.008			0.247	0.008
939	0.023		0.008			0.247	0.008
942	0.017		0.007			0.247	0.004
945	0.017		0.007				0.004
948	0.017		0.006				0.004
951	0.011		0.006				
954	0.011		0.006				
957	0.011		0.005				
960	0.011		0.005				
963	0.006		0.004				
966	0.006		0.004				
969	0.006		0.004				
972			0.004				
975			0.003				
978			0.003				
981			0.003				
984			0.002				
987			0.002				
990			0.001				
993			0.001				

APPENDIX M

TOTAL RELEASE PROFILE FROM GREISS REAGENT ANALYSIS OF DIAZENIUMDIOLATES

Table M.1 Total Nitric Oxide Release Profile using Greiss Reagent

UV/Vis Diazeniumdiolate Release Profile							
Time (min)	DTBSNO	DLSNO	DHSNO	DISOSNO	DEANO	DEEDANO	PEG/DABNO
0	2.250	0.981	0.072	0.241	0.474	4.780	5.533
3	4.500	1.962	0.179	0.481	1.023	5.907	9.680
6	6.403	2.943	0.297	0.722	1.572	7.033	13.134
9	8.306	3.786	0.421	0.963	2.120	8.159	16.029
12	10.210	4.628	0.548	1.203	2.708	9.147	18.618
15	12.113	5.470	0.678	1.444	3.296	10.134	20.973
18	14.017	6.232	0.814	1.643	3.884	11.122	23.211
21	15.920	6.993	0.954	1.843	4.471	12.029	25.377
24	17.620	7.697	1.096	2.042	5.059	12.935	27.476
27	19.321	8.401	1.239	2.242	5.647	13.842	29.483
30	21.022	9.104	1.385	2.417	6.235	14.691	31.461
33	22.722	9.764	1.529	2.592	6.783	15.540	33.384
36	24.423	10.423	1.677	2.767	7.332	16.389	35.254
39	26.123	11.046	1.825	2.943	7.843	17.237	37.098
42	27.680	11.668	1.973	3.101	8.353	18.042	38.894
45	29.381	12.291	2.124	3.259	8.828	18.846	40.643
48	31.081	12.883	2.274	3.417	9.302	19.614	42.348
51	32.638	13.475	2.424	3.575	9.777	20.382	44.031
54	34.195	14.040	2.576	3.733	11.186	21.150	45.693
57	35.752	14.605	2.728	3.878	12.507	21.887	47.314
60	37.197	15.147	2.881	4.023	13.829	22.624	48.897
63	38.642	15.688	3.035	4.168	15.071	23.361	50.441
66	39.996	16.209	3.187	4.313	16.313	24.071	51.931
69	41.350	16.729	3.340	4.458	17.480	24.782	53.387
72	42.704	17.231	3.494	4.592	18.648	25.492	54.793
75	44.058	17.732	3.646	4.726	19.746	26.179	56.168
78	45.335	18.234	3.801	4.860	20.845	26.866	57.512
81	46.612	18.718	3.955	4.994	21.879	27.553	58.811
84	47.889	19.202	4.107	5.128	22.913	28.239	60.082
87	49.166	19.670	4.260	5.252	23.887	28.905	61.311
90	50.376	20.138	4.412	5.377	24.860	29.571	62.501
93	51.586	20.591	4.566	5.502	25.776	30.236	63.652
96	52.796	21.031	4.719	5.627	26.693	30.883	64.767

TOTAL RELEASE PROFILE FROM GREISS REAGENT ANALYSIS OF DIAZENIUMDIOLATES (continued)

99	54.007	21.457	4.873	5.752	27.555	31.530	65.846
102	55.158	21.872	5.025	5.877	28.417	32.176	66.902
105	56.309	22.275	5.178	6.001	29.228	32.806	67.913
108	57.461	22.667	5.330	6.118	30.039	33.435	68.893
111	58.612	23.049	5.482	6.235	30.801	34.064	69.841
114	59.710	23.421	5.634	6.352	31.563	34.694	70.759
117	60.809	23.793	5.785	6.469	32.325	35.307	71.648
120	61.908	24.156	5.937	6.579	33.041	35.920	72.509
123	63.006	24.510	6.087	6.689	33.757	36.533	73.342
126	64.057	24.864	6.237	6.799	34.428	37.132	74.157
129	65.108	25.218	6.387	6.908	35.099	37.730	74.954
132	66.159	25.563	6.537	7.018	35.770	38.329	75.725
135	67.167	25.909	6.688	7.122	36.399	38.927	76.471
138	68.174	26.246	6.836	7.226	37.027	39.512	77.192
141	69.182	26.583	6.984	7.329	37.656	40.096	77.897
144	70.189	26.913	7.132	7.433	38.244	40.681	78.579
147	71.156	27.242	7.280	7.536	38.832	41.253	79.245
150	72.124	27.564	7.428	7.640	39.419	41.824	79.895
153	73.091	27.886	7.574	7.738	39.968	42.396	80.531
156	74.059	28.200	7.720	7.836	40.516	42.968	81.151
159	74.989	28.508	7.866	7.934	41.065	43.540	81.758
162	75.919	28.816	8.010	8.032	41.576	44.099	82.342
165	76.850	29.116	8.153	8.130	42.087	44.659	82.913
168	77.780	29.417	8.295	8.222	42.597	45.218	83.463
171	78.676	29.712	8.439	8.315	43.072	45.766	83.999
174	79.572	30.006	8.581	8.408	43.546	46.315	84.515
177	80.468	30.294	8.723	8.501	44.021	46.863	85.011
180	81.331	30.582	8.865	8.593	44.495	47.411	85.488
183	82.195	30.863	9.007	8.681	44.935	47.959	85.953
186	83.059	31.139	9.147	8.769	45.374	48.497	86.399
189	83.892	31.415	9.286	8.857	45.813	49.034	86.826
192	84.725	31.685	9.424	8.945	46.219	49.571	87.242
195	85.559	31.955	9.562	9.033	46.624	50.109	87.639
198	86.392	32.219	9.700	9.121	47.030	50.636	88.019
201	87.225	32.478	9.838	9.205	47.435	51.163	88.382
204	88.058	32.737	9.974	9.288	47.808	51.690	88.734
207	88.863	32.991	10.110	9.372	48.181	52.207	89.074
210	89.668	33.244	10.244	9.455	48.553	52.725	89.398
213	90.473	33.492	10.378	9.539	48.926	53.242	89.711
216	91.277	33.741	10.512	9.618	49.267	53.759	90.013
219	92.055	33.984	10.646	9.698	49.608	54.277	90.305
222	92.833	34.222	10.780	9.777	49.949	54.785	90.586
225	93.610	34.461	10.912	9.857	50.290	55.293	90.862
228	94.388	34.694	11.044	9.932	50.600	55.801	91.128
231	95.166	34.928	11.176	10.008	50.910	56.309	91.388

TOTAL RELEASE PROFILE FROM GREISS REAGENT ANALYSIS OF DIAZENIUMDIOLATES (continued)

234	95.918	35.157	11.308	10.084	51.220	56.817	91.638
237	96.670	35.385	11.440	10.159	51.530	57.325	91.883
240	97.422	35.610	11.572	10.235	51.811	57.833	92.123
243	98.174	35.834	11.702	10.311	52.091	58.341	92.358
246	98.926	36.054	11.833	10.383	52.371	58.849	92.589
249	99.678	36.273	11.963	10.455	52.651	59.348	92.814
252	100.406	36.489	12.091	10.527	52.932	59.847	93.039
255	101.133	36.704	12.219	10.599	53.212	60.346	93.259
258	101.861	36.915	12.348	10.667	53.463	60.845	93.474
261	102.565	37.126	12.476	10.736	53.715	61.345	93.689
264	103.270	37.333	12.602	10.805	53.966	61.835	93.900
267	103.974	37.540	12.727	10.873	54.217	62.326	94.110
270	104.656	37.742	12.852	10.942	54.469	62.816	94.316
273	105.338	37.945	12.976	11.010	54.692	63.299	94.521
276	106.020	38.144	13.101	11.076	54.915	63.781	94.722
279	106.703	38.342	13.224	11.141	55.138	64.264	94.923
282	107.364	38.537	13.347	11.207	55.361	64.746	95.118
285	108.024	38.732	13.468	11.272	55.584	65.221	95.314
288	108.685	38.922	13.589	11.337	55.780	65.696	95.510
291	109.326	39.113	13.710	11.400	55.976	66.170	95.706
294	109.966	39.300	13.829	11.462	56.172	66.645	95.902
297	110.607	39.487	13.946	11.524	56.367	67.119	96.098
300	111.247	39.671	14.066	11.587	56.563	67.587	96.289
303	111.868	39.854	14.183	11.646	56.759	68.054	96.480
306	112.489	40.037	14.299	11.706	56.928	68.521	96.671
309	113.110	40.217	14.416	11.765	57.097	68.980	96.862
312	113.712	40.396	14.532	11.824	57.266	69.440	97.053
315	114.314	40.572	14.648	11.884	57.435	69.900	97.244
318	114.916	40.748	14.762	11.941	57.604	70.360	97.430
321	115.518	40.921	14.876	11.997	57.773	70.813	97.621
324	116.120	41.093	14.990	12.054	57.942	71.265	97.808
327	116.703	41.262	15.102	12.111	58.111	71.718	97.994
330	117.287	41.431	15.214	12.165	58.255	72.171	98.180
333	117.871	41.597	15.327	12.219	58.398	72.624	98.367
336	118.437	41.762	15.437	12.273	58.541	73.077	98.553
339	119.004	41.924	15.548	12.327	58.684	73.523	98.739
342	119.570	42.090	15.657	12.381	58.827	73.969	98.925
345	120.136	42.252	15.766	12.432	58.970	74.415	99.112
348	120.685	42.411	15.875	12.484	59.113	74.861	99.298
351	121.235	42.570	15.982	12.535	59.231	75.307	99.484
354	121.784	42.729	16.090	12.587	59.349	75.753	99.666
357	122.333	42.884	16.195	12.638	59.467	76.199	99.847
360	122.866	43.037	16.301	12.690	59.584	76.638	100.029
363	123.399	43.189	16.407	12.739	59.702	77.077	100.210
366	123.932	43.342	16.511	12.788	59.820	77.517	100.392

TOTAL RELEASE PROFILE FROM GREISS REAGENT ANALYSIS OF DIAZENIUMDIOLATES (continued)

369	124.465	43.491	16.615	12.837	59.938	77.956	100.573
372	124.982	43.640	16.719	12.886	60.055	78.396	100.755
375	125.499	43.789	16.823	12.935	60.173	78.835	100.936
378	126.016	43.936	16.925	12.984	60.266	79.268	101.113
381	126.518	44.082	17.028	13.031	60.359	79.701	101.290
384	127.019	44.225	17.130	13.077	60.452	80.135	101.462
387	127.521	44.368	17.233	13.124	60.546	80.568	101.634
390	128.023	44.511	17.333	13.171	60.639	81.001	101.806
393	128.509	44.651	17.434	13.218	60.732	81.428	101.978
396	128.996	44.791	17.534	13.262	60.825	81.855	102.151
399	129.483	44.929	17.633	13.307	60.918	82.282	102.318
402	129.955	45.066	17.731	13.351	61.011	82.709	102.485
405	130.427	45.203	17.828	13.395	61.104	83.135	102.653
408	130.900	45.337	17.924	13.438	61.197	83.556	102.820
411	131.372	45.468	18.021	13.480	61.290	83.977	102.983
414	131.830	45.597	18.115	13.522	61.359	84.398	103.146
417	132.288	45.723	18.210	13.565	61.428	84.819	103.304
420	132.733	45.846	18.304	13.605	61.497	85.240	103.467
423	133.177	45.966	18.399	13.645	61.566	85.655	103.625
426	133.621	46.083	18.492	13.685	61.635	86.071	103.783
429	134.066	46.198	18.585	13.726	61.704	86.486	103.941
432	134.497	46.311	18.678	13.766	61.773	86.901	104.099
435	134.928	46.423	18.770	13.804	61.842	87.311	104.257
438	135.359	46.533	18.860	13.842	61.911	87.720	104.411
441	135.790	46.640	18.950	13.880	61.980	88.130	104.564
444	136.208	46.747	19.040	13.919	62.049	88.539	104.718
447	136.627	46.854	19.129	13.957	62.118	88.949	104.866
450	137.032	46.959	19.218	13.993	62.187	89.353	105.020
453	137.437	47.063	19.305	14.029	62.233	89.757	105.169
456	137.843	47.166	19.392	14.066	62.278	90.161	105.318
459	138.248	47.268	19.479	14.100	62.324	90.565	105.467
462	138.642	47.368	19.565	14.134	62.369	90.969	105.616
465	139.035	47.467	19.651	14.169	62.415	91.368	105.764
468	139.428	47.564	19.735	14.203	62.460	91.766	105.909
471	139.809	47.662	19.819	14.237	62.505	92.165	106.053
474	140.190	47.757	19.902	14.270	62.551	92.564	106.197
477	140.571	47.852	19.985	14.303	62.596	92.963	106.342
480	140.952	47.944	20.068	14.335	62.642	93.356	106.486
483	141.321	48.037	20.149	14.368	62.687	93.750	106.626
486	141.691	48.129	20.230	14.398	62.733	94.143	106.766
489	142.060	48.219	20.310	14.429	62.778	94.537	106.905
492	142.418	48.310	20.390	14.460	62.824	94.930	107.045
495	142.776	48.397	20.470	14.491	62.869	95.319	107.185
498	143.133	48.485	20.549	14.521	62.915	95.707	107.325
501	143.480	48.573	20.628	14.550	62.960	96.096	107.460

TOTAL RELEASE PROFILE FROM GREISS REAGENT ANALYSIS OF DIAZENIUMDIOLATES (continued)

504	143.827	48.661	20.705	14.579	62.983	96.484	107.595
507	144.173	48.749	20.782	14.608	63.028	96.868	107.730
510	144.509	48.834	20.859	14.637	63.050	97.251	107.865
513	144.844	48.920	20.935	14.667	63.073	97.635	108.001
516	145.180	49.006	21.011	14.694	63.095	98.018	108.131
519	145.505	49.089	21.087	14.721	63.118	98.402	108.262
522	145.830	49.172	21.161	14.749	63.140	98.780	108.393
525	146.154	49.256	21.236	14.776	63.163	99.159	108.524
528	146.469	49.337	21.309	14.802	63.185	99.538	108.654
531	146.783	49.418	21.382	14.827	63.208	99.917	108.785
534	147.097	49.497	21.455	14.853	63.230	100.291	108.911
537	147.412	49.576	21.527	14.877	63.253	100.665	109.037
540	147.726	49.654	21.598	14.901	63.275	101.039	109.164
543	148.030	49.731	21.668	14.925	63.298	101.413	109.290
546	148.334	49.808	21.737	14.950	63.320	101.787	109.416
549	148.638	49.882	21.806	14.974	63.343	102.156	109.538
552	148.942	49.957	21.876	14.996	63.365	102.525	109.660
555	149.236	50.031	21.943	15.019	63.388	102.895	109.781
558	149.530	50.104	22.011	15.042	63.410	103.264	109.903
561	149.824	50.176	22.078	15.064	63.433	103.629	110.025
564	150.117	50.249	22.144	15.085	63.455	103.994	110.142
567	150.401	50.319	22.211	15.106	63.477	104.359	110.259
570	150.685	50.389	22.276	15.127	63.500	104.724	110.377
573	150.969	50.459	22.342	15.148	63.522	105.084	110.494
576	151.253	50.528	22.406	15.168	63.545	105.445	110.611
579	151.528	50.596	22.470	15.188	63.567	105.805	110.729
582	151.802	50.664	22.533	15.207	63.590	106.166	110.841
585	152.076	50.730	22.596	15.227	63.612	106.522	110.954
588	152.351	50.796	22.659	15.245	63.612	106.878	111.067
591	152.615	50.862	22.720	15.263	63.635	107.235	111.176
594	152.880	50.928	22.782	15.281	63.635	107.591	111.284
597	153.145	50.993	22.842	15.300	63.635	107.947	111.392
600	153.400	51.057	22.902	15.318	63.635	108.299	111.501
603	153.656	51.121	22.961	15.335	63.635	108.651	111.609
606	153.911	51.183	23.020	15.351	63.635	109.003	111.718
609	154.157	51.245	23.079	15.368	63.635	109.355	111.822
612	154.404	51.307	23.137	15.384	63.635	109.703	111.926
615	154.650	51.367	23.195	15.399	63.635	110.051	112.030
618	154.896	51.427	23.251	15.414	63.635	110.399	112.134
621	155.133	51.487	23.308	15.430	63.635	110.746	112.238
624	155.370	51.545	23.363	15.444	63.635	111.090	112.338
627	155.608	51.603	23.418	15.458	63.635	111.434	112.437
630	155.836	51.661	23.472	15.472	63.635	111.778	112.537
633	156.064	51.717	23.526	15.486	63.635	112.122	112.637

TOTAL RELEASE PROFILE FROM GREISS REAGENT ANALYSIS OF DIAZENIUMDIOLATES (continued)

636	156.293	51.773	23.580	15.499	63.635	112.462	112.736
639	156.513	51.829	23.633	15.512	63.635	112.802	112.832
642	156.732	51.883	23.685	15.524	63.635	113.141	112.927
645	156.952	51.937	23.737	15.537	63.635	113.481	113.022
648	157.163	51.991	23.788	15.550	63.635	113.817	113.118
651	157.374	52.044	23.839	15.561	63.635	114.153	113.213
654	157.585	52.096	23.889	15.573	63.635	114.489	113.304
657	157.796	52.148	23.939	15.584	63.635	114.825	113.395
660	157.999	52.200	23.989	15.596	63.635	115.157	113.486
663	158.202	52.250	24.039	15.606	63.635	115.490	113.577
666	158.405	52.299	24.088	15.616	63.635	115.822	113.668
669	158.607	52.349	24.137	15.626	63.635	116.154	113.759
672	158.810	52.397	24.186	15.637	63.635	116.482	113.845
675	159.005	52.444	24.234	15.646	63.635	116.811	113.932
678	159.199	52.489	24.281	15.655	63.635	117.139	114.019
681	159.393	52.533	24.328	15.664	63.635	117.464	114.105
684	159.580	52.576	24.374	15.673	63.635	117.789	114.188
687	159.766	52.617	24.419	15.680	63.635	118.114	114.270
690	159.952	52.656	24.464	15.688	63.635	118.438	114.352
693	160.139	52.693	24.509	15.696	63.635	118.760	114.435
696	160.317	52.729	24.553	15.704	63.635	119.081	114.517
699	160.496	52.765	24.596	15.711	63.635	119.402	114.595
702	160.674	52.798	24.639	15.717	63.635	119.723	114.673
705	160.844	52.830	24.681	15.724	63.635	120.041	114.751
708	161.015	52.863	24.722	15.729	63.635	120.358	114.829
711	161.185	52.893	24.764	15.735	63.635	120.676	114.907
714	161.356	52.923	24.805	15.740	63.635	120.994	114.981
717	161.518	52.954	24.845	15.746	63.635	121.308	115.055
720	161.681	52.982	24.886	15.750	63.635	121.622	115.129
723	161.844	53.011	24.926	15.754	63.613	121.936	115.203
726	162.007	53.039	24.965	15.759	63.613	122.247	115.276
729	162.162	53.066	25.003	15.763	63.613	122.558	115.346
732	162.317	53.093	25.041	15.766	63.613	122.868	115.416
735	162.472	53.120	25.079	15.769	63.613	123.179	115.485
738	162.627	53.147	25.116	15.773	63.613	123.486	115.555
741	162.774	53.172	25.153	15.776	63.613	123.794	115.624
744	162.922	53.198	25.189	15.778	63.613	124.101	115.694
747	163.070	53.223	25.225	15.780	63.613	124.409	115.759
750	163.210	53.248	25.260	15.782	63.613	124.713	115.824
753	163.350	53.273	25.294	15.783	63.591	125.017	115.890
756	163.490	53.297	25.328	15.784	63.569	125.321	115.955
759	163.623	53.320	25.362	15.785	63.547	125.622	116.016
762	163.756	53.344	25.395	15.786	63.547	125.922	116.077
765	163.881	53.366	25.428	15.787	63.525	126.223	116.138

TOTAL RELEASE PROFILE FROM GREISS REAGENT ANALYSIS OF DIAZENIUMDIOLATES (continued)

768	164.007	53.388	25.461		63.503	126.524	116.200
771	164.133	53.410	25.492		63.481	126.822	116.261
774	164.251	53.431	25.524		63.459	127.119	116.322
777	164.370	53.453	25.556		63.437	127.417	116.379
780	164.488	53.474	25.586		63.437	127.711	116.436
783	164.600	53.494	25.617		63.415	128.006	116.493
786	164.711	53.514	25.646		63.393	128.300	116.549
789	164.823	53.533	25.676		63.393	128.592	116.602
792	164.935	53.551	25.705		63.393	128.883	116.655
795	165.039	53.570	25.734		63.393	129.174	116.708
798	165.144	53.589	25.762		63.371	129.463	116.760
801	165.242	53.606	25.790		63.349	129.751	116.813
804	165.340	53.623	25.817		63.327	130.039	116.866
807	165.438	53.640	25.843		63.305	130.328	116.915
810	165.535	53.657	25.870		63.283	130.613	116.963
813	165.627	53.674	25.895		63.261	130.898	117.012
816	165.718	53.689	25.921		63.239	131.184	117.060
819	165.809	53.704	25.945		63.217	131.466	117.109
822	165.900	53.720	25.969		63.195	131.748	117.153
825	165.991	53.734	25.993		63.173	132.031	117.198
828	166.076	53.747	26.016		63.151	132.310	117.242
831	166.160	53.761	26.039		63.129	132.589	117.287
834	166.245	53.775	26.061		63.107	132.869	117.327
837	166.329	53.787	26.083		63.085	133.145	117.367
840	166.407	53.799	26.105		63.063	133.422	117.408
843	166.485	53.812	26.126		63.041	133.698	117.448
846	166.563	53.824	26.147		63.019	133.975	117.488
849	166.641	53.834	26.167		62.997	134.249	117.525
852	166.713	53.845	26.186		62.975	134.522	117.561
855	166.785	53.856	26.206		62.953	134.796	117.597
858	166.856	53.865	26.224		62.931	135.067	117.633
861	166.928	53.874	26.243		62.909	135.338	117.669
864	166.993	53.883	26.261		62.887	135.609	117.706
867	167.058	53.892	26.279		62.866	135.877	117.738
870	167.123	53.900	26.296		62.844	136.145	117.770
873	167.182	53.907	26.313		62.822	136.413	117.802
876	167.241	53.915	26.329		62.800	136.679	117.834
879	167.300	53.921	26.346		62.778	136.944	117.862
882	167.353	53.927	26.361		62.756	137.210	117.890
885	167.405	53.933	26.377		62.734	137.472	117.918
888	167.452	53.939	26.392		62.712	137.735	117.946
891	167.498	53.943	26.407		62.690	137.998	117.970
894	167.545	53.948	26.421		62.668	138.258	117.994
897	167.585	53.952	26.435		62.646	138.518	118.014

TOTAL RELEASE PROFILE FROM GREISS REAGENT ANALYSIS OF DIAZENIUMDIOLATES (continued)

900	167.626	53.957	26.449		62.624	138.778	118.034
903	167.666	53.960	26.461		62.602	139.036	118.054
906	167.707	53.963	26.474		62.580	139.293	118.074
909	167.741	53.966	26.486		62.558	139.551	118.090
912	167.776	53.967	26.498		62.536	139.805	118.106
915	167.810	53.969	26.508		62.514	140.060	118.122
918	167.839	53.970	26.519		62.492	140.313	118.138
921	167.867	53.972	26.529		62.470	140.565	118.150
924	167.896		26.539		62.448	140.817	118.162
927	167.925		26.548		62.426	141.067	118.174
930	167.947		26.557		62.404	141.317	118.186
933	167.970		26.566		62.382	141.567	118.194
936	167.993		26.574		62.360	141.814	118.202
939	168.016		26.582		62.338	142.062	118.210
942	168.032		26.589		62.316	142.309	118.214
945	168.049		26.596		62.294		118.218
948	168.066		26.603		62.272		118.221
951	168.078		26.609		62.250		
954	168.089		26.615		62.228		
957	168.100		26.620		62.206		
960	168.111		26.626		62.184		
963	168.117		26.630		62.162		
966	168.122		26.634		62.140		
969	168.128		26.639		62.118		
972			26.642		62.096		
975			26.645		62.074		
978			26.648		62.052		
981			26.650		62.030		
984			26.652		62.008		
987			26.654		61.986		
990			26.655		61.964		
993			26.656		61.942		
996					61.920		

APPENDIX N

ECOSY NMR SPECTRA FOR PEG/DAB NO AND PEG/EDA NO

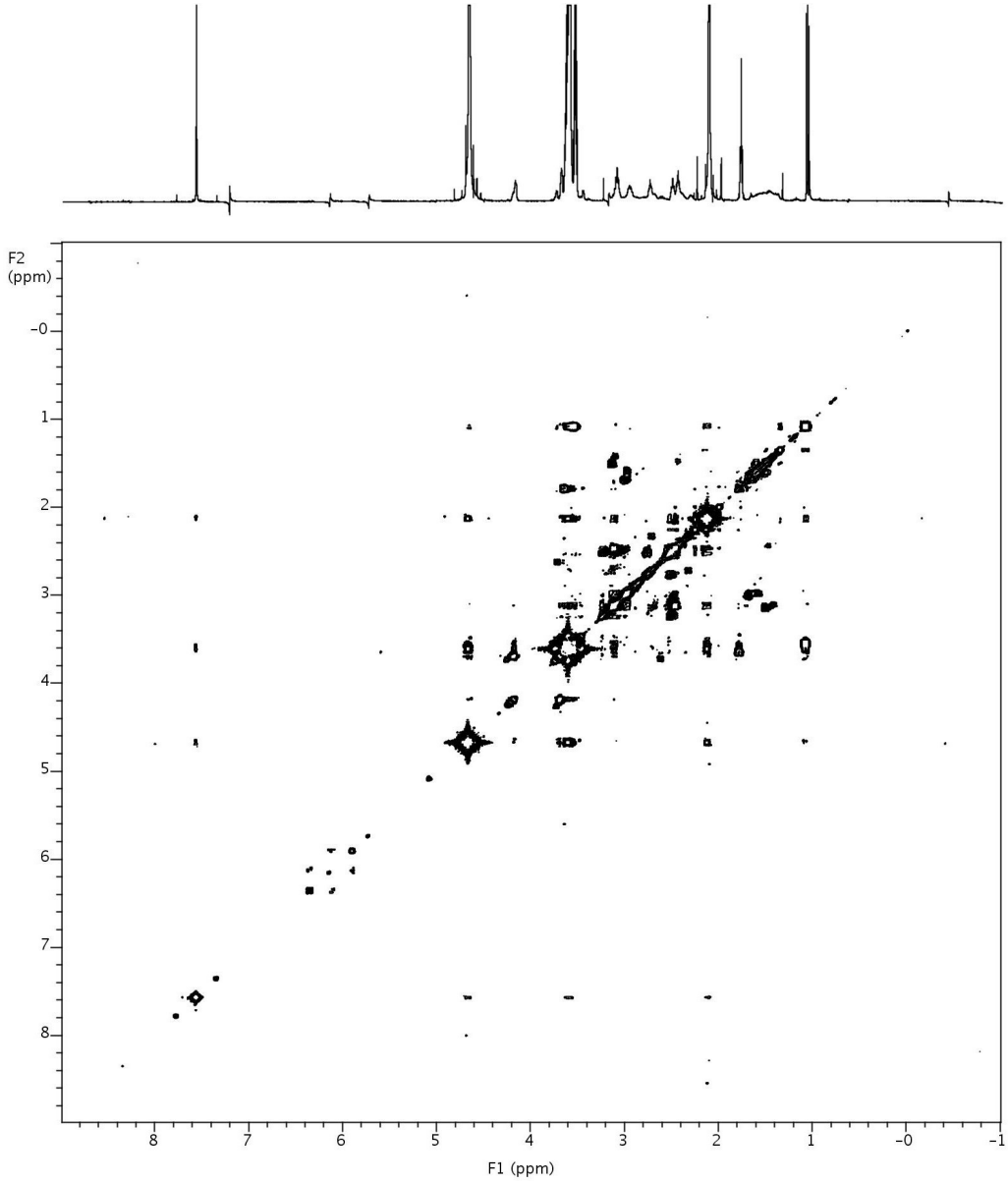

ECOSY spectrum of PEG/DAB NO

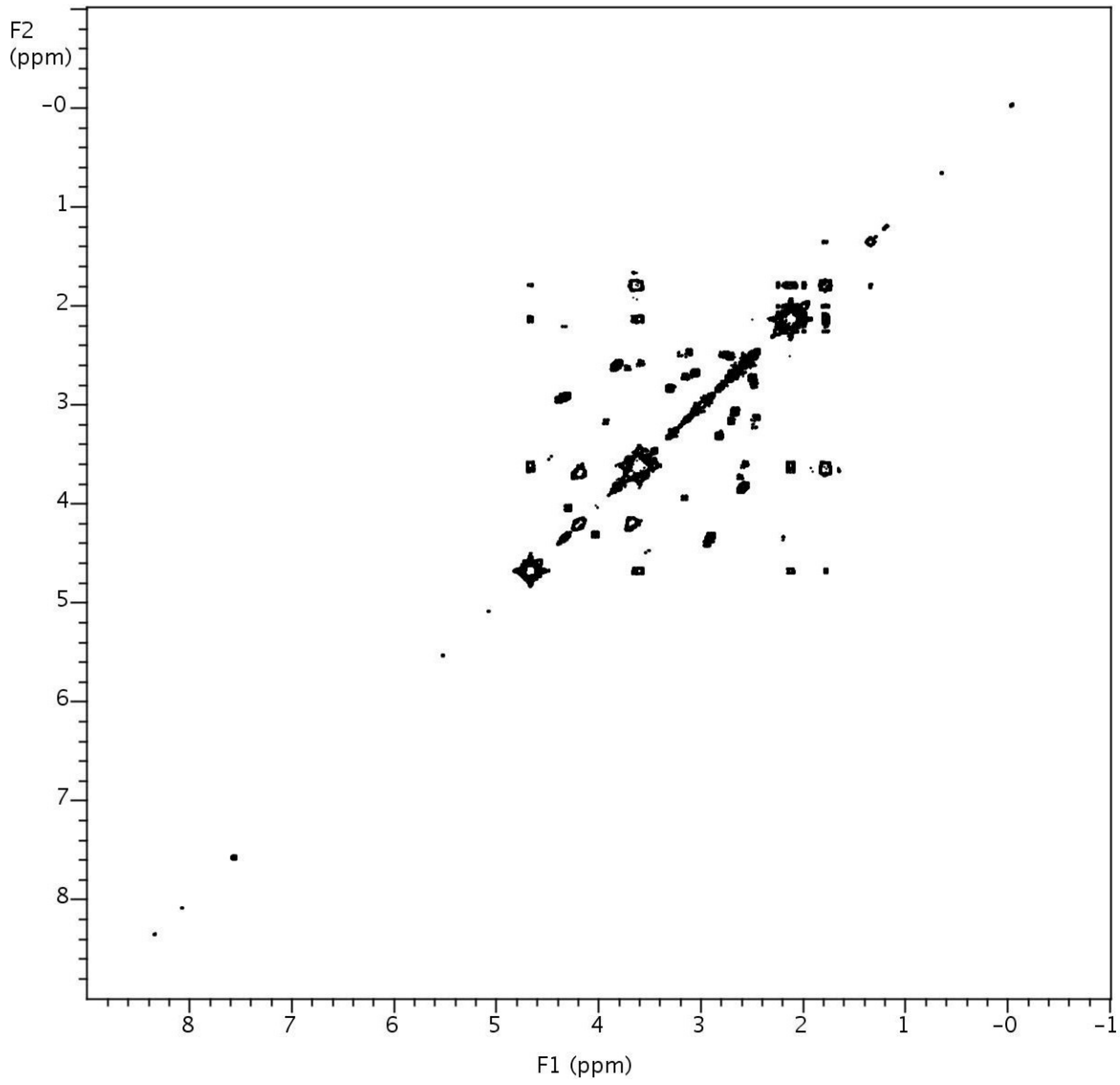

ECOSY spectrum of PEG/EDA NO